

South Dakota State University  
**Open PRAIRIE: Open Public Research Access Institutional  
Repository and Information Exchange**

---

Theses and Dissertations

---

2016

# Composite Gel Polymer Electrolyte for Lithium Ion Batteries

Roya Naderi

South Dakota State University, roya.naderi@sdstate.edu

Follow this and additional works at: <http://openprairie.sdstate.edu/etd>

 Part of the [Materials Science and Engineering Commons](#), and the [Power and Energy Commons](#)

---

## Recommended Citation

Naderi, Roya, "Composite Gel Polymer Electrolyte for Lithium Ion Batteries" (2016). *Theses and Dissertations*. Paper 1061.

This Thesis - Open Access is brought to you for free and open access by Open PRAIRIE: Open Public Research Access Institutional Repository and Information Exchange. It has been accepted for inclusion in Theses and Dissertations by an authorized administrator of Open PRAIRIE: Open Public Research Access Institutional Repository and Information Exchange. For more information, please contact [michael.biondo@sdstate.edu](mailto:michael.biondo@sdstate.edu).

COMPOSITE GEL POLYMER ELECTROLYTE FOR LITHIUM ION BATTERIES

BY

ROYA NADERI

A thesis submitted in partial fulfillment of the requirements for the

Master of Science

Major in Electrical Engineering

South Dakota State University

2016

## COMPOSITE GEL POLYMER ELECTROLYTE FOR LITHIUM ION BATTERIES

This thesis is approved as a creditable and independent investigation by a candidate for the Master of Science degree in Electrical Engineering and is acceptable for meeting the thesis requirements for this degree. Acceptance of this thesis does not imply that the conclusions reached by the candidate are necessarily the conclusions of the major department.

Qiquán Qiao, Ph.D.  
Thesis Advisor

Date

Steven Hietpas, Ph.D.  
Head, Department of Electrical  
Engineering and Computer science

Date

Dean, Graduate School

Date

This thesis is dedicated to my parents, Bahador Naderi and Homeira Sam-Daliri for their love, encouragement, support and always teaching me “Educate for betterment of the world, education is waste of time if can’t make our lives easier!”

## ACKNOWLEDGEMENTS

The work presented in this thesis was supported by NASA EPSCoR (Award #: NNX14AN22A), and by the State of South Dakota.

First and foremost, my deepest gratitude would be extended to Dr. Qiao as my supervisor and graduate coordinator for providing me the opportunity of working in his research group as a research assistant and his enormous help throughout this project..

My committee members, Dr. Yoon and Prof. Galipeau are appreciated for the the time and consideration they spent on improving my presentation skills and upgrading the contents of this dissertation.

Much indebtedness goes to Prof. Delfanian and his wife, Mrs. Christie Delfanian that blessed me with their consistent inspirations throughout my degree program.

Equal gratefulness goes to Ashim Gurung, the senior PhD student for his continuous guidance towards mentoring the battery researchers.

## TABLE OF CONTENTS

LIST OF FIGURES .....	viii
LIST OF TABLES .....	xii
ABSTRACT .....	xv
CHAPTER 1. INTRODUCTION .....	1
1.1. Background .....	1
1.2. Literature review .....	7
1.3. Motivation.....	18
1.4. Objectives .....	18
CHAPTER 2. THEORY .....	19
2.1. Charge and discharge principles and reactions of lithium ion batteries .....	19
2.1.1. Basic components of lithium ion batteries.....	35
2.2. All solid state lithium ion batteries .....	43
2.2.1. Solid polymer electrolyte .....	47
2.2.2. Gel polymer electrolyte.....	48
2.2.3. Composite solid/gel polymer electrolyte .....	51
2.2.4. Ionic liquid-based gel polymer electrolyte .....	52
2.3. Ionic conductivity mechanism of gel polymer electrolyte.....	54
2.3.1. Adding plasticizers to improve ionic conductivity of gel polymer electrolyte	54
2.3.2. Effect of concentration of lithium salt .....	56

2.3.3. Effect of adding inorganic nano fillers .....	58
2.3.4. Effect of plasma treatment of trilayer PP (polypropylene-polypropylene-polypropylene) separator.....	60
CHAPTER 3. EXPERIMENTAL PROCEDURES.....	61
3.1. Materials .....	61
3.1.1. PVDF-HFP.....	61
3.1.2. DMF.....	63
3.1.3. PC.....	64
3.1.4. SiO <sub>2</sub> .....	66
3.1.5. TiO <sub>2</sub> .....	67
3.1.6. Trilayer PP separator membrane.....	69
3.1.7. LiClO <sub>4</sub> .....	70
3.1.8. LiPF <sub>6</sub> in EC:DMC:DEC (4:2:4 in volume).....	71
3.1.9. NH <sub>3</sub> OH.....	72
3.1.10. TEOS.....	73
3.1.11. HNO <sub>3</sub> .....	74
3.2. Preparation of the CGPE coated PP separators.....	75
3.2.1. O <sub>2</sub> plasma treatment of trilayer PP separator membrane .....	75
3.2.2. Preparation of modified inorganic fillers .....	76
3.2.3. Composite gel polymer coating on trilayer PP separator.....	77

3.2.4. Incorporation of liquid electrolyte into composite gel polymer coated trilayer PP separator membrane.....	78
3.2.5. Characterization of the trilayer PP before and after coating the CGPE.....	79
3.2.6. Electrochemical measurements.....	80
CHAPTER 4. RESULTS AND DISCUSSIONS.....	83
4.1. Characterization of trilayer PP separator before and after O <sub>2</sub> plasma treatment ...	83
4.2. Characterization of modified inorganic nano fillers .....	86
4.3. SEM images of the composite gel polymer electrolyte before and after coating on trilayer PP separator .....	87
4.4. EDS measurement of CGPE membrane after LiClO <sub>4</sub> +LiPF <sub>6</sub> solution bath.....	90
4.5. Electrochemical measurements.....	91
4.5.1. Electrochemical Impedance Spectroscopy (EIS).....	91
4.5.2. Cyclic Voltammetry (CV) measurement of the half cell lithium ion battery .	93
4.5.3. Charge and discharge cycle of the half cell lithium ion battery .....	95
4.5.4. Rate capability measurement of the half cell lithium ion batteries.....	96
CHAPTER 5. CONCLUSIONS .....	99
5.1. Summary .....	99
5.2. Conclusion .....	101
5.3. Future work.....	102
REFERENCES .....	104



## LIST OF FIGURES

Figure 1.1. Global warming due to the emission of greenhouse gases; increases in the Earth's average temperature by 14.47% in 2010 [2]. .....	1
Figure 1.2. Rapid growth of demand on electric cars by 2040, accounting for 35% of all new vehicle sales [6]. .....	4
Figure 1.3. 50 MW battery vs. 50 MW gas peaker as backup systems for renewable energy based plants [8]. .....	5
Figure 1.4. Global market share of different applications of lithium ion batteries from 2005 to 2025 reported by the Nikkei BP consulting Inc [10]. .....	6
Figure 1.5. Boeing 787-Dreamliner lithium ion battery explosion [12]. .....	7
Figure 1.6. Dell laptop explosion at a Japanese conference [13]. .....	7
Figure 1.7. A prehistoric Parthian battery [15]. .....	8
Figure 1.8. Voltaic battery, stacks of zinc and copper/silver separated by a blotting paper [19]. .....	9
Figure 1.9. Franklin battery made of a series of connected capacitors [20]. .....	10
Figure 1.10. Daniel's cell as the first practical battery [21]. .....	10
Figure 1.11. The first rechargeable Gaston's lead acid battery [25]. .....	12
Figure 1.12. The first wet Leclanché's cell [26]. .....	12
Figure 1.13. The first dry Gassner's dry cell in the market [27]. .....	12
Figure 1.14. Commercialized zinc-carbon battery, an alkaline primary battery [29]. .....	13
Figure 2.1. Ion/electron transfer within the atomic structure of the electrodes through electrolyte in a LiCoO <sub>2</sub> -Graphite full cell lithium ion battery. ....	20

Figure 2.2. Contribution of secondary batteries based on their specific power vs. specific energy [45].	24
Figure 2.3. Volumetric energy density of different rechargeable battery prototypes vs. specific energy density [52].	30
Figure 2.4. Charge (1&2) and discharge (3&4) diagram of a rechargeable battery [54].	31
Figure 2.5. Finger like lithium dendrites growth on lithium anode surface with possibility of internal short circuit in higher cycles [55].	34
Figure 2.6. Schematic of lithium ion battery charge and discharge process [56].	34
Figure 2.7. polymer electrolyte in a lithium ion battery where electrolyte and separator are both in one membrane [57].	35
Figure 2.8. Potential vs. capacity of alternative anode/cathode material for lithium ion batteries [60].	37
Figure 2.9. chemical structure of PC (a) with an additional methyl group vs. EC (b).	41
Figure 2.10. segmental motion of lithium ion batteries in a PEO electrolyte membrane [74].	44
Figure 2.11. some transport paths of lithium ions in a ceramic membrane through the point defects and grain boundaries [75].	46
Figure 2.12. Ionic liquid enriched polymer host where polymer chains are modified using cross linking agents [86].	53
Figure 2.13. adding plasticizer can provide the free volume within a polymer host matrix [94].	56
Figure 3.1. resonance form of PVDF polymer host [112].	62
Figure 3.2. resonance form of the PVDF-HFP copolymers [114].	62

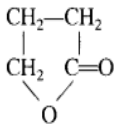
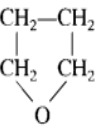
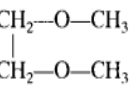
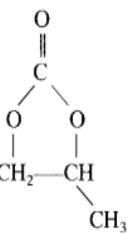
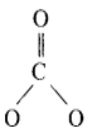
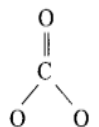
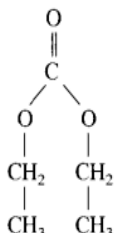
Figure 3.3. Two different resonance forms of DMF [115].	64
Figure 3.4. resonance form of PC [119].	65
Figure 3.5. Resonance form of SiO <sub>2</sub> [121].	67
Figure 3.6. Resonance forms of (a) rutile (b) brookite (c) anatase phases of TiO <sub>2</sub> [122].	68
Figure 3.7. Chemical structure of LiClO <sub>4</sub> [8].	70
Figure 3.8. Chemical structures of LiPF <sub>6</sub> , EC, DEC and DMC [129].	72
Figure 3.9. Chemical structure of NH <sub>3</sub> OH [131].	73
Figure 3.10. Molecular structure of Si(OC <sub>2</sub> H <sub>5</sub> ) <sub>4</sub> used as a precursor for preparing SiO <sub>2</sub> [132].	74
Figure 3.11. Molecular structure of HNO <sub>3</sub> [17].	75
Figure 3.12. Cleaning the separator using acetone vapored lab tissues.	76
Figure 3.13. Phase separated gel TEOS after hydrolyzation and before drying.	77
Figure 3.14. (a) Basic CGPE coated on trilayer PP separator before dipping in lithium salt solution. (b) Schematic diagram of a trilayer PP separator coated by composite gel electrolyte.	78
Figure 3.15. CGPE coated PP separators in Petri dishes covered by aluminum foil with holes.	78
Figure 3.16. Contact Angle Measurement system.	79
Figure 3.17. SEM-EDS Measurement system.	80
Figure 3.18. System setup used for Electrochemical Impedance Spectroscopy (EIS) and Cyclic Voltammetry (CV).	81
Figure 3.19. LAND CT2001A battery tester system setup.	82

Figure 4.1. Trilayer PP separator (a) before O <sub>2</sub> plasma treatment (b) after 10 minutes , (c) after 15 minutes and (d) after 20 minutes of O <sub>2</sub> plasma treatment at each side respectively. ....	83
Figure 4.2. Trilayer PP membrane (a) after 20 minutes (b) after 25 minutes of plasma treatment at each side respectively. ....	84
Figure 4.3. Formation of polar groups on trilayer PP membrane [142]. ....	85
Figure 4.4. acid treated TiO <sub>2</sub> coated on pH strip on the left and hydrolyzed TEOS coated on the pH strip on the right; colors comparison with the pH numbers. ....	87
Figure 4.5. SEM image of (a&b): CGPE before coating on trilayer PP separator, (c&d): Coated CGPE before LiClO <sub>4</sub> +LiPF <sub>6</sub> solution bath and (e&f): Coated CGPE after LiClO <sub>4</sub> +LiPF <sub>6</sub> solution bath with 200 & 10 μm magnification respectively.....	89
Figure 4.6. EIS of (a) GPE without nano fillers (b) acidic CGPE and (c) basic CGPE. ..	91
Figure 4.7. Cyclic voltammograms of (a) acidic CGPE and (b) basic CGPE. ....	94
Figure 4.8. Galvanostatic charge-discharge voltage profiles of acidic and basic CGPE for (a) 1st cycle and (b) 40 <sup>th</sup> cycle @ C/20.....	96
Figure 4.9. Rate capability of acidic and composite gel polymer electrolyte half cells @ different constant current rates.....	97

## LIST OF TABLES

Table 1.1. Alkali metals' oxidation energies. Lithium has the highest potential and energy per electron [3].	2
Table 2.1. fundamental differences between primary and secondary batteries [43] .	22
Table 2.2. examples of primary and secondary batteries' types [43].	23
Table 2.3. some of advantages and disadvantages of lead acid batteries [46].	25
Table 2.4. some of advantages and disadvantages of Nickel based batteries [44].	27
Table 2.5. some of advantages and disadvantages of lithium ion batteries [50].	29
Table 2.6. Ionic conductivity ranges of several electrolyte types of lithium ion batteries [53].	32
Table 2.7. Electrochemical comparison of anode materials for lithium ion batteries [53].	37
Table 2.8. Electrochemical comparison of cathode materials for lithium ion batteries [53].	38
Table 2.9. Compatible anode and cathode electrodes for lithium ion batteries [61].	38
Table 2.10. Types of typical lithium salts, commonly used solvents and conductivities in - 40° to 80° C range temperature for lithium ion batteries [61].	40

Table 2.11. Lithium salt aprotic solvents, chemical structure and essential characteristics [53].

Characteristic	$\gamma$ -BL	THF	1,2-DME	PC	EC	DMC	DEC
Structural formula							
Boiling point, °C	202–204	65–67	85	240	248	91	126
Melting point, °C	-43	-109	-58	-49	-39–40	4.6	-43
Density, g/cm <sup>3</sup>	1.13	0.887	0.866	1.198	1.322	1.071	0.98
Viscosity at 25°C, cP	1.75	0.48	0.455	2.5	1.86	0.59	0.75
					(at 40°C)		
Dielectric constant at 20°C	39	7.75	7.20	64.4	89.6	3.12	2.82
					(at 40°C)		
Molecular weight	86.09	72.10	90.12	102.0	88.1	90.08	118.13
Typical H <sub>2</sub> O content, ppm	<10	<10	<10	<10	<10	<10	<10
Electrolytic conductivity at 20°C, 1M LiAsF <sub>6</sub> , mS/cm	10.62	12.87	19.40	5.28	6.97	11.00 (1.9 M)	5.00 (1.5 M)

.. 42

Table 3.1. Some main physical properties of PVDF-HFP [114].	63
Table 3.2. Main physical properties of DMF [115].	64
Table 3.3. Main physical properties of PC [119].	65
Table 3.4. Physical properties of SiO <sub>2</sub> [3].	67
Table 3.5. Physical properties of TiO <sub>2</sub> [7].	68
Table 3.6. Physical properties of a Celgard 2500 separator [127].	69
Table 3.7. Physical properties of LiClO <sub>4</sub> [8].	70
Table 3.8. Physical properties of LiPF <sub>6</sub> in EC:DMC:DEC [130].	72
Table 3.9. Physical properties of NH <sub>3</sub> OH [13].	73
Table 3.10. Physical properties of TEOS.	74
Table 3.11. Physical properties of HNO <sub>3</sub> .	75

Table 4.1. Pore diameter range of CGPE under different conditions. ....	90
Table 4.2. Weight contribution of carbon, oxygen, hydrogen (3 dominant elements of PVDF-HFP) and lithium in CGPE.....	90
Table 4.3. Bulk resistance and ionic conductivity of different types of GPE.....	92
Table 4.4. Specific capacity of acidic CGPE at different cycle numbers and constant current rates.....	98
Table 4.5. Specific capacity of basic CGPE at different cycle numbers and constant current rates.....	98

## ABSTRACT

## COMPOSITE GEL POLYMER ELECTROLYTE FOR LITHIUM ION BATTERIES

ROYA NADERI

2016

Batteries have been ubiquitously utilized in enormous applications such as portable electronics, satellites, computers, medical instruments, and electric cars. The development of battery technology has been through a long journey since the 17<sup>th</sup> century, paving its way to commercialization of lithium ion batteries in 1991 by Sony. Rechargeable lithium ion batteries represent the most favorable type of batteries for portable applications due to their high energy density compared to other alkali metals. In 1997, lithium polymer batteries with solid polymer/composite electrolyte were introduced where the safety drawbacks of the liquid electrolyte were eliminated but the ionic conductivity of the batteries was lower than that of a liquid. In this work, composite gel polymer electrolyte (CGPE) films, consisting of poly (vinylidene fluoride-hexafluoropropylene) (PVdF-HFP) as the membrane, dimethylformamide (DMF) and propylene carbonate (PC) as solvents and plasticizing agent, mixture of charge modified TiO<sub>2</sub> and SiO<sub>2</sub> nano particles as ionic conductors, and LiClO<sub>4</sub>+LiPF<sub>6</sub> as lithium salts were fabricated. CGPE was coated on an O<sub>2</sub>-plasma treated trilayer polypropylene-polyethylene-polypropylene (PP) membrane separator using solution casting technique. In acidic CGPE, the mixture of acid treated TiO<sub>2</sub> and neutral SiO<sub>2</sub> nano particles played the role of the charge modified nano fillers with enhanced hydroxyl groups. The mixture of neutral TiO<sub>2</sub> nano particles with basic SiO<sub>2</sub> prepared through the hydrolyzation of



tetraethyl orthosilicate (TEOS) provided a more basic environment due to the residues of  $\text{NH}_4\text{OH}$  (Ammonium hydroxide) catalyst. The CGPE exhibited submicron pore size while the ionic conductivities were in order of  $10^{-3}$  -  $10^{-5}$   $\text{S}\cdot\text{cm}^{-1}$  with and without modified nano-fillers respectively. Half-cells with graphite anode and Li metal as reference electrode were then assembled and the electrochemical measurements and morphology examinations were successfully carried out. Half-cells demonstrated a considerable change in their electrochemical performance upon the enhancement of acidic properties of the CGPE, gaining the reversible specific capacity of  $372 \text{ mAh}\cdot\text{g}^{-1}$  in acidic CGPE vs.  $270 \text{ mAh}\cdot\text{g}^{-1}$  in basic CGPE @ C/20 after 40 cycles.

## CHAPTER 1. INTRODUCTION

### 1.1. Background

Batteries have been ubiquitously utilized in enormous applications such as portable electronics, satellites, computers, medical instruments, and electric cars. The American Physical Society presaged that the household demands of energy is claimed to increase by 30% in next 10 years. Simultaneously, the current non-renewable resources are rapidly diminishing along with global warming due to the emission of greenhouse gas as shown in Figure 1.1. Substituting our dependence to renewable resources, devising methods to efficiently store the generated energy has been an undeniable component. Particularly, the fluctuating nature of sunlight and wind at any given location necessitates the inclusion of storage system in the overall design [1].

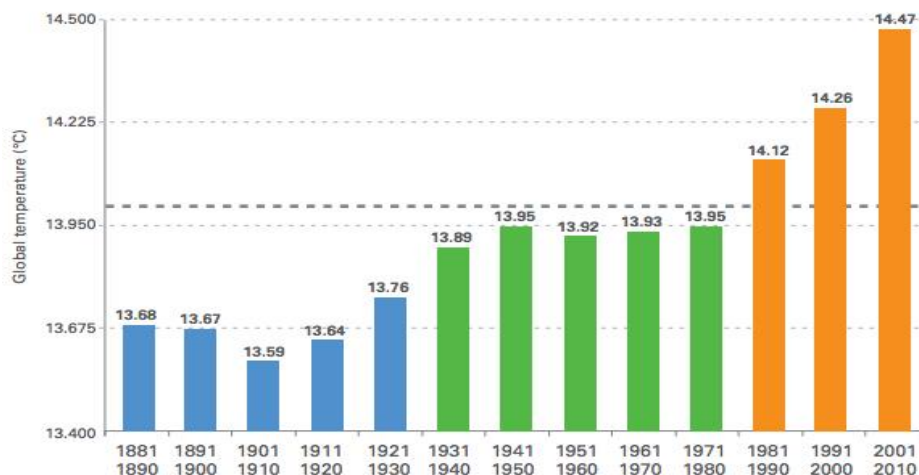


Figure 1.1. Global warming due to the emission of greenhouse gases; increases in the Earth's average temperature by 14.47% in 2010 [2].

Meanwhile that the rechargeable lithium ion batteries represent the most favorable type of batteries for portable applications due to their high energy density compared to other Alkali metals shown in Table 1.1, the selectivity of pertinent elements in the

electrode and electrolyte would be another controversial topic to determine time scale, which is one of the most critical concerns of any battery user. It may take seconds, minutes, hours or days for a battery to charge or discharge reflects to full capacity.

Table 1.1. Alkali metals' oxidation energies. Lithium has the highest potential and energy per electron [3].

Oxidation energies of Alkali Metals

Alkali Metal	$E^0_{\text{oxidation}}$ (V vs. SHE)	$\Delta G^0$ (kJ/mol)
$\text{Li} \rightarrow \text{Li}^+ + \text{e}^-$	3.04	293.3
$\text{Na} \rightarrow \text{Na}^+ + \text{e}^-$	2.71	261.5
$\text{K} \rightarrow \text{K}^+ + \text{e}^-$	2.93	282.7
$\text{Rb} \rightarrow \text{Rb}^+ + \text{e}^-$	2.98	287.5
$\text{Cs} \rightarrow \text{Cs}^+ + \text{e}^-$	3.03	292.0
$\text{Fr} \rightarrow \text{Fr}^+ + \text{e}^-$	2.90	279.8

\*potentials are vs. standard hydrogen electrode (SHE)

Commonly, a battery structure accommodates two electrodes separated by an electrically insulator porous membrane. The electrodes possess opposed chemical potentials and soluble ions in the electrolyte transition from one electrode to the other through an ionically conducting membrane. As discussed earlier, the emphasis on rechargeable/secondary batteries has arisen from two fundamental motivations; portable applications and environmentally friendly energy production. With this being claimed,

light weight batteries which allocate the higher energy density with minimized safety issues are of our interest.

Additionally, rechargeable batteries are being widely used in electric and hybrid vehicles. The attention to electric vehicles is directly associated with the oil crisis all around the world. The constantly increasing price of the fossil fuels and greenhouse emission concerns along with those sophisticated industrial steps subjected to the preparation of gasoline have necessarily led to persuading the electric vehicles. Figure 1.2 demonstrates the very rapid growth of demand on electric cars by 2040 as 35% of all new vehicle sales. Reported by Bloomberg new energy finance, last year the sale rate for electric vehicles grew by roughly 60% worldwide in which 2 million barrels of oil will be saved daily by 2023. However, this growth rate was predicted by Tesla to happen through 2020 [4]. Furthermore, batteries account for at least one third of the electric vehicle's manufacturing price. Consequently, if the price of the battery heads into the right direction, the issues that are bringing the oil production under reevaluation such as the increasing price and greenhouse effects will deteriorate.

The urge for a affordable and clean source of energy as an alternative for the fossil fuel for industrial, residential applications as well as the transportation paved the way for establishing and then advancing the renewable energy power plants such as wind and solar. Unfortunately, the fluctuation nature of these sources makes them insufficient for all time use. However, introducing the storage system could be as influential as the researches being done on promoting the efficiency and quality of solar panels or wind turbines themselves [5].

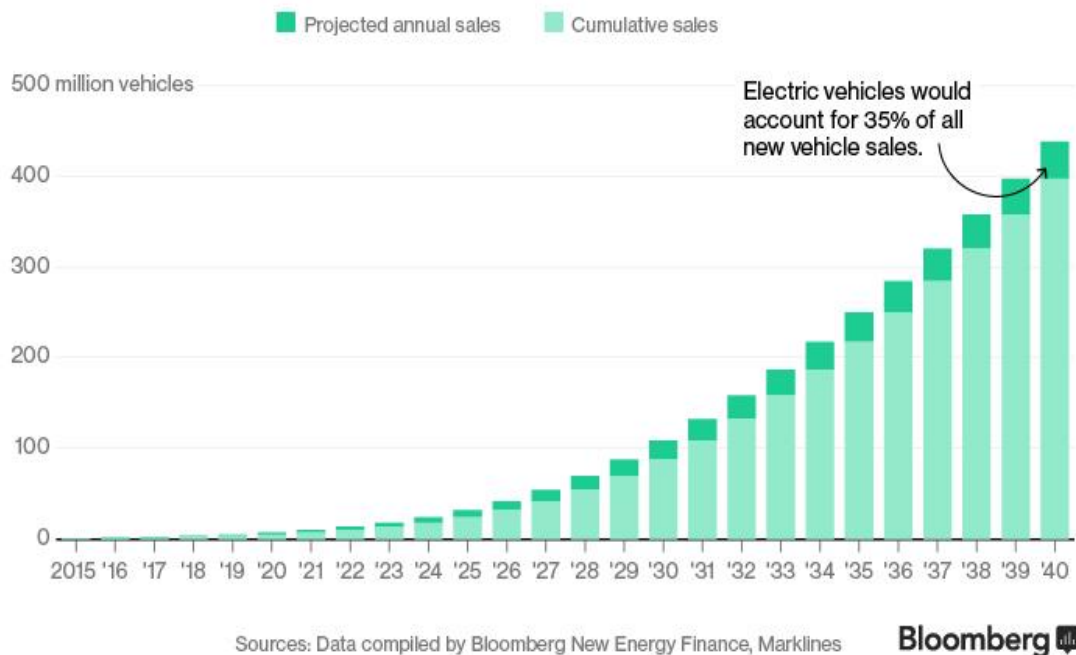


Figure 1.2. Rapid growth of demand on electric cars by 2040, accounting for 35% of all new vehicle sales [6].

Reported by the Energy storage association in 2015, availability of battery backup at the grid has several advantages compared to that of a hybrid solar/wind-gas peaker plant. While the peakers are designed to compensate the energy requirements in peak hours, they are encountered with the same arguments as are subjected to the fossil fuels since they are mostly petroleum based. In Figure 1.3, advantages of a renewable energy plant with 50 MW battery backup system over its 50 MW gas peaker counterpart is illustrated in a diagram. It is investigated that gas peakers are followed by significantly high stand by costs and emissions where in contrary, storage units of battery backup system would have zero direct emission and very negligible standby cost. Also, It will take minutes for gas peakers to dispatch where it is a matter of some seconds for battery backups to dispatch to the renewable energy based plant. Accordingly, engineering a high

energy/power density secondary battery system for several aforementioned functions can genuinely fulfill the rapid growth of global energy demands [7].

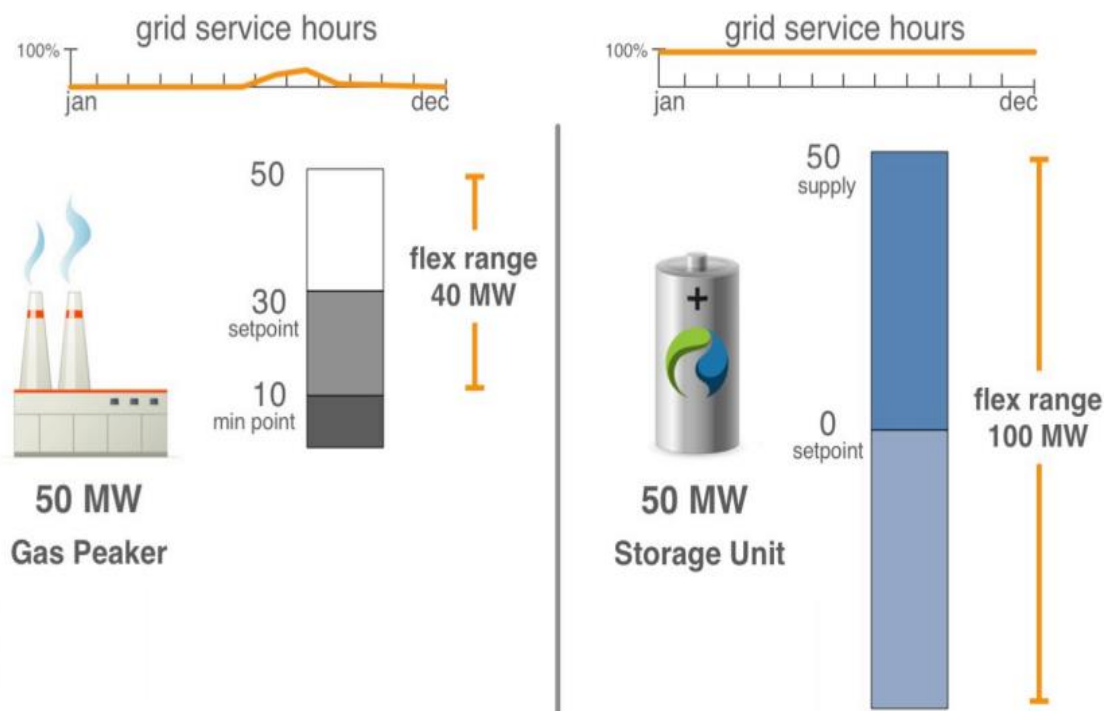


Figure 1.3. 50 MW battery vs. 50 MW gas peaker as backup systems for renewable energy based plants [8].

In 2012, 660 million of cylindrical lithium ion batteries were produced by industries. 40,000 Model S electric vehicles were produced by Tesla in 2014 which operated on 7,104 numbers of same kinds of the cell with total energy of 85 kWh. The global media reported Asia-Pacific accounts for the 43% market share of the lithium ion batteries from 2013 onward due to its demand in laptops, smart phones and tablets. Meanwhile, 34.7% of the lithium ion battery market was allocated to North America and 16% to European. This number is expected to grow since the prime target of North American is to invest more on electric or hybrid vehicles for local and global market [9].

Figure 1.4 shows the global market share of different applications of lithium ion batteries from 2005 to 2025 reported the Nikkei BP consulting Inc.

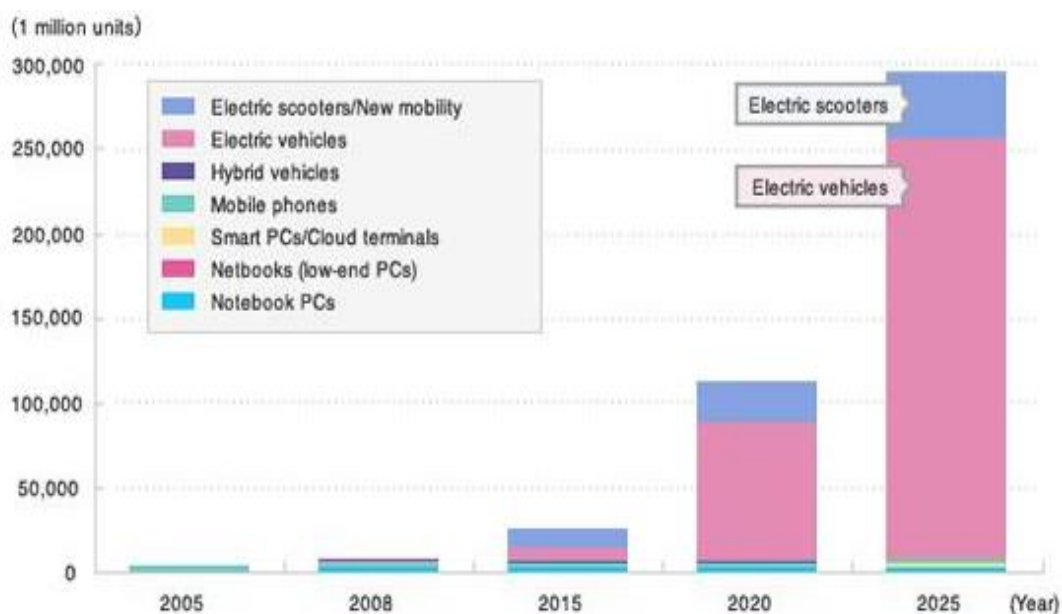


Figure 1.4. Global market share of different applications of lithium ion batteries from 2005 to 2025 reported by the Nikkei BP consulting Inc [10].

It should be mentioned that lithium ion batteries are still suffering from safety issues. While researchers are trying to achieve outstanding improvements on energy density, cycle and time durability over the years, the safety issues such as sudden explosions or fires due to over-charging, over-heating or internal short circuit are still unsolved. The electrolyte physical and chemical structures and interfacial properties of the electrodes play the most important role in the safety issues. Organic solvents having the disadvantages of leakage and ignition in higher battery cycles are prone to be replaced by gel or solid counterparts. Likely, there are several methods to modify the interfacial properties of the electrodes where the interface contacts of the electrolyte and electrodes exist. Figures 1.5 and 1.6 show the explosion of the Boeing 787-Dreamliner and Dell lithium ion batteries. [11].

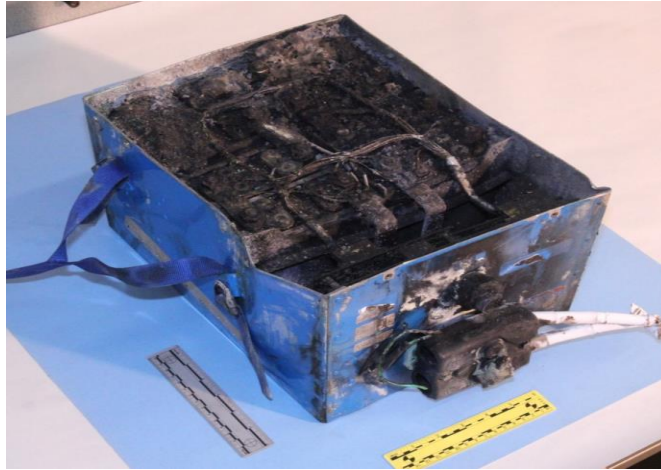


Figure 1.5. Boeing 787-Dreamliner lithium ion battery explosion [12].



Figure 1.6. Dell laptop explosion at a Japanese conference [13].

## 1.2. Literature review

Batteries have gone through a long journey since 17<sup>th</sup> century to reach the appearance and performance that they are now. Battery can be traced back to more than 2000 years ago when Parthians Empire was ruling in Middle East, reported by BBC. In 1936, when workers were conducting railway construction in Baghdad, they revealed a battery made of a jar of clay filled with vinegar where a rod of Iron covered by a copper



cylinder was dipped into it [14]. Figure 1.7 is a picture of the device taken at the Baghdad museum. This device could store 1.1 to 2 V electricity.

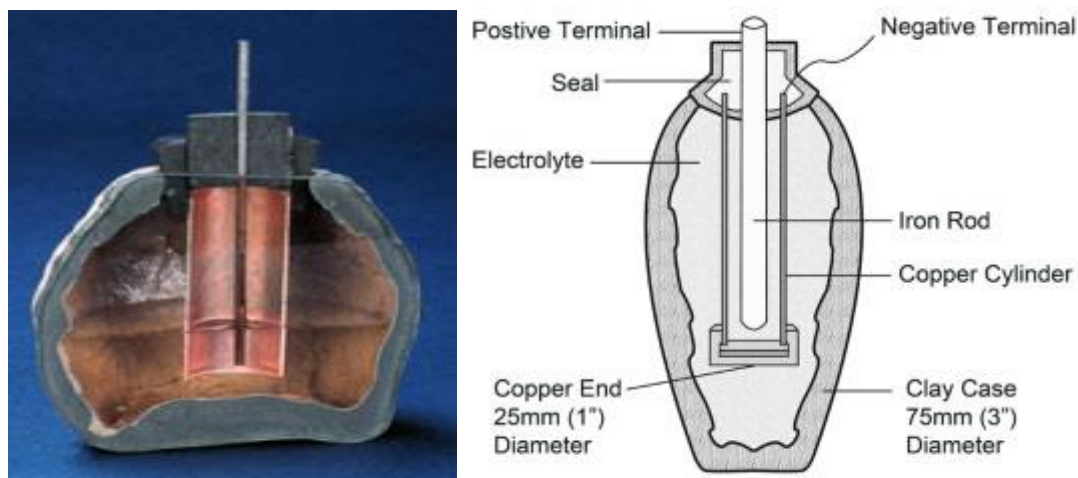


Figure 1.7. A prehistoric Parthian battery [15].

In 1749, Benjamin Franklin was the first to use the word “battery” to define a set of connected capacitors [16, 17]. Then in 1800, Alessandro Volta came up with the first functional battery called Voltaic Pile. The voltaic pile was made of zinc and copper/silver discs pairs stacked on top of each other in which a cardboard soaked in brine or a piece of cloth (current electrolyte/separator) was separating the electrode layers. Figures 1.8 & 9 show the structure of a Franklin and Volta’s battery. Volta’s battery model suffered from some fundamental pitfalls. The leakage of the electrolyte occurred due to the compression caused by the weight of the discs on the soaked cloth. This phenomenon could possibly lead to an internal short circuit. Soon after, this problem was solved by William Cruickshank by changing the device packaging from a stack of layers to a box where the layers are laid accordingly. Additionally, the short battery life in Volta’s model was influenced by Hydrogen bubble reactions at the copper electrodes

through electrolysis as well as the zinc degradation during the operation of the battery.

The latter issue was figured out by William Sturgeon by coating mercury on Zinc surface [17].

In 1836, John Frederic Daniell solved the hydrogen bubbler issue subjected to Volta's model which later managed to be the first practical battery. His battery was made of a copper bowl filled with a solution of copper sulfate in which a smaller size porous earthenware bowl filled with a zinc plate and sulfuric acid were dipped into.

The earthenware bowl acted as the separator in which only ions could pass through but solutions did not mix with each other. The device produced 1.1 V at room temperature [18]. Figure 1.10 shows the structure of the Daniel's purposed cell.

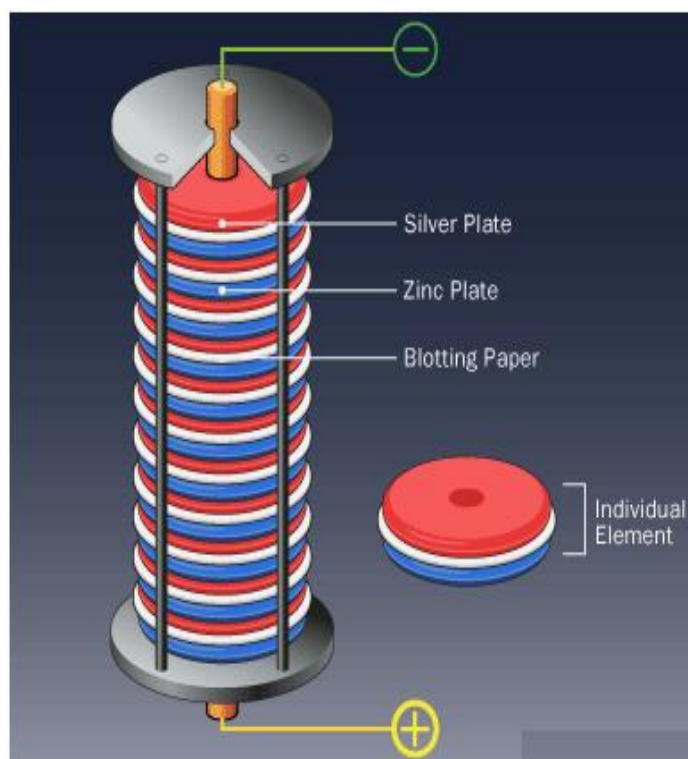


Figure 1.8. Voltaic battery, stacks of zinc and copper/silver separated by a blotting paper [19].



Figure 1.9. Franklin battery made of a series of connected capacitors [20].

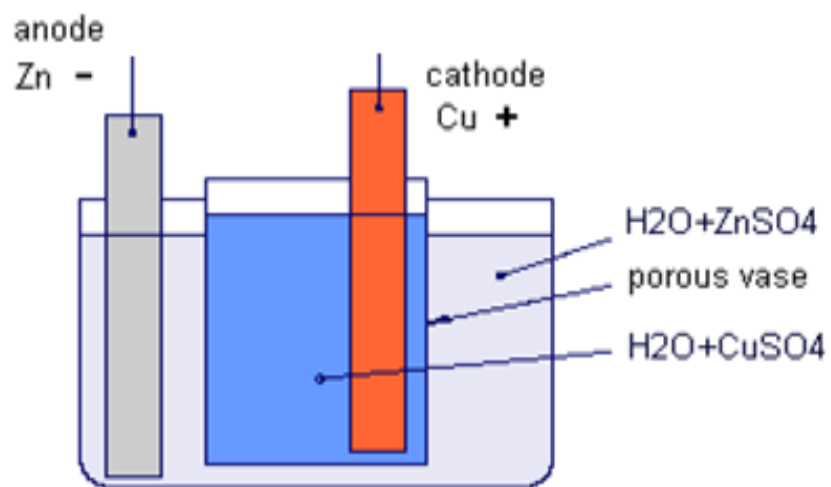


Figure 1.10. Daniel's cell as the first practical battery [21].

From 1837 until 1885, Daniel's cell was compromised and eventually improved to a safer model which lasted longer. During almost half of the 19<sup>th</sup> century, other prototypes such as Birds' cell, Gravity cell, porous pot cell, Poggendorff cell, Grove cell and Dun cell paved the way to the newer era in which the industrial primary and secondary batteries emerged [20].

In 1859, Gaston Planté developed a lead acid battery, which is an electrochemical cell and can be recharged through passing a reverse current [22]. Beside its unique rechargeable nature, lead acid batteries were too heavy to be sufficient for multiple applications except where the weight was not a detrimental factor such as in automobiles. In 1881, Camile Alphonse Faure improved the Gaston's version of lead acid battery making it more suitable for mass production. Figure 1.11. shows the device structure of a Gaston's lead acid battery [23].

In 1930, gel electrolyte was used in vacuum-tube radio's battery with no danger of electrolyte leakage and performance failure. Meanwhile, Georges Leclanché developed his modified electrode batteries in which the mixture of metal oxides and carbon accommodated a better absorption of the electrolyte as well as the ionic and electrical conductivity. The initial model consisted of manganese dioxide as cathode, zinc as anode and ammonium chloride as electrolyte solution [23]. The earliest commercial dry cell can be dated back 1896 where the improved version of Leclanché's cell was made by Carl Gassner. Carl simply replaced the liquid ammonium chloride by mixing the same solution with Gypsum plaster (plaster of Paris) with a small amount of zinc chloride additives to create a dry-like electrolyte. National Carbon Company was the first to

market this product [24]. Figures 1.12 & 13 show the overall structure of Leclanché's wet cell and Gassner's dry cell respectively.

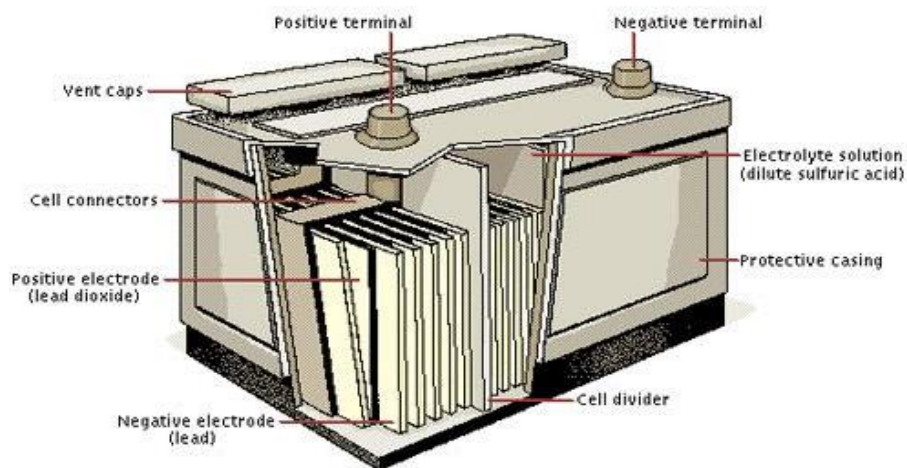


Figure 1.11. The first rechargeable Gaston's lead acid battery [25].

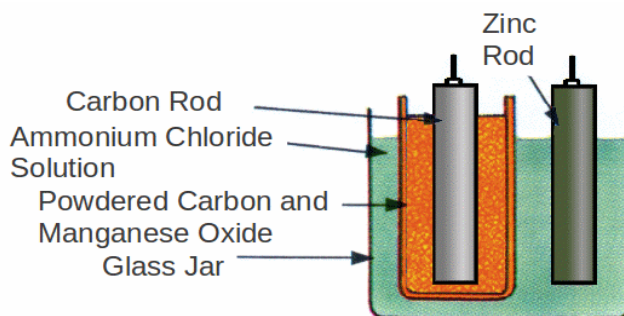


Figure 1.12. The first wet Leclanché's cell [26].

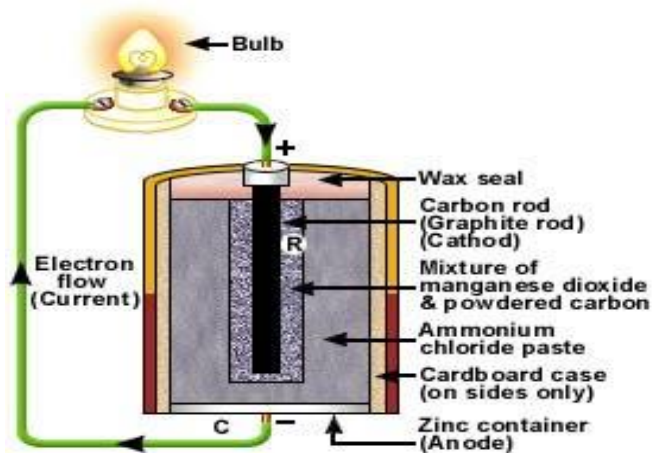


Figure 1.13. The first dry Gassner's dry cell in the market [27].

Along with the multiple developments for more reliable dry cells through the 19<sup>th</sup> century, rechargeable batteries had their own contribution yet minor. In 1899, Waldemar Jungner invented the second rechargeable battery as nickel-cadmium battery in which nickel acted as positive electrode, cadmium as negative electrode and potassium hydroxide solution as the electrolyte [28]. The battery was not commercialized until 1910 in Sweden and 1946 in United States. Nickel cadmium favored the above lead acid battery in case of the energy density and lighter weight. Thomas Edison solved some minor issues about Jungner's nickel-iron battery and commercialized it in 1903. A lighter weight version of Gaston's lead acid battery was proposed by Edison which had a great advancement for electric and diesel-electric rail vehicle applications. Then until 1959, progress on primary (non-rechargeable) cells have been made; and zinc carbon and later zinc-manganese dioxide batteries based on alkaline electrolyte entered the market [28].

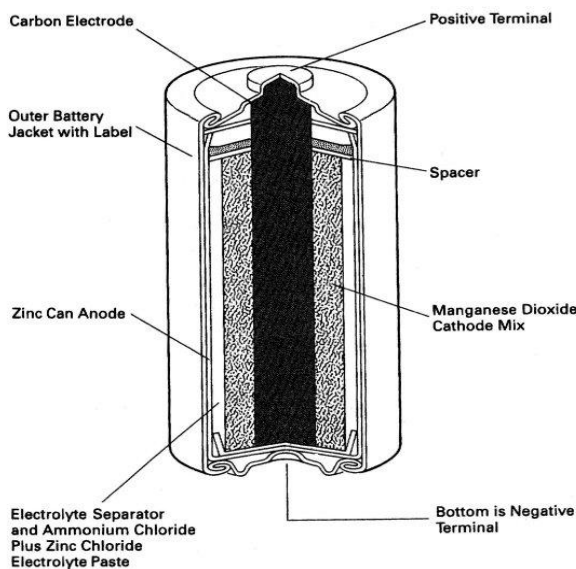


Figure 1.14. Commercialized zinc-carbon battery, an alkaline primary battery [29].

It is very challenging to extend the life of primary alkaline batteries and replace cadmium by other favorable metals due to its toxicity. Various efforts have been tried

such as using Nickel-hydrogen and nickel-metal hydrides and development of rechargeable lithium ion batteries. Theoretically, lithium as the lightest metal in periodic table and highest ratio of specific energy (energy to weight) with most positive potential is the best choice for the battery manufacturing. The first lithium ion battery hit the market in 1970 by G. N. Lewis. In 1980, John B. Goodenough used  $\text{LiCoO}_2$  as positive electrode and graphite as anode [30, 31]. In 1985, Japanese scientist Akira Yoshino managed to build the first lithium ion battery device where the battery was rechargeable with dominant advantages over its lithium battery prototypes in regard to the electrode stability over charge and discharge cycling. Later in 1991, Sony produced lithium ion batteries on commercial scales. One of the biggest challenges is to develop electrodes with the lowest degradation rate during cycling while maintaining a higher specific energy and capacity by adapting new conductive materials, and a safer electrolyte with minimized danger of leakage, ignition or explosion in higher cycles [32].

Technically, the initial lithium ion battery electrolyte consisted of an organic solvent mixed with lithium salt. In 1997, lithium polymer batteries with solid polymer/composite polymer electrolyte were introduced where the safety drawbacks of the initial prototypes were eliminated. However; the ionic conductivity of the batteries has been critical due to the lower ion transfer rate in a solid state compared to that of a liquid. In polymer lithium ion batteries, the electrolyte consists of a solid polymer matrix such as Poly(ethylene oxide) (PEO) , poly(methyl methacrylate) (PMMA) or poly(vinylidene fluoride) (PVDF) in which the lithium salt is inserted in [28].

Generally speaking, solid state lithium battery electrolyte can be classified in 3 categories: dry-solid polymer, gel-solid polymer and porous solid polymer electrolyte. In

1987, Michel Armand from Domain University built an all solid state lithium ion battery with dry-solid polymer electrolyte [33]. Later by 1990, several researchers were performing experiments on gel polymer electrolyte in which the advantages of a solid and a liquid state electrolyte have been combined. GS Yuasa, Valence and Mead were the first to commercialize this type of the electrolyte [28]. Although Fenton *et al.* first casted polymer electrolyte in 1973, its advancement has experienced three phases: solid state polymer, gel or plasticized polymer, and polymer composite [34]. Since then, the most popular polymer hosts of gel polymer electrolyte membranes for lithium ion batteries have been poly(vinylidene) (PVdF), poly(acrylonitrile) (PAN), poly(methyl methacrylate) (PMMA), poly(ethylene oxide) (PEO), polyacrylates and poly(vinylidene fluoride-hexafluoropropylene) (PVdF-HFP).

In 1978, Armand *et al.* introduced poly(ethylene oxide) (PEO) as a the first solid polymer host with a low ionic conductivity in order of  $10^{-8}$  S.cm<sup>-1</sup> at room temperature and low cycling rate (optimum performance in the first 200/300 cycles). The emergence of gel or plasticized polymer electrolyte which shares the properties of both solid and liquid electrolyte while maintaining the similar transport properties to that of liquid. Kucharski *et al.* reported the first plasticized PEO with an increased ionic conductivity of  $10^{-4}$  S.cm<sup>-1</sup> at room temperature compared to that of solid PEO using no plasticizing agent [35, 36]. The same matrix increased the salt content by 10 wt% and improved the ionic conductivity up to  $6.4 \times 10^{-3}$  S.cm<sup>-1</sup>. The most recent category of polymer electrolytes includes the polymer composites where the ceramic nano ceramic fillers such as TiO<sub>2</sub>, SiO<sub>2</sub>, and Al<sub>2</sub>O<sub>3</sub> are incorporated into the gel or plasticized polymer membranes [37].



Gel polymer electrolyte containing PVdF-HFP as the polymer host was first developed by Capiglia et al. where changing the concentration of lithium salt altered the ionic conductivity in a wide range of  $10^{-8}$  to  $10^{-2}$  S.cm<sup>-1</sup>. The maximum ionic conductivity was reported when LiBF<sub>4</sub> was used as the lithium salt; however the formation of LiF provided a very reactive environment for anode material [38]. Saika and Kumar carried out fundamental studies on PVdF-HFP based polymer electrolytes including LiClO<sub>4</sub> as lithium salt and PC-DEC as plasticizers [39].

Due to the sticky and wobbly nature of PVdF-HFP gel polymer electrolyte, researchers have been actively looking for alternative methods for preparing and casting the gel polymer films. Telcordia Technologies (former Bellcore Company) brought up a new technique for the formation of PVDF-HFP heterogeneous polymer gel electrolytes in which the liquid electrolyte was incorporated into the porous gel polymer membranes after the solvents were completely evaporated from the polymer matrix. They reached the ionic conductivity of  $2 \times 10^{-4}$  S.cm<sup>-1</sup> @ 25° C. Later, Tarascon *et al.* made further improvements on their procedure. The importance of the porous gel polymer membrane inspired many researchers for developing newer materials and procedures in which NIPS (nonsolvent-induced phase separation), EIPS (evaporation-induced phase separation/inversion) and TIPS (thermally induced phase separation) have been the most practical ones [40]. The mentioned methods deal with the choice of the solvent or nonsolvent used for the polymer host. Aravindan *et al.* selected acetone as the solvent and ethanol as the nonsolvent. Once the volatile solvents were evaporated from the polymer matrix, the pores were simply left behind. They obtained the ionic conductivity of  $1.57 \times 10^{-3}$  S.cm<sup>-1</sup>. Chiu *et al.* reached the higher ionic conductivity of  $2.93 \times 10^{-3}$  S.cm<sup>-1</sup>

and electrochemical potential up to 4.7 V (vs. Li/Li<sup>+</sup>) using a TIPS method [41].

Meanwhile, Kim *et al.* introduced the fibrous PVDF-HFP where the copolymer was prepared through electrospinning. The Kim group reached the ionic conductivity of  $1 \times 10^{-3}$  S.cm<sup>-1</sup> @ 25° C and electrochemical potential up to 4.5 V (vs. Li/Li<sup>+</sup>).

The mixed PVDF-HFP/X where X could stand for PEO, PMMA and PAN were further studied by Cui *et al.* using electrospinning. Cui *et al.* gained the high electrochemical potential of the 5.1 V (vs. Li/Li<sup>+</sup>) which represented the high stability of this type of electrolyte. They also reached a higher ionic conductivity of  $7.8 \times 10^{-3}$  S.cm<sup>-1</sup> @ 25° C [42]. Accordingly, Zhao *et al.* introduced PVDF-HFP-poly(ethylene glycol dimethacrylate) cross-linking where the flexibility and stability of the membrane were improved but the ionic conductivity was slightly lower at  $2.82 \times 10^{-3}$  S.cm<sup>-1</sup> [35].

With these being said, the gel polymer electrolyte must be able to transfer the highest rate of lithium ion with high cycling properties and can provide a specific capacity close to a theoretical graphite anode as 372 mAhg<sup>-1</sup>.

In summary, although lithium polymer electrolytes have appeared to be vastly applicable in portable electronics use, they have encountered enormous failures in commercialization due to their demanding ionic transportation mechanism. Compared to liquid electrolyte with ionic conductivity in the range of  $10^{-2}$  Scm<sup>-1</sup> in room temperature, gel and solid polymer have been fluctuating between  $10^{-2}$  to  $10^{-8}$  Scm<sup>-1</sup> depending on the structure of the electrolyte membranes. Enhancing the ion transport rate in a solid membrane is one of the most challenging approaches for developing a safer lithium ion battery with a lower fabrication cost.

### 1.3. Motivation

There is a strong need for a highly conductive gel polymer electrolyte for lithium polymer batteries to replace the current organic liquid electrolyte with leakage, high reactivity when exposed to the air and ignition issues.

### 1.4. Objectives

The objective of this work is to develop a gel polymer electrolyte with ionic conductivity of  $\sim 10^{-3} \text{ S.cm}^{-1}$  with a specific capacity close to  $372 \text{ mAh.g}^{-1}$  for that of graphite in a half cell lithium ion battery through modification of passive nano fillers to active nano fillers by pH treatment. In order to accomplish the mentioned objectives, the following tasks were performed:

- 1) Identify sufficient solvent and polymer membrane to fulfill a submicron pore sized gel polymer layer with softened polymeric chain.
- 2) Enhance hydrophilicity of the trilayer PP (polypropylene-polypropylene-polypropylene) separator for higher interfacial contact properties.
- 3) Surface modify the passive inorganic nano fillers to achieve active nano fillers with enhanced ionic properties for gel polymer electrolyte.
- 4) Select sufficient organic lithium salt and solvent for the highest conductivity and lowest preparation cost.
- 5) Fabricate gel polymer electrolyte based on optimized thickness and liquid/solid weight ratio.
- 6) Obtain 0-3 V voltage window for lithium ion battery half-cell with a specific capacity close to a  $372 \text{ mAg/h}$  capacity of graphite anode.
- 7) Study the cycling capacity for the first 40 cycles using a variety of C-rates.

## CHAPTER 2. THEORY

### 2.1. Charge and discharge principles and reactions of lithium ion batteries

Basically, a battery is an electrochemical system converting chemical energy to electricity. Batteries are generally classified into two categories of primary and secondary cells. The so called non-rechargeable batteries or primary cells possess irreversible discharge reactions where they must be disposed after one time use. The reaction of discharging in the secondary batteries (rechargeable batteries) is reversible in which the battery material can move back to their initial position after every discharge cycle.

Figure 2.1 shows a general approach on how the energy would be reserved within the atomic structure of the electrodes in the shape of traveling ions which will then be transmitted to the current collectors in the shape of moving electrons. Over the discharging process, the electrode that gives up the electron is the anode and the one that gains the electron is called cathode. The flow of ions in electrochemical cell through the charging process and electrons in external circuit through the discharging persuade the suitability of rechargeable batteries in portable uses [5].

In all battery applications, columbic efficiency of charge/discharge cycling, immunity from safety hazards, nominal voltage window, time and cycle endurance are of compelling factors. Accordingly, the weight and size of the storing system would play a critical role as it can define both time and cycle durability of the battery.

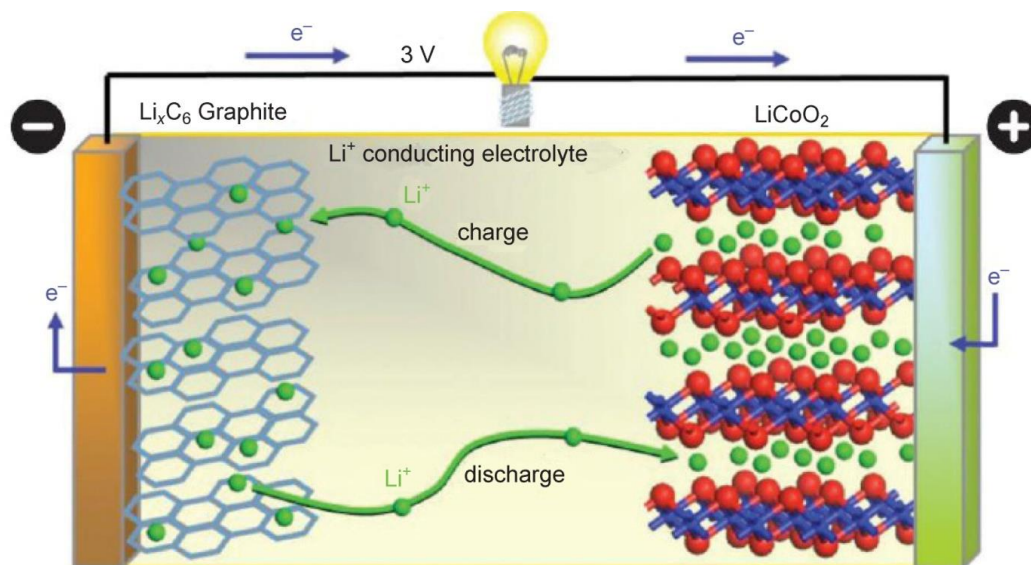


Figure 2.1. Ion/electron transfer within the atomic structure of the electrodes through electrolyte in a LiCoO<sub>2</sub>-Graphite full cell lithium ion battery.

Secondary batteries can be justified by their rechargeable nature with compared to primary batteries. However, Table. 2.1 and 2.2 emphasize the fundamental differences between these two types and some examples of each category respectively. The variables that determine the characteristic of batteries as tools for comparison between different types. In this sense, users can decide which battery type fits their demand the most. As an instance, a battery cannot possess a high specific power and energy at the same time which means manufacturers would possibly classify their battery productions accordingly [4].

The detrimental parameters would generally be:

- **C-rate:** the C-rate explains the rate at which the cell discharges respective to the maximum capacity allocated by it. Subsequently, for a battery with 1C rate, it takes one hour to discharge under the designed constant current. So likely, if the battery has the capacity of 500 AH (Ampere-Hour), the discharge current of 500 A will be needed to fully discharge this battery in one hour at 1C rate. A 5C for

this battery means it will take  $60 \text{ min}/5=12 \text{ min}$  for the battery to discharge at the constant current rate of 2500 A.

- **State of Charge (SOC %):** The ratio of the current capacity of a battery to its maximum capacity in percentage.
- **Depth of Discharge (DOD %):** The ratio of the discharged capacity of a battery to its maximum capacity in percentage in which the DOD= 80% is called a deep discharge.
- **Open Circuit Voltage (V):** The battery voltage when there is no load connected which thoroughly depends on the kind of the potential of the materials used in battery fabrication.
- **Cut Off voltage (V):** This parameter represents the lowest allowed level of voltage for a battery to be discharged at.
- **Specific Capacity (AH/kg for a known C-rate):** The specific capacity is calculated by multiplication of constant discharge current (A) by the time it takes to discharge (H) and then dividing it to the weight of the active material within anode electrode (kg). It is mainly considered for a cycle where the state of charge reaches to cut off voltage from a fully charged level.
- **Specific energy (Wh/kg):** The specific capacity is calculated by multiplication of discharge power (W) by the time it takes to discharge (H) and then dividing it to the weight of the active material within anode electrode (kg).
- **Specific power (W/kg):** This parameter defines the ratio of the available power to the weight of the active material within anode electrode (kg).

- **Internal (bulk) Resistance ( $\Omega_{Rb}$ ):** The resistance inside the battery; mostly influenced by the materials incorporated into electrode/separator/electrolyte structure and also depends whether the charge or discharge cycle is taking place.

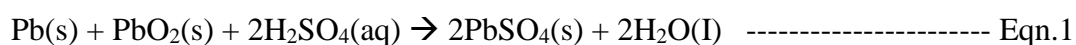
Table 2.1. fundamental differences between primary and secondary batteries [43] .

<b>Type</b>	<b>Cost Effectiveness</b>	<b>Performance</b>	<b>Safety and Environmental Effects</b>	<b>Applications</b>
<b>Primary</b>	Cheaper individual batteries but must be replaced after every discharge	Higher energy density, initial voltage and capacity	Producing toxic wastes and minerals and mostly non-recyclable such as non-rechargeable AA,AAA,C and D cells	Watches, electronic keys, flashlights, toys, military devices in combat
<b>Secondary</b>	Rechargeable	Lower energy density, initial voltage and capacity compensated by its significantly longer life time in terms of energy supplement	Almost non-hazardous wastes, but heavy metals such as Lithium and Lead must be recycled.	Telecommunication, portable electronics, electric vehicles, starting and ignition of cars, emergency power supplies and etc

Table 2.2. examples of primary and secondary batteries' types [43].

<b>Primary</b>	<b>Secondary</b>
Alkaline battery	Flow battery
Zinc-carbon battery	Fuel cell
Bunsen cell	Lead acid battery
Atomic battery	Lithium-air battery
Molten salt battery	Lithium-ion battery
Chromic acid cell	Nickel-cadmium battery
Nickel oxyhydroxide battery	Polymer based battery
Clark battery	Sodium ion battery
Mercury battery	Magnesium-ion battery
Weston battery	Molten salt battery
Zamboni battery	Silicon-air battery
Daniell cell	Sodium/Lithium-sulfur battery

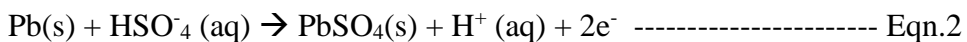
The most popular types for rechargeable batteries among all the types listed in Table 2.2 are lithium based, nickel based and lead based batteries in which the contribution of each is roughly explained in Figure 2.2 based on their specific power vs. specific energy. The longest history goes to lead based batteries in which lead is used as anode material and lead dioxide and sulfuric acid as cathode and electrolyte in the charged state respectively [44]. The total reaction of discharging a lead acid battery can be written as Eqn. 1;





Splitting Eqn.1 into reactions happening at each electrode, Eqn. 2&3 will be gained;

At the anode side:



At the cathode side:

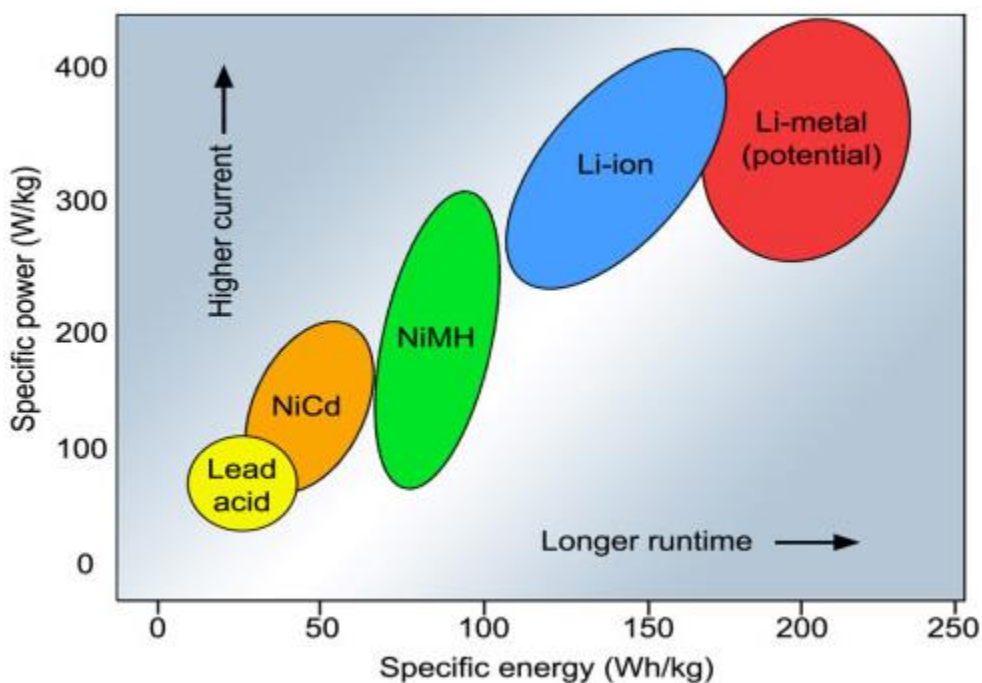


Figure 2.2. Contribution of secondary batteries based on their specific power vs. specific energy [45].

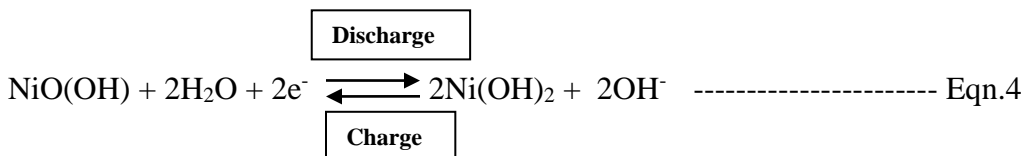
As can be seen in equations 1,2&3, both anode and cathode become  $\text{PbSO}_4$ ; lead(II) sulfate while the electrolyte gives up a great amount of the dissolved  $\text{HSO}_4^-$ ; sulfuric acid and mainly develop into the  $\text{H}_2\text{O}$ ; water. The diffusion of  $\text{H}^+$  from anode to cathode in discharging process and reversely from cathode to anode in charging process takes place when at the same time as shown in Eqn. 2, at every discharge cycle 2 free electrons will be sent to the external circuit which will be then inserted into the positive

electrode; cathode when the cell is being charged. The drawbacks of the aqueous nature of the reactions in lead acid battery make them insufficient for use in winter due to the risk of easily reaching to the freezing point. Also, the accumulated  $O_2$  and  $H_2$  gasses or water vapor in high temperatures can cause an internal ignition, push the top case of the battery to fly off and spray the acid and other hazardous materials such as lead into the environment. However, it has been reported that since 2003, Environment Defense and Ecology Center of Ann Arbor at Michigan announced the “Getting the lead out” bulletin through the media as lead compounds are severely toxic and can potentially originate several health issues such as kidney and brain damage and learning impairments in children in long term. While the recycling of lead acid battery has gone through a successful trend from 2009 onwards with 99% of all lead acid batteries being recycled, the use of this type of electrochemical cells as bulk or robust applications such as in vehicles’ starter and stationary backup system at power plants are still promising [46]. As a summery, some of advantage and disadvantages of lead acid batteries are mentioned in Table 2.3.

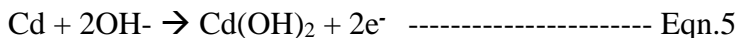
Table 2.3. some of advantages and disadvantages of lead acid batteries [46].

<b>Advantages</b>	<b>Disadvantages</b>
Cheap to manufacture	Low specific energy
Low self discharge (lowest vs. Ni and Li based secondary batteries)	Slow charge/discharge
High specific power	Short life cycle unless it’s stored in charged condition with limited deep cycling
Good low temperature and excellent high temperature performance	Environmentally hazardous

After lead acid batteries dominance in market has fallen due to its safety reasons, Nickel based batteries started developing in which Nickel-Cadmium, Nickel-Iron, Nickel-Hydrogen, Nickel-Zinc and Ni-metal hydride were of the most popular prototypes. In all Nickel based batteries the reaction at the positive plate; cathode would be as illustrated in Eqn. 4:



According to the Eqn. 4, the nickel (III) oxide-hydroxide NiO(OH) which has been the active material of the cathode will produce Ni(OH)<sub>2</sub> as a product of the discharge. Likely, during the charge or preferably recharge process the NiO(OH) will be reconstituting in the presence of the water again. Just like lead acid battery, Nickel based battery's reactions happen in a aqueous environment as well. Considering Cd or any of the aforementioned combinations as negative plate, the electrolyte for nickel based batteries are alkaline based solutions such as potassium hydroxide (KOH) [47]. If the anode is designed to be cadmium, the reaction during discharge process would be as expressed in Eqn. 5:



Unlike the lead acid battery, the alkaline electrolyte is not consumed in recharge reaction. This will lead to the further stability of the cell since the specific gravity of the electrolyte does not determine the state of the charge. Additionally, Nickel based batteries could fulfill a more stable and robust structure with compared to that of lead based ones with specific application in spacecraft and memory devices. Also, the lighter weight,

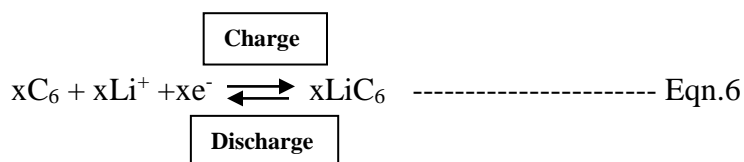
higher energy density and deeper charge/discharge tolerance of the nickel provide several advantages over its lead acid counterpart. However, their higher cost, higher self-discharge rate, environmental issues of recycling the heavy metals and over current phenomena during charging process affected by its very low temperature coefficient which leads to extreme fall in resistant in higher temperatures have been the logics behind reevaluating this type of batteries. As a summery, some of advantage and disadvantages of Nickel based batteries are mentioned in Table 2.4.

Table 2.4. some of advantages and disadvantages of Nickel based batteries [44].

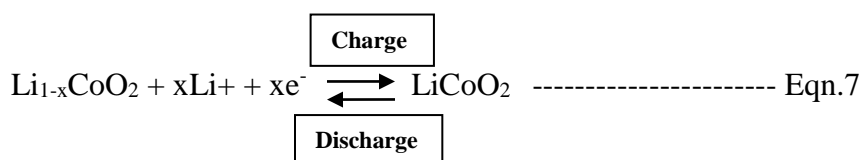
<b>Advantages</b>	<b>Disadvantages</b>
Fast charge/discharge rate with minimum stress compared to other secondary batteries	Memory effect; the sudden drop in voltage at the start point of recharging cycle
Mechanically robust structure	In case of Ni-Cd, Cd is a toxic heavy metal; needs regulations to be followed for disposal
Excellent low temperature performance	High rate of self discharge if the charged battery is left unused
NiCd is one of the cheapest in terms of price per cycle	Typically low open circuit voltage (below 2 V) ; compromising of anode materials needed
Long life, can be stored in discharged state.	Low specific energy

With these issues being argued, one more time the industry paved its way to develop a new generation of rechargeable batteries at which the toxicity of the materials, low energy density, temperature dependence and self-discharge properties do not affect the cell improvements as much. Rechargeable lithium based batteries were introduced into the market where the most promising prototype was released in 1991 by Asahi Kasaei and Sony as the first commercial lithium ion battery. Unlike the other two types of secondary batteries that were mentioned above, lithium ion batteries provide a non

aqueous environment where the electrolyte is an aprotic mixture of lithium salt and respective solutions. It should be mentioned that, the incorporation of other transition metal oxide such as cobalt into the structure of the lithium cathode material makes distinction between a lithium battery and a lithium ion battery [48]. Primarily, carbon compounds are used as negative electrode for lithium ion batteries where lithium salt dissolved in organic solution acts as electrolyte and lithiated metal oxide as cathode. Depending on the selection of the electrolyte and electrode materials, the energy density, voltage, charge capacity, life and cycle durability of the battery alter dramatically. Considering  $\text{LiCoO}_2$  (lithium cobalt dioxide) as cathode and  $\text{C}_6$  (graphite) as anode for a full cell lithium ion battery, the reactions happening at each plate will be as demonstrated in Eqn. 6 & 7. The reaction taking place at negative plate; anode side:



The reaction taking place at positive plate; cathode side:



The non-aqueous electrolyte in lithium ion batteries can electrolyze the larger potentials. Under this circumstance, there will be a wider open circuit voltage window. Also, lithium as the most positive metal in the periodic table with lightest weight can serve the highest potential and specific energy density. Charging this type of cell is performed through two steps of constant current and constant voltage charge where the

constant voltage is applied to the cell after the cell is charged to its maximum voltage using constant current. The cell will then stay at the same maximum voltage while the constant current gradually falls to the cut off current which is typically 3% of the designed constant current [49]. Table 2.5 summarizes the advantage and disadvantages of lithium ion batteries.

Table 2.5. some of advantages and disadvantages of lithium ion batteries [50].

<b>Advantages</b>	<b>Disadvantages</b>
High specific energy per unit weight	Thermal runaway if the cell is stressed ; protection circuit needed
High specific capacity , cycle durability and columbic efficiency	Degrades at very high or very low temperature; best performance in 0-45° C
Long life cycling with minimum degradation ; easy maintenance	Expensive manufacturing process; almost 40% NiCd
Very low self discharge rate	Transportation of large quantities are subjected to the safety regulations
More simple charge and discharge process compared to other secondary batteries	Electrode and electrolyte material are changing on a continuous trend

The energy density of lithium ion batteries is higher than nickel cadmium and lead acid batteries due to lithium outstanding electrochemical properties and lowest potential among other alkali metals [51]. Figure 2.3 shows the volumetric energy density of different rechargeable battery prototypes vs. specific energy density.

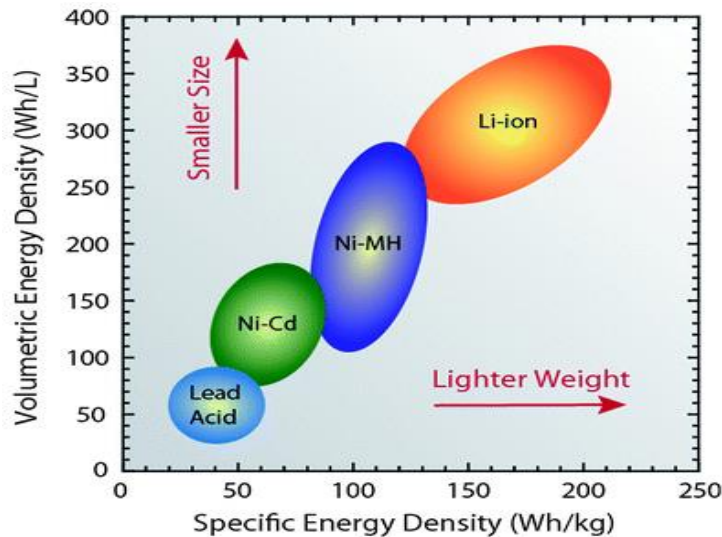


Figure 2.3. Volumetric energy density of different rechargeable battery prototypes vs. specific energy density [52].

The electrochemical characteristics of electrode components are extremely dependent on chemical and physical features such as the size of the atoms or compounds within the structure, surface area, and ionic number [53].

According to Figure 2.4, ions stored at the negative plate will be used during discharge process and the cell needs to be charged again. Charging occurs in exactly opposite direction where ions travel from positive electrode to negative electrode. Basically, the negative electrode or anode goes through the oxidation process and releases the electrons towards the external circuit when discharging. Whereas in cathode, positive electrode undergoes the reduction process during charging by an external voltage source. In a secondary battery, anode is the negative electrode during discharge and positive electrode when charging occurs.

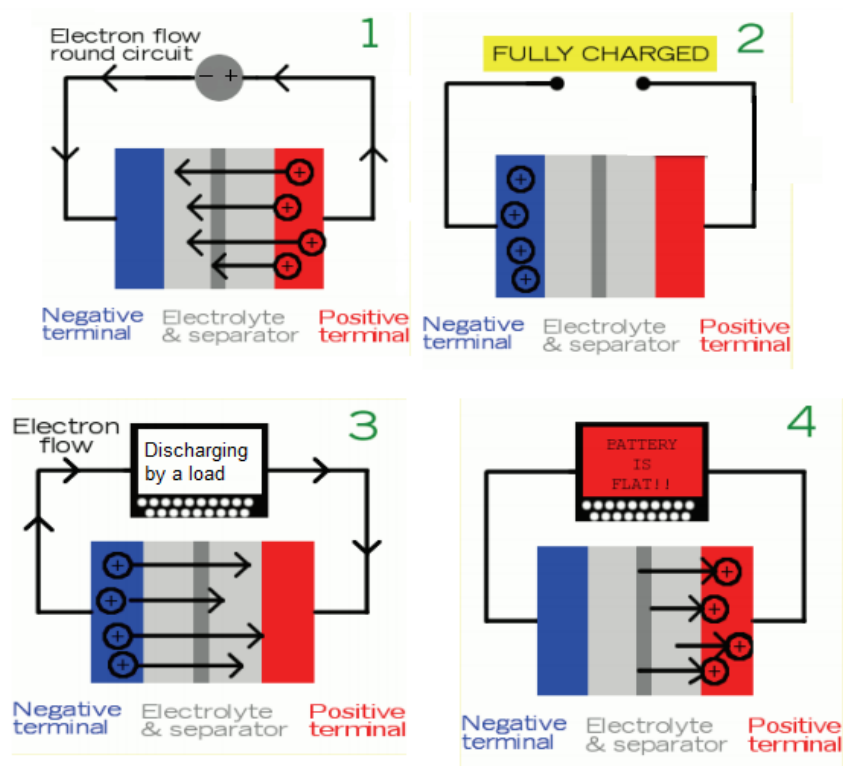


Figure 2.4. Charge (1&2) and discharge (3&4) diagram of a rechargeable battery [54].

The highest electric energy transferred by the chemicals within the battery is strongly relied on the free energy changes ( $\Delta G$ ) regarding to the electrochemical couples in a reaction. The most favorable case is when through the discharge process, all the energy transforms to the electric energy. However, there will still be losses at electrode sides where the load current flows towards the electrodes and polarization occurs. Consequently, two types of losses can take place: (i) activation polarization that deals with the reactions happening at the electrode interfaces; (ii) concentration polarization that deals with the differences in reactants and products concentration at the interfaces or even through the bulk caused by chemical transfer. Lithium ion batteries similar to other types of electrochemical cells are made of active materials, conductive ceramic fillers, electrode materials binder, and cyclic improving additives, etc.



Bulk or internal impedance of the battery is another critical issue that directly affects the battery performance by causing a voltage drop through the battery cycling and is usually regarded as  $R_b$  (bulk resistance) or IR (Internal resistance) loss. Under this circumstance, the electrolyte ionic conductivity must be high enough to overcome the effect of IR polarization. Acceptable ranges of ionic conductivities of several electrolyte types for lithium ion batteries are listed in Table 2.6 [53].

Table 2.6. Ionic conductivity ranges of several electrolyte types of lithium ion batteries [53].

Electrolyte system	Ionic conductivity, $\Omega^{-1} \text{ cm}^{-1}$
Aqueous electrolytes	$1-5 \times 10^{-1}$
Molten salt	$\sim 10^{-1}$
Inorganic electrolytes	$2 \times 10^{-2}-10^{-1}$
Organic electrolytes	$10^{-3}-10^{-2}$
Polymer electrolytes	$10^{-7}-10^{-3}$
Inorganic solid electrolytes	$10^{-8}-10^{-5}$

In addition to the ionic conductivity rates, there are some more critical rules to be considered when designing a lithium ion battery to minimize side reactions:

- The chemical dependability of electrolyte, salt and solvent components to stay immune from direct reaction with electrode materials.
- The reaction rate at the electrode sides needs be relatively fast so that the applied current/voltage does not damage cell components. Presence of porous electrode structure is sufficient, since the local density of the current does not exceed at one particular are of the cell.
- The transport rate of reactants and products must be equal to avoid the buildup of excessive mass concentration. The selections of the right electrode, porous

electrolyte/separator structure, and effective concentration of active material in electrolyte and optimized thickness of electrolyte are important.

- The selection of current collectors and the quality of the interface they form with electrode materials are extremely important since they are associated with the polarization and internal impedance.
- It is required to save as much as reaction products at the electrodes sides other than the bulk to facilitate the reversible reactions in a rechargeable lithium ion battery.

Two exceptional electrochemical properties of lithium with high oxidation potential and light weight show that either lithium ion or lithium metal can be used to fabricate batteries. The current popularity of lithium ion instead of lithium metal batteries is the more immune nature of lithium ion batteries due to unfavorable reactions. Before the emergence of lithium ion batteries, lithium metal batteries were vastly utilized where lithium metal itself was used as the anode electrode. The lithium metal and liquid electrolyte suffer from safety issues in higher cycles when they are in contact with each other due to the decomposition of organic liquid electrolyte and lithium dendrites formation on metal electrode which could lead to internal short circuit and later explosion and decrease in columbic efficiency of the cell [51, 53]. The lithium dendrite or solid electrolyte interface (SEI) growth, if not controlled, will form a barrier between the electrode and electrolyte which will accordingly affect the ions transfer properties. Figure 2.5 shows the finger like lithium dendrite formation on lithium anode surface.

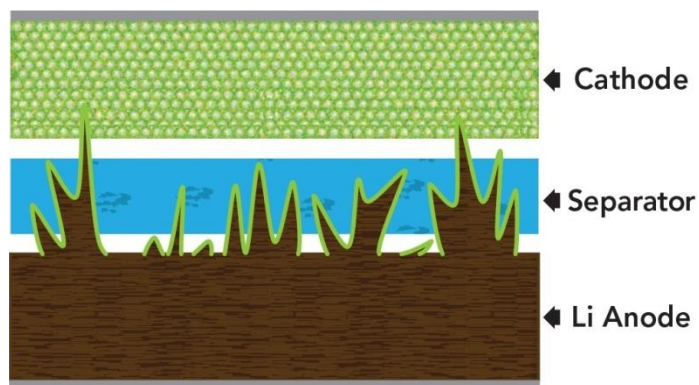


Figure 2.5. Finger like lithium dendrites growth on lithium anode surface with possibility of internal short circuit in higher cycles [55].

Two approaches have been used to tackle this issue. One is to replace lithium metal electrode with lithium ion electrode. Through this replacement, lithium ions bond with carbon at one side and metal oxides at the other side acting as electrode couple which will lower the accumulation of the lithium metal-decomposed liquid electrolyte compounds at the electrode. Figure 2.6 illustrates a typical schematic of lithium ion transport through the electrolyte.

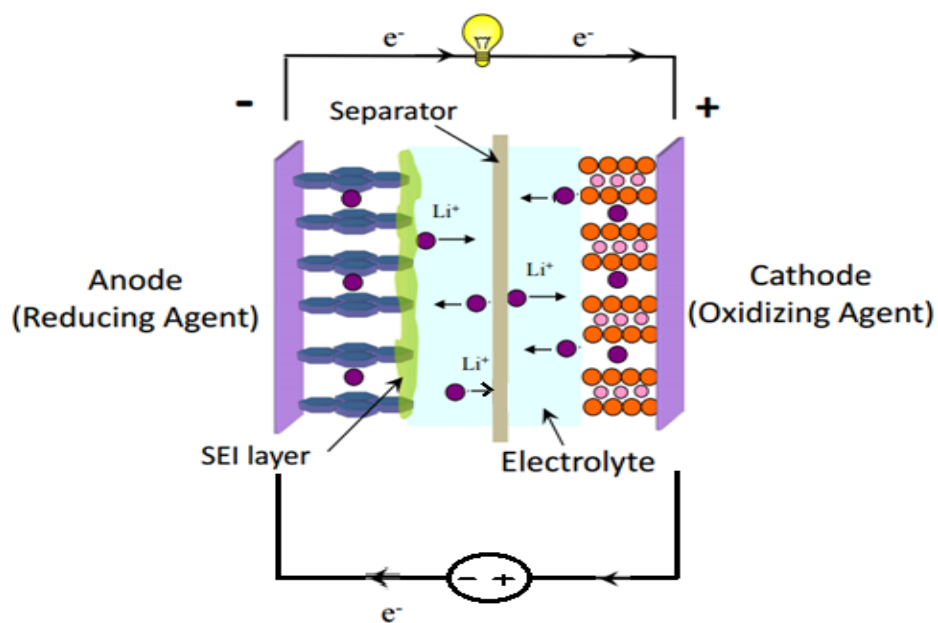
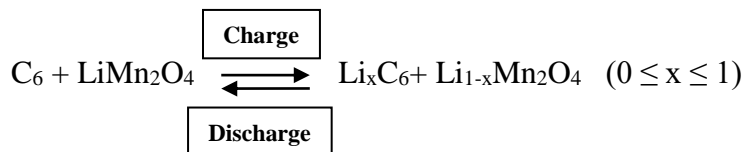


Figure 2.6. Schematic of lithium ion battery charge and discharge process [56].

If graphite is considered as anode material and  $\text{LiMn}_2\text{O}_4$  as cathode material, reactions happening at anode and cathode sides could be illustrated as:



The second approach is to replace the organic liquid electrolyte with a solid membrane with high mechanical stability that minimizes the growth pace of the SEL layer. A thin membrane of polymer electrolyte would be a desirable candidate in such a case. Figure 2.7 shows how a polymer electrolyte membrane can play the role of a separator and electrolyte at the same time.

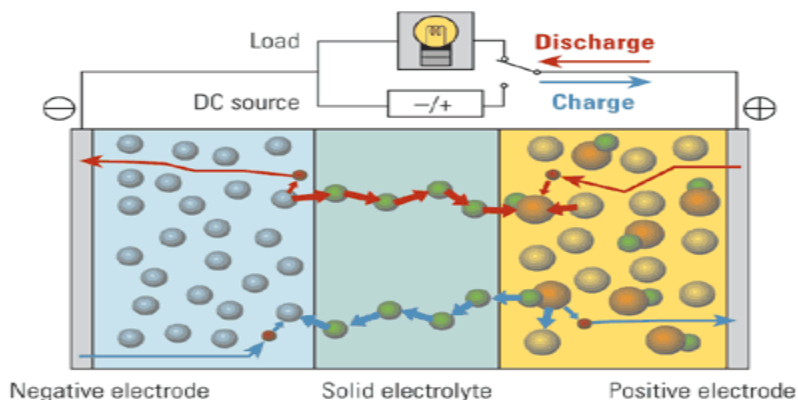


Figure 2.7. polymer electrolyte in a lithium ion battery where electrolyte and separator are both in one membrane [57].

### 2.1.1. Basic components of lithium ion batteries

Three main parts of a battery are anode, electrolyte and cathode. Cathode is the positive electrode where the external electron from the electrical circuit is inserted into and reduction happens during discharging, whereas in the negative electrode, anode gives

up the electron where earlier reduced at anode surface during charging process. The separation between the electrodes happens through an ionic conductor porous structure called electrolyte [51, 58].

Carbonated materials such as graphite, carbon nanotubes, graphene, and super carbon have been among the most preferred selections for anode material in lithium ion batteries [2, 59]. Lithium has a density of 0.534g/cc and high specific capacity of 3.86Ah/g. The intercalation of the lithium with electrode material directly depends upon the number of lithium that can be accommodated into the structure. As for graphite, one lithium can be intercalated by 6 carbon atoms with the theoretical specific capacity of 372 mAhg<sup>-1</sup>. Low price, excellent structural properties of graphite, small redox potential and availability of carbonated anode material make them suitable for commercial applications.

Crystalline metal oxides have been frequently used as cathode materials. The cathode material must be capable of accommodating and releasing lithium ions into its structure during the recharge process. To achieve higher cycles, a stable crystal structure is needed for a number of material decomposition/composition processes. This stability becomes more challenging when targeting the maximum amount of lithium being extracted from cathode material through charging process [60]. Figure 2.8 contains some alternatives for anode/cathode electrodes based on their potential vs. specific capacity relationship. Table 2.7 & 2.8 show the comparison of electrochemical properties of various types of anode and cathode materials, respectively. Table 2.9 lists compatible anode and cathode electrodes for lithium ion batteries.

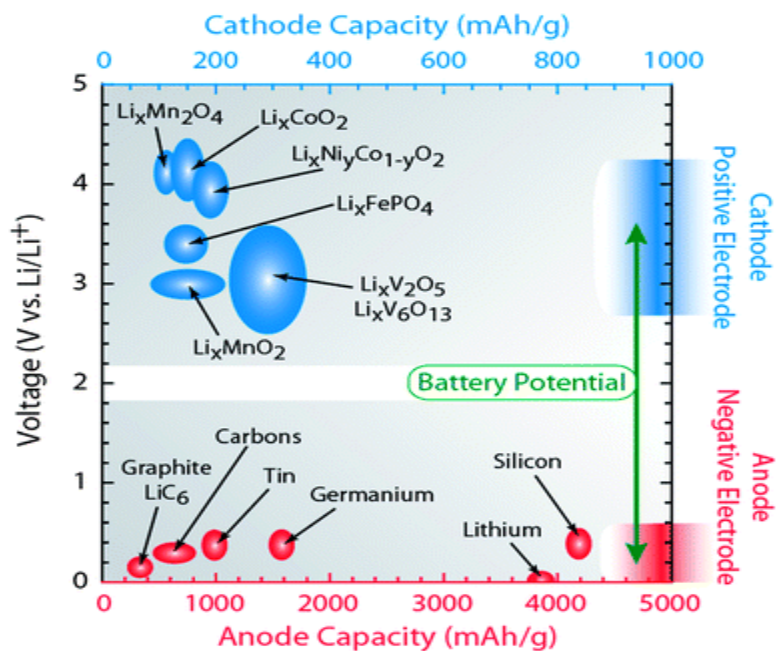


Figure 2.8. Potential vs. capacity of alternative anode/cathode material for lithium ion batteries [59].

Table 2.7. Electrochemical comparison of anode materials for lithium ion batteries [53].

Material	Voltage range vs. lithium, V	Theoretical specific capacity, Ah/g	Comments
Li metal	0.0	3.86	Lithium foils readily available Generally brittle foils, difficult to handle
LiAl	0.3	0.8	
Li <sub>0.5</sub> C <sub>6</sub> (coke)	0.0–1.3	0.185	Used for lithium-ion cells
LiC <sub>6</sub> (MCMB (b), or graphite)	0.0–0.1	0.372 (a)	
LiWO <sub>2</sub>	0.3–1.4	0.12	Possible use for lithium-ion cells
LiMoO <sub>2</sub>	0.8–1.4	0.199	
LiTiS <sub>2</sub>	1.5–2.7	0.266	

(a) Based on weight of carbon only.

(b) Mesocarbon microbeads.

Table 2.8. Electrochemical comparison of cathode materials for lithium ion batteries [53].

Material	Average voltage vs. lithium,* V	Lithium/mole	Practical specific energy, † Wh/kg	Comments
MoS <sub>2</sub>	1.7	0.8	230	Naturally occurring
MnO <sub>2</sub>	3.0	0.7	650	Inexpensive
TiS <sub>2</sub>	2.1	1	550	Costly
NbSe <sub>3</sub>	1.9	3	450	Costly
LiCoO <sub>2</sub>	3.7	0.5	500	Good for lithium-ion system
LiNiO <sub>2</sub>	3.5	0.5	480	Good for lithium-ion system
LiMn <sub>2</sub> O <sub>4</sub>	3.8	0.8	450	Good for lithium-ion system, safe
VO <sub>x</sub>	2.3	2.5	300	Good for SPE system
V <sub>2</sub> O <sub>5</sub>	2.8	1.2	490	Good for SPE system
SO <sub>2</sub>	3.1	0.33	220	Good for pulse power applications, safety issues
CuCl <sub>2</sub>	3.3	1	660	Good for pulse power applications, safety issues
Polyacetylene	3.2	1	340	For polymer electrodes
Polypyrrole	3.2	1	280	For polymer electrodes

\* At low rates.

† Based on cathode material only and average voltage and lithium/mole as shown.

Table 2.9. Compatible anode and cathode electrodes for lithium ion batteries [61].

Application	Positive electrode	Negative electrode	Remarks
High energy	LiCoO <sub>2</sub> (L)	Graphite, Si, SnO <sub>x</sub> ,	M = Mn, Al, Cr named "LMO"
	LiNi <sub>x</sub> Co <sub>y</sub> Mn <sub>1-y-z</sub> O <sub>2</sub> (L)	CoO <sub>x</sub> , FeO <sub>x</sub> , CuO <sub>x</sub> ,	
	LiMn <sub>2</sub> O <sub>4</sub> (S)	NiO <sub>x</sub> , etc.	
High power	LiMn <sub>2-y</sub> Al <sub>y</sub> O <sub>4+z</sub> (S)	hard carbon,	named "NMC" "LFP//LTO" cell
	LiNi <sub>x</sub> Mn <sub>y</sub> Co <sub>2-y</sub> O <sub>2</sub> (L)	graphite	
	LiFePO <sub>4</sub> (O)	Li <sub>4</sub> Ti <sub>5</sub> O <sub>12</sub> (S)	
Long cycle life	LiMn <sub>2-y</sub> Al <sub>y</sub> O <sub>4+z</sub> (S)	Graphite	named "LFP"
	LiFePO <sub>4</sub> (O)	Li <sub>4</sub> Ti <sub>5</sub> O <sub>12</sub> (S)	
	LiFe <sub>1-y</sub> Mn <sub>y</sub> PO <sub>4</sub> (O)	Li <sub>4</sub> Ti <sub>5</sub> O <sub>12</sub> (S)	

Electrolyte has two significant roles in a battery: separating electrodes and passing the lithium ions between the electrodes. Electrolyte is a critical factor to define the electrochemical properties of the battery such as charge and discharge capacity,

current density and safety. Basically, electrolyte regardless of the type of materials need to have the following properties:

- Acceptable electrochemical window: minimized side reactions at electrode/electrolyte contact surface.
- High ionic conductor: low bulk resistance making it easier for lithium ions to pass through.
- High mechanical stability: safety and easier manufacturing.
- Non-toxicity: minimized reactivity in environment and electrode material.
- Cost effectiveness
- Safety: minimized lithium dendrites layer formation and high flash point.
- High thermal stability: controlled vapor release in over heating conditions and freezing point for cold environments.
- 

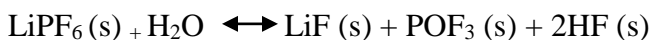
There are two physical states for electrolyte material: liquid electrolyte and solid electrolyte. Liquid electrolyte is mostly an organic alkyl carbonate mixed with lithium salts such as:  $\text{LiClO}_4$ ,  $\text{LiBF}_6$ ,  $\text{LiPF}_6$ , and  $\text{Li}[\text{PF}_3(\text{C}_2\text{CF}_5)_3]$ . Initially,  $\text{LiClO}_4$  was the most common lithium salt which was later replaced by  $\text{LiPF}_6$  because of some hazards caused by highly oxidative  $\text{ClO}_4^-$  ions.  $\text{LiPF}_6$  possessed improved safety and ionic conductivity but exhibited decreased thermal stability since it decomposes at temperatures as low as  $80^\circ\text{C}$ . The decomposition of  $\text{LiPF}_6$  happens through following equation.



The  $\text{PF}_5 (\text{g})$  is a very reactive Lewis acid gas and can react with the solvent and increase the pressure within the cell.  $\text{LiPF}_6$  is highly reactive to  $\text{H}_2\text{O}$  and needs a moisture free



environment for maintenance. The following equation expresses the reactivity of  $\text{LiPF}_6$  to  $\text{H}_2\text{O}$  molecules:



All the experimental procedures to fabricate a lithium ion battery using  $\text{LiPF}_6$  as salt need an inert environment to minimize the side reactions caused by moisture.  $\text{LiF}$  is a non-conductive salt which will deposit on electrodes and contribute to the EIS layer formation. Table 2.10 shows various types of typical lithium salts, commonly used solvents and conductivities in  $-40^\circ$  to  $80^\circ$  C range temperature for lithium ion batteries.

Table 2.10. Types of typical lithium salts, commonly used solvents and conductivities in  $-40^\circ$  to  $80^\circ$  C range temperature for lithium ion batteries [61].

Salt	Solvents	Solvent, vol %	Conductivities at $^\circ\text{C}$ , mS/cm						
			-40	-20	-0	20	40	60	80
$\text{LiPF}_6$	EC/PC	50/50	0.23	1.36	3.45	6.56	10.34	14.63	19.35
	2-MeTHF/EC/PC	75/12.5/12.5	2.43	4.46	6.75	9.24	11.64	14.00	16.22
	EC/DMC	33/67	—	1.2	5.0	10.0	—	20.0	—
	EC/DME	33/67	—	8.0	13.6	18.1	25.2	31.9	—
	EC/DEC	33/67	—	2.5	4.4	7.0	9.7	12.9	—
$\text{LiBF}_4$	EC/PC	50/50	0.19	1.11	2.41	4.25	6.27	8.51	10.79
	2-MeTHF/EC/PC	75/12.5/12.5	—	0.38	0.92	1.64	2.53	3.43	4.29
	EC/DMC	33/67	—	1.3	3.5	4.9	6.4	7.8	—
	EC/DEC	33/67	—	1.2	2.0	3.2	4.4	5.5	—
	EC/DME	33/67	—	6.7	9.9	12.7	15.6	18.5	—
$\text{LiClO}_4$	EC/DMC	33/67	—	1.0	5.7	8.4	11.0	13.9	—
	EC/DEC	33/67	—	1.8	3.5	5.2	7.3	9.4	—
	EC/DME	33/67	—	8.4	12.3	16.5	20.3	23.9	—

The solvents need to be abundant and have promising solubility for  $\text{LiPF}_6$  as the most common lithium salt. They should also be non-aqueous because  $\text{LiPF}_6$  reacts with

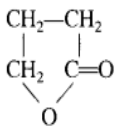
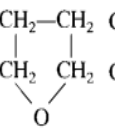
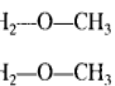
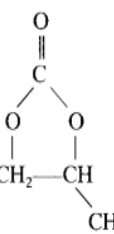
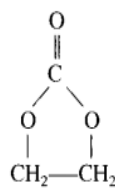
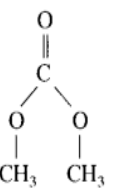
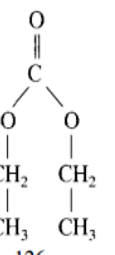
water. Organic alkyl carbonates offer suitable performance and safety [62, 63]. The most commonly used carbonate solvents are a mixture of these solvents: ethylene carbonate (EC), ethyl methyl carbonate (EMC), dimethyl carbonate (DMC), diethyl carbonate (DEC), ethyl methyl carbonate (EMC) or propylene carbonate (PC). Large flash point and dielectric constant are two significant features of an applicable solvent.

The selection of ethylene carbonate (EC) or propylene carbonate (PC) based solvents is associated with the chemical structure of their functional groups. Figure 2.9 shows that PC has an additional methyl group. The PC based electrolyte possesses high conductivity and more importantly low viscosity properties. However, PC cannot be used as a single solvent because the decomposition of PC exfoliates the graphite. EC can establish a reliable SEI that further saves the graphite from extra reactions with electrolyte components. Since graphite is a conventional anode material for lithium ion batteries, the EC groups will always be present in lithium ion battery liquid electrolyte solvent. Table 2.11 summarizes lithium salt aprotic solvents, chemical structures and essential characteristics.



Figure 2.9. chemical structure of PC (a) with an additional methyl group vs. EC (b).

Table 2.11. Lithium salt aprotic solvents, chemical structure and essential characteristics [52].

Characteristic	$\gamma$ -BL	THF	1,2-DME	PC	EC	DMC	DEC
Structural formula							
Boiling point, °C	202–204	65–67	85	240	248	91	126
Melting point, °C	-43	-109	-58	-49	-39–40	4.6	-43
Density, g/cm <sup>3</sup>	1.13	0.887	0.866	1.198	1.322	1.071	0.98
Viscosity at 25°C, cP	1.75	0.48	0.455	2.5	1.86	0.59	0.75
					(at 40°C)		
Dielectric constant at 20°C	39	7.75	7.20	64.4	89.6	3.12	2.82
					(at 40°C)		
Molecular weight	86.09	72.10	90.12	102.0	88.1	90.08	118.13
Typical H <sub>2</sub> O content, ppm	<10	<10	<10	<10	<10	<10	<10
Electrolytic conductivity at 20°C, 1M LiAsF <sub>6</sub> , mS/cm	10.62	12.87	19.40	5.28	6.97	11.00 (1.9 M)	5.00 (1.5 M)

Solid electrolytes have two main categories: (I) inorganic solid electrolyte such as ceramics, and (II) solid/gel organic polymer electrolyte that can be doped with inorganic fillers and shape the composite polymer electrolyte. Organic polymer electrolyte can also be dry or gel form. In dry polymer electrolyte, the host solid polymer has the role of the solvent in which the Li salts are incorporated in the solid polymer and the ionic conduction occurs by hopping of ions through a porous solid structure. Table 2.6 contains ionic conductivity ranges of different types of lithium battery electrolyte including solid polymers.

Polymer gels own a closer conduction mechanism to liquid electrolyte than solid electrolytes. While gel polymer electrolyte normally possesses a lower ionic conductivity of around  $10^{-3} \text{ Scm}^{-1}$  at room temperature compared to  $10^{-2} \text{ Scm}^{-1}$  for liquid electrolytes, gel polymers have improved safety and flexibility. Basically, a more porous or

amorphous the structure of a gel/solid polymer leads to a better accommodation and movement of the lithium salt and a higher ionic conductivity [64].

## 2.2. All solid state lithium ion batteries

Lithium ion batteries containing polymeric or ceramic components as electrolyte are called all solid state lithium ion batteries. Polymeric electrolyte or more commonly said lithium polymer batteries offer enhanced safety due to the reduced reaction of lithium with polymer electrolyte and resilience in their design since they possess higher form factor. In a lithium polymer battery, depending on the state of the electrolyte whether solid or gel, there may or may not be a separator required. In fully solid batteries where the need for organic solvents is eliminated, a thin layer is formed by coating cathode and electrolyte onto a current collector. This process is known as cathode lamination. Later, the lithium foil is placed onto the laminate cathode. These components allocate a highly porous structure to maximize the surface area between the layers and reduce the internal/bulk resistance as well.

Earlier, Poly-(ethylene oxide) (PEO) was one of the most well-known solid polymer matrixes used for Li ion batteries. However, the PEO-Li Salt system has a low ionic conductivity of  $10^{-6} \text{ S.cm}^{-1}$  at room temperature. This makes it impossible for portable applications [65]. Later, newer polymer electrolytes such as copolymers of PEO, plasticized PEO and gel electrolytes were introduced, which offered higher ionic conductivities.

Meanwhile, poly-(vinylidene fluoride) (PVDF), a chemically inert polymer, has attracted significant attention among all other polymer electrolyte hosts. The dielectric constant of PVDF is 8.4 due to the intense electron withdrawal of  $-\text{C}-\text{F}-$  functional

groups. The large dielectric constant facilitates the ionization of Li salts and consequently there are more dissociated ions and more charge carriers. Recently, the poly (vinylidene fluoride-hexafluoropropylene) (PVdF-HFP) copolymer has attracted attentions from many researchers. HFP provides an amorphous phase in which the liquid electrolyte is trapped and ion movements happen through the more porous structure. Also, the PVdF phase due to its crystalline properties contributes to mechanical stability [65-71]. Other popular polymer hosts used in gel polymer electrolytes are poly(methylmethacrylate) (PMMA) and Polyacrylonitrile (PAN) that have considerable drawbacks compared to PVDF such as poor ionic conductivity at room temperature and compatibility with limited choice of Li salts [72, 73]. Figure 2.10 shows the segmental motion of lithium ion batteries in a PEO electrolyte membrane.

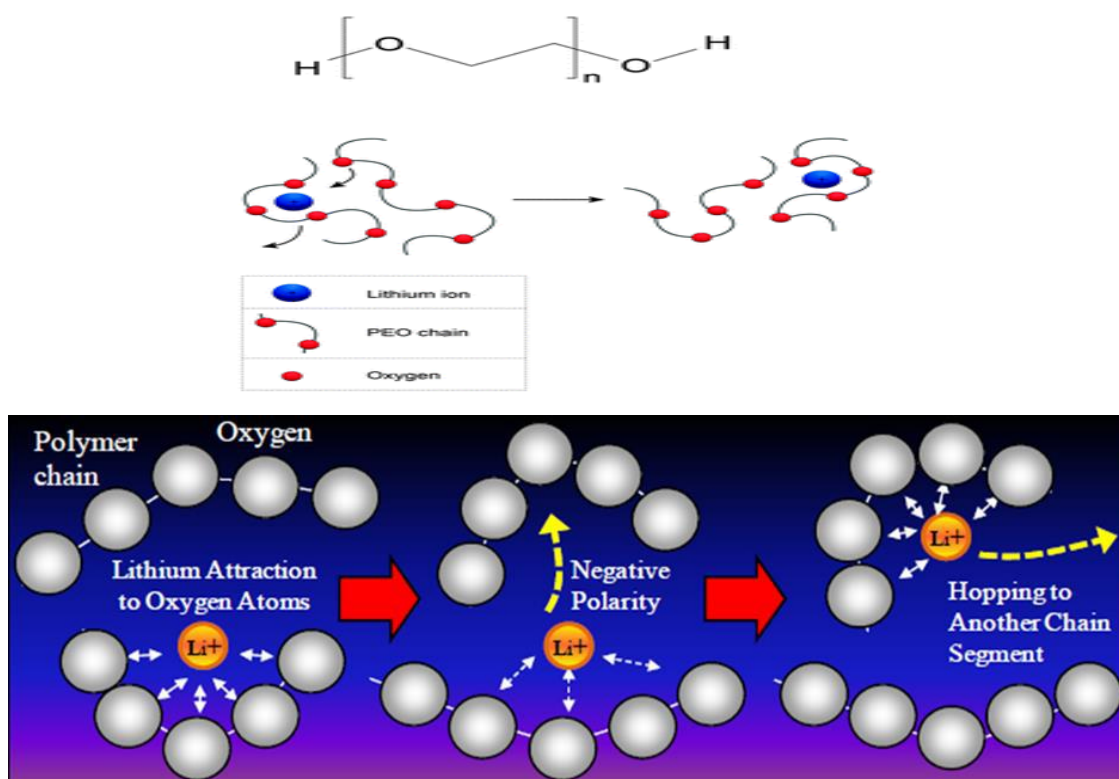


Figure 2.10. segmental motion of lithium ion batteries in a PEO electrolyte membrane [74].

While the most critical drawback of polymer electrolytes still remains to be its lower ionic conductivity in normal ambient temperature, use of polymer electrolyte in lithium ion batteries provides several other significant advantages. Improved safety, higher flexibility, lower fabrication cost due to the elimination of separator, reduced side reactions such as SEI layer formation, and acceptable energy and power density are among the most critical ones. This deficiency can be tackled by enhancing the amorphous regions in a host polymer matrix. There are alternative methods to approach the amorphousness enhancement such as adding plasticizers to make the polymer chains smoother and create easier paths for ion movement. Another alternative is to add nano-sized ceramic fillers to produce a composite gel/solid polymer electrolyte where the Lewis acid-base reactions assist the lithium ions dissociation rate. Polymer electrolytes can be divided into three categories: (1) solid polymer electrolyte, (2) gel polymer electrolyte and (3) composite solid/gel polymer electrolyte.

In general, the solid polymer electrolyte (SPE) can act as the separator, solvent and salt host all together. Gel polymer electrolyte (GPE) is based on a semi-liquid, semi-solid structure where the liquid electrolyte is incorporated into a solid polymer matrix and unlike the SPE the host polymer itself does not contribute into the conductivity or dissolving the ions. Composite gel/solid polymer electrolyte has the same features, but in which the nano-sized ceramic fillers are dispersed into the polymer matrix.

Ceramic based electrolyte follows a slightly different mechanism in regard to the ionic conductivity. The ionic conductivity in an all solid ceramic membrane happens by the movement of lithium ion through the point defects or grain boundaries. Increasing the temperature in such a membrane will improve the conductivity which makes them

sufficient for high temperature use. Ceramics can be in crystalline, amorphous or partially amorphous structure. The lower degree of crystallinity is preferred for higher ionic conductivity. Ceramic electrolytes in general are divided into three types: (1) sulfides, (2) oxides, and (3) phosphates. Regarding ceramic electrolytes, the conductive additive plays a critical role. For example, addition of Zirconium into the lithium-phosphate ( $\text{Li-PO}_4$ ) leads to higher ionic conductivity than those of germanium or titanium based phosphates. Pervoskite based electrolytes ( $\text{(La,Li)TiO}_3$ ) have enjoyed the highest conductivity among other oxides. Figure 2.11 highlights some transport paths of lithium ions in a ceramic membrane through the point defects and grain boundaries.

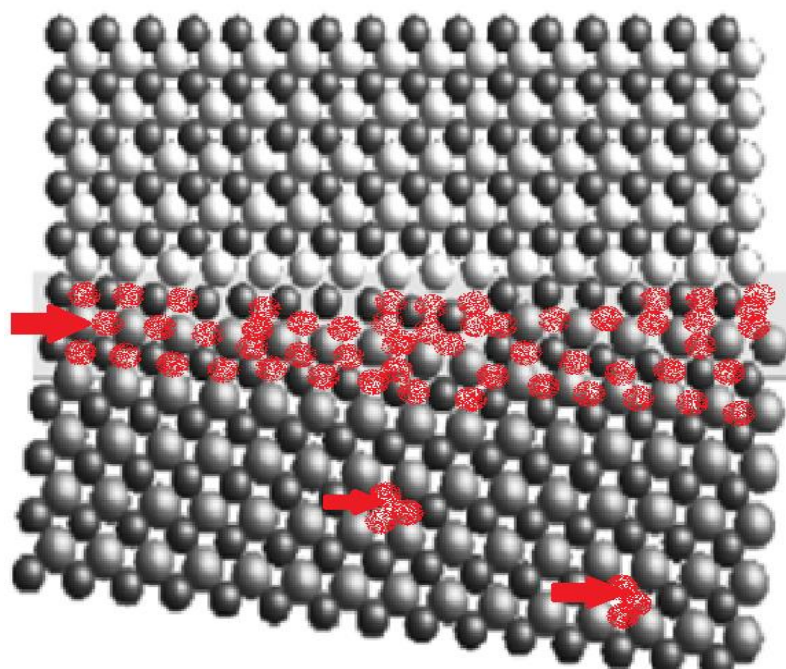


Figure 2.11. some transport paths of lithium ions in a ceramic membrane through the point defects and grain boundaries [75].

All solid state batteries own high thermal durability, low self-discharge rate which leads to longer life time (5 to 10 years in average), high energy densities, and high

mechanical stability over different environmental circumstances (pressure, temperature, etc). However, their limited ionic conductivity (or high bulk resistance) at room temperature make them insufficient for portable applications. In addition, the volume change due to insertion and extraction of lithium ions into and out of the electrode material causes mechanical stresses at high charge or discharge rates. However, many of these issues have been solved using gel polymer electrolytes which share common features with both solid and liquid electrolyte in certain ways [53].

### **2.2.1. Solid polymer electrolyte**

SPE is determined to be a solid solution enriched with lithium conducting ions. Under an electric field, the ions will transport through the solid interface. In a solid polymer electrolyte, the solid polymer host is made of polymer backbones which are connected to ionizing functional groups through covalent bonding. The interaction between donor groups in polymer with lithium cations leads to dissociation of lithium salt where the transport of dissociated lithium ions is done through hopping of ions. This mechanism can be determined in Figure 2.10 where the negatively charged oxygen groups on PEO chains are interacting with positively charged Lithium cations. More pores in a solid membrane corresponds to more amorphous structure, decreased activation energies and packing density in order to transport the lithium ions [76].

To improve the dissociation rate of lithium salts in a polymer host, salt must possess relatively low lattice energy. The host polymer must have a high dielectric constant ( $\epsilon$ ). As an example, the ionic conductivity of polyethylene oxide (PEO) is considerably larger than polypropylene oxide (PPO) where PPO has lower  $\epsilon$ . Additionally, concentration of the salt itself must be optimized; otherwise it will affect



the mobility of the free lithium ions. The equation below shows the mobility of the ions is related to the final ionic conductivity, where  $n$  is the density of the free ions,  $e$  is the electric charge and  $\mu$  is the ion mobility.

$$\sigma = ne\mu$$

As can be seen in Figure 2.10, the ionic conduction in a polymer membrane is based on the segmental motion of the polymer in which the lithium ions flow through the polymer chains. Accordingly, the temperature dependence of this conduction mechanism is based on the glass transition temperature (GTT) of the polymer host, where GTT must be the lowest value possible providing a more elastic system [53]. With increasing the temperature, some local micro/nano-sized vacancies are produced by expansion of the membrane which lets the ionic species to hop through. In the PEO solid polymer membranes, above 60 °C, the melting temperature and crystallization point is surpassed where the highest ionic conductivity of around  $10^{-4} \text{ Scm}^{-1}$  is achieved [51].

Figure 2.10 also illustrates that the mobility of the lithium ion is associated with the movement of the PEO polymeric chains. Followed by the polymer chain motion, lithium ions can hop between the neighboring chains which is also known as intrachain and interchain. The dynamic properties of the polymeric chains turn to be the focus of the conduction enhancement.

### **2.2.2. Gel polymer electrolyte**

The low ionic conductivity of solid polymer electrolyte paves the way to introduce the gel polymer electrolyte where similar features of solid and liquid conduction mechanisms should be considered. Adding plasticizer to the polymer membranes has been the most practical method to provide the smoother polymeric chains

for lithium ions segmental motion. The diffusive motion of the lithium ions within the semi-solid, semi-liquid structure of gel electrolytes is highly considered to follow the ionic conduction mechanism of liquid electrolyte. Table 2.1 contains the typical range of ionic conductivities for several states of electrolyte materials. The gel polymer electrolyte enjoys a higher conductivity at room temperature than solid polymer electrolyte. Gel polymer electrolyte offers some significant advantages that overcome the drawbacks of fully solid and fully liquid electrolytes, although the mechanical stability of GPE is still controversial. Addition of nano-sized ceramic fillers can considerably improve the mechanical properties of GPE which helps develop a new class of GPEs, composite gel polymer electrolyte (CPE).

Ionic conductivity of gel polymer membranes is associated with low molecular weight solvent diffusive motion within the polymer membrane. Reported by Daka and Kumar, ionic conductivity of gel polymer electrolyte can be as high as  $10^{-3} \text{ S cm}^{-1}$ . In the equation of  $\sigma = ne\mu$ ,  $n$  is the density of the free ions and  $\mu$  as the ion mobility are mainly responsible for the ionic conductivity. In GPE, the ion aggregation can possibly cause a block on the ions motion path if the concentration of the salt is not optimized. In addition, the other drawback shall be unfavorable re-association of the ions which again will lower the conductivity [76].

Technically, a gel polymer membrane is a modified version of a solid polymer membrane in which the polymer electrolyte is plasticized. Plasticizing the polymer matrix will decrease the regional viscosity and facilitate the transfer of the mobile lithium ions through smoother paths. This class of polymer electrolytes typically allocates a trapped solution mixture of lithium salt and aprotic solvents inside a solid polymer membrane

[51]. Presently, there are four main host polymer matrixes for gel polymer electrolytes [29, 40, 76]: (1) Polyethylene oxide (PEO), (2) Polymethyl methacrylate (PMMA) or Polymethacrylate/Poly(vinyl chloride) (PMMA/PVC), (3) Polyacrylonitrile (PAN), and (4) Polyvinylidene fluoride (PVDF) or Polyvinylidene fluoride-co-hexafluoropropylene (PVDF-HFP). Initially, PEO-based polymer electrolytes attracted a lot of attention.

Considerable efforts have been done regarding its development as it was the first polymer system that was casted as thin film relatively easy. As shown in Figure 2.10, the conduction mechanism in PEO-based gel polymer electrolyte depends on the interaction between lithium ions and oxygen atom in an ether functional group. As reported by Song *et al.*, low ionic conductivity in PEO was attributed to its high degree of crystallinity which can vary in a range of  $10^{-8}$  S  $\text{cm}^{-1}$  to  $10^{-4}$  S  $\text{cm}^{-1}$  when the temperature altered between 40°C and 100°C [64, 77].

A few years later, PAN was introduced as a replacing polymer host material due to its flame retardant and poor thermal resistance features. Feuliade *et al.* investigated that PAN-based gel polymer electrolytes enjoy the higher ionic conductivity of between  $10^{-5}$  to  $10^{-3}$  S  $\text{cm}^{-1}$ . The major drawback for PAN is the internal resistance of the cell which increases through higher cycles. It was observed that if combining PAN with PEO, it will enhance the ionic conductivity, mechanical resilience and also interfacial properties of PAN-based gel polymer electrolyte [78].

Among other host polymers, PMMA-based polymer matrixes became popular since they possess increased interfacial stability and lower preparation cost because of the smoother synthesis process. However its limited mechanical durability is still an issue.

Copolymerization of PMMA with other polymer matrixes could significantly recover the

mentioned disadvantage. Accordingly, reported by Ramesh *et al.*, copolymerization of PMMA with PVC had the best performance in case of ionic conductivity and life time of the lithium ion battery using PMMA-based gel polymer electrolytes.

Poly-(vinylidene fluoride) (PVDF), a chemically inert polymer, has attracted significant attention among all other polymer electrolyte hosts. The dielectric constant of PVDF is equal to 8.4 due to the intense electron withdrawal of  $-C-F-$  functional groups. The large dielectric constant facilitates the ionization of Li salts and consequently there will be more dissociated ions and more charge carriers. Recently, the poly (vinylidene fluoride-hexafluoropropylene) (PVdF-HFP) copolymer has impressed many researchers. HFP provides a dominated amorphous phase in which the liquid electrolyte is trapped and ion movements happens through the more porous structure versus the dominated crystalline structure of PVdF. Also, the PVdF phase due to its crystalline properties contributes to the mechanical stability [65-71]. Amorphous PVDF-HFP based gel polymers own higher ionic conductivity at room temperature and compatibility with more choice of Li salts [79, 80].

### **2.2.3. Composite solid/gel polymer electrolyte**

The mechanical stability of the polymer matrix can be enhanced by adding nano fillers such as  $Al_2O_3$ ,  $TiO_2$ , and  $SiO_2$ . The addition of metal oxide ceramic fillers have been one of the most significant ways to advance the electrochemical, interfacial and morphological properties of gel polymer electrolytes [81]. Ceramic-ion matrix does not directly contribute to the ionic conductivity mechanism, however majority of the ion transfer still happen through the softened polymeric chains. Croce *et al.* investigated that

the enhancement of the conductivity is mostly affected by the reduction of polymer crystallinity level because of the presence of fillers [82].

A variety of the fillers have been studied in recent years. The macro and micro fillers initially were purposed but the unfavorable toughness and stiffness of them paved its way to change the nature of the fillers to nano dimension. The idea has been based on uniformly dispersed nano filler content into the matrix of the polymer host where the filler's agglomeration was minimized. The ceramic particles in particular, depending on their size and volume fraction minimize the space where the electrodes are exposed to polymer components such as -O and -OH containing groups and consequently decreases the electrolyte/electrode interface passivation development. The fact that nano sized ceramic particles can provide more surface area gives rise to the better performance of nano particles compared to those of micro or macro [51].

#### **2.2.4. Ionic liquid-based gel polymer electrolyte**

In recent years, room temperature ionic liquids (RTIL) salts which own low temperature melting points were extensively explored. They can function as an electrolyte in a battery cell where the solvents do not contain any volatile components, making them safe and nonflammable. Typical room temperature ionic liquids based on ammonium salts own a very limited vapor pressure and broad (usually > 4V) electrochemical window. RTILs based on ammonium cations are not direct options for primary or secondary batteries, however it is feasible to diffuse a  $[\text{Li}^+][\text{X}^-]$  lithium salt system in  $[\text{A}^+][\text{X}^-]$  ionic liquid system or even a two-cation system  $[\text{Li}^+]_m[\text{A}^+]_n[\text{X}^-]_{m+n}$ . Ionic liquid's structure is comprised of ions, interacting with other ions with heavy

coulombic forces. In addition, RTILs have the tendency for super-cooling and very low viscosity [83].

Ionic conductivity of RTILs falls between  $0.1\text{--}18\text{ mScm}^{-1}$  where the mobility of ions within a gel polymer matrix relies on the solubility of ionic liquid with a polymer component. Aprotic ILs offered a higher mobility and concentration of the ions than Zwitter and protic ionic liquids as well as enhanced electrochemical properties. This class of ILs is consisted of small anions and large cations.

Some IRTILs contain imide as anion and quaternary ammonium as cation. The quaternary ammonium cations contain bis(trifluoromethanesulfonyl)imide (TFSI), trimethylpropylammonium (TMPA), 1-ethyl-3-methylimidazolium (EMI), N-methyl-N-propylpiperidinium (PP13) and N-methyl-N-propylpyridinium (P13). They are capable of stabilizing unfavorable reductions occurring on the lithium metal through solid electrolyte interface (SEI) related reactions [84]. Fung *et al.* concluded that adding  $\text{C}_6\text{H}_5\text{SO}_2\text{Cl}$  will help stabilizing the surfacial reactions taking place on the electrodes [85]. RTILs enhanced electrochemical performance of lithium ion polymer batteries by incorporating useful ions [51]. Figure 2.10 shows an ionic liquid enriched polymer host where the polymeric chains are modified using cross linking agents.

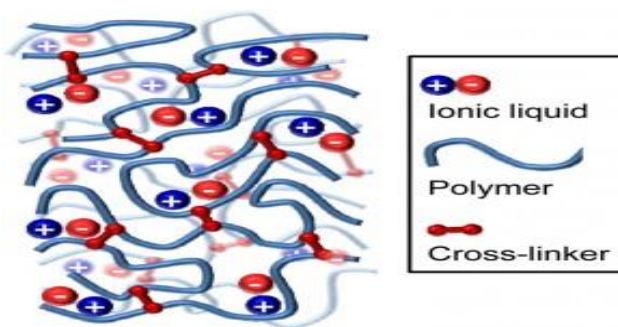


Figure 2.12. Ionic liquid enriched polymer host where polymer chains are modified using cross linking agents [86].

### **2.3. Ionic conductivity mechanism of gel polymer electrolyte**

Ionic conductivity determines the characteristic of an electrolyte, especially for polymer electrolytes where achieving higher ionic conductivity close to that of liquid electrolyte is desired. The conductivity mechanism in a gel polymer membrane occurs through the coupling between the segmental motion of the polymer and ions. The earliest evidence of this phenomenon was dated back to 1986 when Haris *et al.* investigated the ionic conductivity of PEO-based polymer electrolyte particularly happens in the amorphous region [87]. In a semi crystalline polymer host such as PVDF, there are two independent ion transport mechanisms: (1) segmental motions in the amorphous region through the soft polymeric chains and (2) ion hopping in the crystalline region through grain boundaries or point defects [88]. Consequently, in a polymer electrolyte, the efforts are made to increase the amorphous region by incorporating plasticizers. The mobility of the polymeric chains will be improved. It has also been reported that adding plasticizers not only reduces the crystallinity, but also enhances dielectric constant of the polymer, leading to a higher dissociation of the ions at room temperature.

In general, extensive efforts have been devoted for improving ionic conductivity of polymer electrolytes. These include incorporation of non-flammable/volatile organic plasticizers, addition of large size anions, use of polymer blends and co-polymers, modification of polymer host by incorporating side chains and adding micron/nano-sized ceramic fillers [55].

#### **2.3.1. Adding plasticizers to improve ionic conductivity of gel polymer electrolyte**

Ionic conductivity of a polymer electrolyte is associated with the amorphousness of the polymer with decreased energy barrier for segmental motions of polymeric chains in

order for transferring lithium ions within the host polymer matrix. Technically, polymer electrolyte must own a low glass transition temperature ( $T_g$ ), corresponding to a lower energy barrier for the segmental motion of the ions. Hence, plasticizers can enhance the ionic conductivity by lowering the  $T_g$  and [89, 90].

The nature of the plasticizer can define the effect of its addition to the polymer segments. These natural features could be the dielectric constant of the plasticizer, its physical interaction with the ions and the polymer segments and its viscosity. It was studied by Mahendran *et al.* that, plasticizer have relatively smaller size molecules compared to those of polymer. Therefore, they can invade the polymer host and cause electrostatic force between the molecules of the polymeric chain and the plasticizer. Plasticizers by providing free volume within the matrix of the host polymer decrease the cohesive interaction between the chains of the polymer, giving rise to the increased mobility of the chains and ions transport [91, 92]. In another literature, the effect of adding plasticizer is illustrated upon possible path ways for ions migration. Rajendran *et al.* showed that the extra path ways for ions are provided due to the addition of the plasticizer [93]. Figure. 2.13 shows how adding plasticizer can provide the free volume within a polymer host matrix.



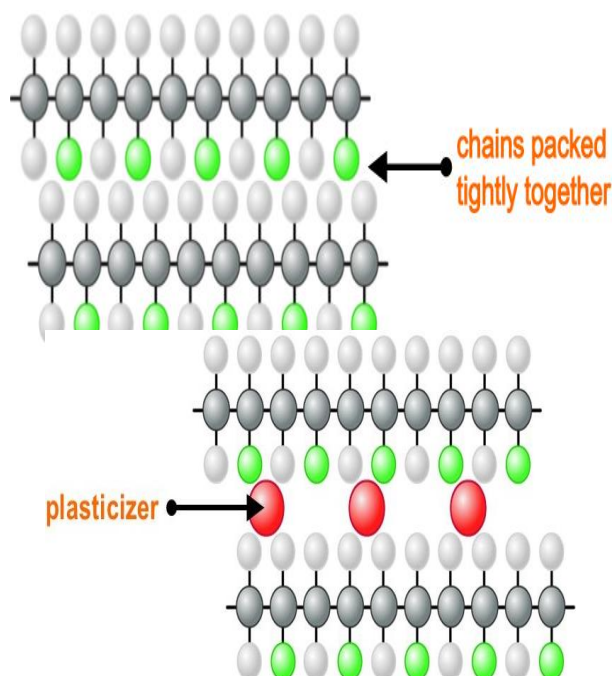


Figure 2.13. adding plasticizer can provide the free volume within a polymer host matrix [94].

Plasticizers such as polyethylene glycol (PEG), Dimethylformamide (DMF), poly carbonate (PC), Dimethyl sulfoxide (DMSO) and Ethylene carbonate (EC) are among the most popular. EC and PC are usually present in the electrolyte structure due to their high dielectric constant of 64.4 and 89.6 respectively. In this work, in addition to EC and PC as aprotic solvents for lithium salt, DMF has been selected to play the role of the solvent for PVDF-HFP polymer host and plasticizer together in which DMF has the dielectric of equal to 37.8. In 2000, Jacob *et al.* has studied multiple additive plasticizers for PVDF-based polymer host and it was concluded that DMF was a sufficient choice for softening the polymer backbones in a PVDF-based polymer matrix [95].

### 2.3.2. Effect of concentration of lithium salt

The number of free ions are directly associated with the ionic conductivity of the electrolyte, giving rise to the need for a lithium salt which can dissociate and re-associate

easily through the ion transfer process. However, an optimum concentration of the salt is still what should be taken into consideration. If the salt is used more than its saturation point, not only the excess ions will not help the ionic conductivity, but also they will establish an unfavorable structure called ions' aggregation, ions's pair or cluster which will lead to some considerable restriction for the polymer chain's mobility [93, 96]. In this work, LiClO<sub>4</sub> and LiPF<sub>6</sub> were the choices of the salts and below is explain why.

Among the variety of the salts that were mentioned in Table. 2.10, LiClO<sub>4</sub> has attracted a lot of attention because of its satisfactory miscibility, less hygroscopic which makes it more stable in atmospheric moisture, large anodic stability of around 5.1 V in contact with a spinel cathode such as LiCoO<sub>2</sub> and relatively high ionic conductivity of around 9 mScm<sup>-1</sup> in a EC/DMC solution @ 20 °C. Also, recent studies have shown that the absence of HF in final product in a dissociation reaction of LiClO<sub>4</sub> leads to the smaller internal resistance and reduced rate of SEI formation compared to LiPF<sub>6</sub> and LiBF<sub>4</sub>. However, the high oxidizing nature of chlorine forms a reactive oxidant which may react organic components under some circumstances like high current or high temperature.

In another hand, none of the salts mentioned in Table. 2.5 could meet the multiple advantages that LiPF<sub>6</sub> simultaneously owns in which the chemical and thermal consistency of LiPF<sub>6</sub> makes it the most balanced salt. For example, the average mobility and dissociation rate of the ions of five different types of salts are mentioned below:

Average mobility of the ions: LiBF<sub>4</sub> > LiClO<sub>4</sub> > **LiPF<sub>6</sub>** > LiAsF<sub>6</sub> > LiTf > LiIm

Dissociation rate constant: LiTf < LiBF<sub>4</sub> < LiClO<sub>4</sub> < **LiPF<sub>6</sub>** < LiAsF<sub>6</sub> < LiIm

Salts, such as  $\text{LiBF}_4$  and  $\text{LiClO}_4$  have higher mobility of ions but they own the lower dissociation rate constants, meaning  $\text{LiPF}_6$  in overall has the most balanced properties as a sufficient lithium salt [97].

### 2.3.3. Effect of adding inorganic nano fillers

Improvement of the mechanical stability of the gel polymer electrolyte is probably the most outstanding effect of adding nano sized ceramic fillers. Additionally, Croce *et al.* has reported that the enhancement in ionic conductivity after adding nano-sized nano fillers is also attributed to the reduction in the crystallinity level of polymers because of the presence of fillers [82].

Besides, prevention from reorganization of polymeric chain which was already dissociated through the use of plasticizer is another advantage of composite gel polymer electrolytes. Lewis acid-base interactions are mainly responsible for the contribution of the nano ceramic particles into the ionic conductivity. The oxygen or hydroxyl (-OH) groups on the surface of the fillers can interact with the anions and cations while creating additional area for lithium ions to get involved with ionic dissociation/re-association [51].

Generally, ceramic fillers for polymer electrolytes are divided into two types: active fillers and passive fillers. The active fillers can contribute in total ionic conduction of the electrolyte due to the presence of the Li ions in their structure e.g.  $\text{LiAl}_2\text{O}_3$  while passive fillers such as  $\text{TiO}_2$  and  $\text{SiO}_2$  are not involved in Li ion conduction process. It should also be taken into account that inorganic fillers can increase the glass transition temperature of polymer which is not favorable, thus the selection of weight ratio of the fillers to the polymer host must be optimized. Following Li *et al.*, in this work, 10 weight percent (wt %) of PVDF-HFP was considered [98]. Fang *et al.* investigated that the nano

sized ceramic particles have better compatibility with electrodes for enhancing the interfacial properties followed by reducing the bulk resistance of the gel electrolyte than the micron sized fillers and the advantages of different types of ceramic particles  $\text{TiO}_2$  and  $\text{SiO}_2$  have been studied in literatures [99-103]. Also, combination of two oxides in this work arises from the fact that titanium tends to agglomerate and the addition of silicon enhances the dispersion level of titanium which avoids the phase transformation of titanium from anatase to rutile form [104-106]. In this work,  $\text{TiO}_2$  and  $\text{SiO}_2$  passive fillers were modified to play the role of the active fillers by pH treatment in which they contribute in total ionic conductivity of the gel polymer electrolyte by enhancing the Li ion dissociation rate.  $\text{TiO}_2$  and  $\text{SiO}_2$  can cause ionic conductivity improvement depending on the filler's surface group properties. According to the Lewis acid/base rules, the interactions between the positive Li ions and enhanced Hydroxyl groups (-OH) in modified metal oxides increases the level of free ions in the electrolytes and thus the ionic conductivity of the nano-composite gel polymer electrolytes [66]. In another word, lithium salt can get dissolved by the treated nano fillers which are assisting the polar groups of the host polymer matrix through Lewis acid-base forces between the surface functional group of the treated fillers and lithium salt [107]. Additionally, Li-metal oxide based active fillers are highly reactive to the air due to high reactivity of lithium to form lithium oxide. this makes these types of active nano fillers to require a high maintenance environment with minimized air diffusion such as a glove box.

#### **2.3.4. Effect of plasma treatment of trilayer PP (polypropylene-polypropylene-polypropylene) separator**

In our work, the gel type polymer electrolyte was coated on to the commercial trilayer PP (polypropylene-polypropylene-polypropylene) separator membrane. Sony, Motorola and Mitsubishi have had a major contribution in developing this technique and claimed that this production is imminent to be commercialized. The majority of predominantly used separators for Li ion batteries such as Polyethylene (PE) and Polypropylene (PP) own poor hydrophilic properties leading to lower liquid electrolyte uptake. To modify the absorption properties of the separators, several techniques were introduced such as UV-Vis ray [108], irradiation of gamma [109], electron beam exposure [110], and irradiation of plasma [106, 111]. In this work, to improve the hydrophilicity of the commercial trilayer PP separator, the separator membranes were O<sub>2</sub> plasma treated with increase in surface energy due to emergence of oxide dangling bonds.

## CHAPTER 3. EXPERIMENTAL PROCEDURES

### 3.1. Materials

Thin films of composite gel polymer electrolyte (CGPE) were prepared using solution casting technique [35, 40, 41]. Poly(vinylidene fluoride-co-hexafluoropropylene) (PVDF-HFP) was selected as polymer host, Dimethylformamide (DMF) and Propylene carbonate (PC) as plasticizers, SiO<sub>2</sub> and TiO<sub>2</sub> as nano fillers, microporous Trilayer polypropylene(PP)-polyethylene(PP)-polypropylene(PP) membrane as separator, lithium perchlorate (LiClO<sub>4</sub>) and lithium hexafluorophosphate (LiPF<sub>6</sub>) in EC: DMC:DEC (4:2:4 in volume) solution as lithium salts, Tetraethyl orthosilicate (TEOS) as primary material for modifying SiO<sub>2</sub> nano particles, Ammonium hydroxide (NH<sub>3</sub>OH) as catalyst for hydrolyzation of TEOS, and Nitric acid (HNO<sub>3</sub>) as primary material for modifying TiO<sub>2</sub> nano particles. The commercial Graphite sheets (Composite Graphite, 0.05mm Thickness) and pure Li chips (99.9%, MTI Corp.) were used as received as working electrode and counter/reference electrode respectively.

#### 3.1.1. PVDF-HFP

PVdF-HFP (density: 1.78 g/mol pellets) from Sigma-Aldrich Co. was applied as the polymer host. PVDF is an extremely non-reactive fluoropolymer made by the vinylidene difluoride's polymerization. The high purity, solvent resistivity and stability when exposed to acidic and basic components make it a perfect choice for the application in lithium ion batteries' electrolyte. More importantly, PVDF has a super hydrophobic structure which will minimize the chance of unwanted moisture related reactions within

the electrolyte. The chemical formula is  $-(C_2H_2F_2)_n-$  with a whitish solid appearance.

Figure 3.1 shows the resonance form of this polymer host.

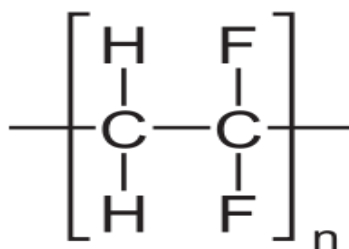


Figure 3.1. resonance form of PVDF polymer host [112].

PVdF-HFP is copolymerized by PVDF and HFP. Depending on the amount of HFP used in the PVDF matrix, different degree of amorphousity will be achieved. For example, if the HFP content lays between 5 - 15 mol%, final copolymers are known as flexible PVDF due to their thermoplastic nature. However, if the HFP content is increased to 20 - 50 mol%, amorphous nature of the copolymer dominates. This is the interest of this research since the highest possible degree of amorphousity is desired for charge transport [113]. Figure 3.2 shows the resonance form of the PVDF-HFP copolymers with chemical formula of  $(-CH_2CF_2-)_x[-CF_2CF(CF_3)-]_y$ . While HFP is known to soften the PVDF backbones to get more amorphousity, PVDF gives rise to a more reliable mechanical stability.

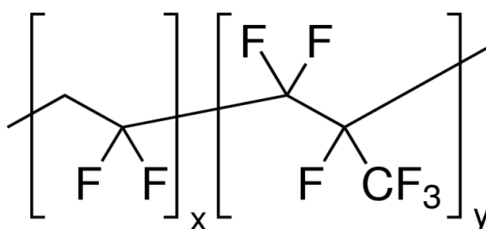


Figure 3.2. resonance form of the PVDF-HFP copolymers [58].

As mentioned in Chapter 2, the major reason behind choosing PVDF-HFP is the dominated amorphous phase of the polymer host with softened and flexible polymer backbones. This will result in enhanced ionic conductivity in ambient temperature. Table 3.1 illustrates some main physical properties of PVDF-HFP. As shown in this table, high dielectric constant, high viscosity, relatively lower melting point compared to other polymer hosts are other significant features of PVDF-HFP for use as the electrolyte material in lithium ion battery.

Table 3.1. Some main physical properties of PVDF-HFP [114].

Form	Pellets
Melting point	4-10 g/10 min (230°C/12.5kg)
Dielectric constant	11.38, 100 Hz (ASTM D 750)
Viscosity	20,000-25,000 poise (Pa.s)
Transition temp	T <sub>m</sub> 135-140 °C (ASTM D 3418)
Density	1.78 g/mL at 25 °C

### 3.1.2. DMF

DMF (99% pure) was applied as plasticizer and solvent for PVDF-HFP polymer host, provided by Acros Organics Co. DMF is a sub-product of formamide which is one of formic acid's amides. Naturally, DMF is a polar solvent with hydrophilic properties. The high polarity of DMF assists those types of reactions that need the particle's dissociation such as ionic dissociation happening in lithium salts. Also, DMF causes swelling in plastics by penetrating into polymer particles which will later lead to better accommodation of liquid electrolyte into thin film polymer membrane matrix. Figure 3.3 shows two different resonance forms of DMF with chemical formula of (CH<sub>3</sub>)<sub>2</sub>NC(O)H.



Table 3.2 contains some main physical properties of DMF. The low viscosity of DMF makes it a suitable choice for PVDF-HFP solvating agent since it can help the lithium ions flow easier. Additionally, its high dipole moment change assists the dissociation/re-association of the ions within the polymer electrolyte matrix.

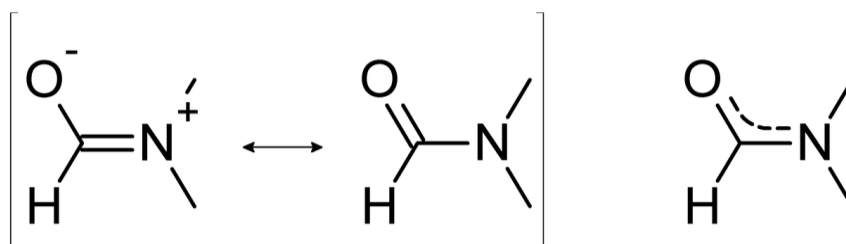


Figure 3.3. Two different resonance forms of DMF [115].

Table 3.2. Main physical properties of DMF [115].

Form	Colorless liquid
Molar mass	73.10 g·mol <sup>-1</sup>
Density	0.948 g mL <sup>-1</sup>
Melting point	-60.5 °C; -76.8 °F; 212.7 K
Boiling point	152 to 154 °C; 305 to 309 °F; 425 to 427 K
Solubility in water	Soluble
Viscosity	0.92 mPa.s (at room temperature)
Dipole moment	3.86 D

### 3.1.3. PC

Propylene carbonate (PC) (provided by Fluka Co., purum; >99% (GC)) is an organic, colorless and odorless solvent. Due to its high dielectric constant, it is typically used for the lithium ion battery salt solvating agent. As shown in Figure 3.4, PC has an

additional methyl group, and therefore the PC based electrolyte possesses high conductivity and low viscosity properties. However, the use of PC as a single solvent is not recommended due to the decomposition of PC which exfoliates the graphite. Since graphite is a conventional anode material for lithium ion battery. Currently, the ethylene carbonate (EC) groups will always be present in lithium ion battery liquid electrolyte solvent since EC can establish a reliable SEI that can further save the graphite from extra reactions with electrolyte components. As reported by Aurbacha *et al.*, PC has been known the best solvent for LiClO<sub>4</sub> salt [116-118]. Table 3.3 contains some main physical properties of PC.

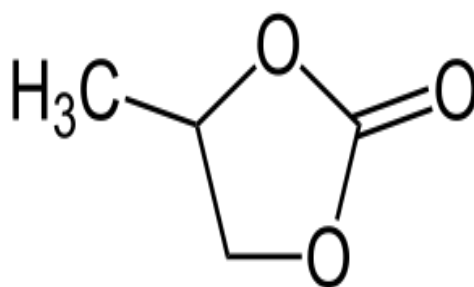


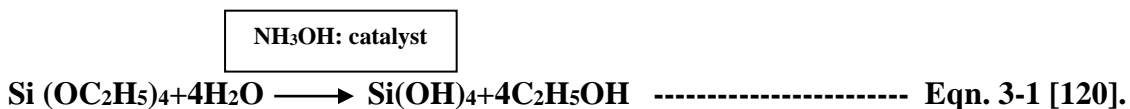
Figure 3.4. resonance form of PC [119].

Table 3.3. Main physical properties of PC [119].

Molar mass	102.09 g.mol <sup>-1</sup>
Density	1.205 g.mol <sup>-1</sup>
Boiling point	241.7°C
Dielectric constant	64.9 at room temperature
Flash point	132 °C - 270 °F-405 °K

### 3.1.4. SiO<sub>2</sub>

SiO<sub>2</sub> or silica (provided by US Research Nanomaterials Inc., Average diameter: 60-70 nm) is an oxide of the silicon, belonging to the inorganic compounds or ceramic filler family. Silica has been vastly used in semiconductor industry from optical fibers to thin films; however its primary use in glass technology is still debatable. Thin films of SiO<sub>2</sub> are prepared by growing the silicon wafers through thermal oxidation where SiO<sub>2</sub> plays the role of an electrical insulator. The unique properties of SiO<sub>2</sub> vary from a controlled pathway for electron flow in a FET, to storing charge in a capacitor. Figure 3.5 shows the resonance form of SiO<sub>2</sub> while Table 3.4 explains some of its physical properties. In lab scale, silicate esters such as tetraethyl orthosilicate (TEOS : Si(OC<sub>2</sub>H<sub>5</sub>)<sub>4</sub>) have been the most widely used route to start many silicon dioxide based reactions. For example, Eqn. 3-1 shows one of the known reactions for extracting the SiO<sub>2</sub> nano fillers by simple hydrolization of TEOS.



In general, Si atoms are tetrahedrally coordinated where 4 atoms of oxygen surround a Si atom in the center with chemical formula of SiO<sub>2</sub>. SiO<sub>2</sub> acts as passive filler, which means there is no direct influence on the lithium ion transport rate by adding this nano filler. However the diffusion of SiO<sub>2</sub> in polymer matrix decreases the glass transition temperature and degree of crystallinity and improves the mechanical stability of the gel polymer film, leading to ionic conductivity enhancement.

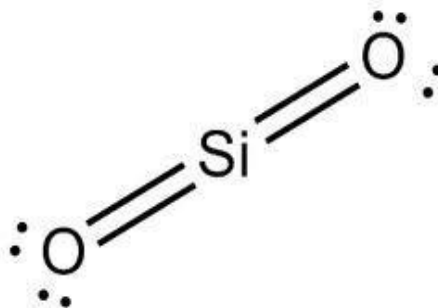


Figure 3.5. Resonance form of SiO<sub>2</sub> [121].

Table 3.4. Physical properties of SiO<sub>2</sub> [3].

Molar mass	60.0843 g.mol <sup>-1</sup>
Melting point	1650(±75) °C
Boiling point	2230 °C
Appearance	white powder
Density	2.634 g.cm <sup>-3</sup>
Solubility in water	0.012 g/100 mL

### 3.1.5. TiO<sub>2</sub>

Titanium dioxide or titania (TiO<sub>2</sub>, provided by Aeroxide Co. Degussa with an average diameter: P25 60-70 nm) is another inorganic filler that has been used in our composite polymer electrolyte. The oxidation process of titanium occurs naturally where three fundamental phases of brookite, rutile and anatase could possibly emerge. The anatase TiO<sub>2</sub> owns a lower degree of crystallinity vs. the rutile phase in Figure 3.6. However, both anatase and rutile phases own the tetragonal coordination, which is different from the brookite form with orthorhombic structure [122].

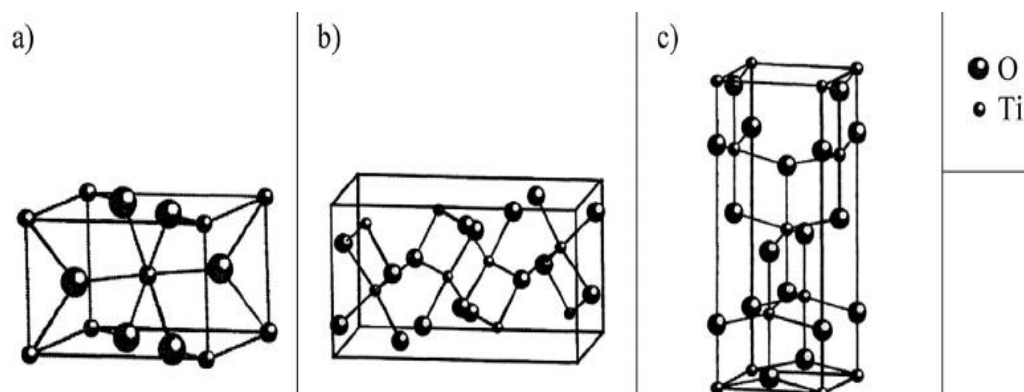


Figure 3.6. Resonance forms of (a) rutile (b) brookite (c) anatase phases of TiO<sub>2</sub> [122].

Reported by Kumar *et al.*, TiO<sub>2</sub> nano fillers within the polymer electrolyte matrix increased the lithium ion transference number and ionic conductivity due to the TiO<sub>2</sub> dipole interaction with the polymer matrix. The lower glass transition temperature caused by adding nano fillers will result in easier segmental motion of the polymeric chains. The voids provided by these sorts of motions give rise to a smoother flow of ions along the polymer backbone and chain [123-125]. Table 3.5 contains some physical properties of TiO<sub>2</sub>.

Table 3.5. Physical properties of TiO<sub>2</sub> [7].

Molar mass	79.866 g.mol <sup>-1</sup>
Appearance	White solid
Density	4.23 g.cm <sup>-3</sup>
Melting point	1,843 °C - 3,349 °F- 2,116 K
Boiling point	2,972 °C - 5,382 °F - 3,245 K
Solubility in water	Non-soluble

### 3.1.6. Trilayer PP separator membrane

Microporous trilayer PP membrane (Celgard 2500, 25  $\mu\text{m}$ ) was applied as the electrodes separator layer. The majority of predominantly used separators for Li ion batteries such as Polyethylene (PE) and Polypropylene (PP) own poor hydrophilic properties leading to lower liquid electrolyte uptake. The polyolefin-based separators (or blends of polyolefins) offer reliable chemical stability and mechanical features. These separators can be produced by dry or wet chemical processes in which the orientation steps enhance the porosity and tensile stability [126]. To modify the absorption properties of the separators, several techniques were used such as UV-Vis illumination [108], gamma irradiation [109], electron beam exposure [110], and plasma irradiation [106, 111]. In our work, the gel type polymer electrolyte was coated onto the commercial trilayer polypropylene-polyethylene-polypropylene membrane separator membrane. Sony, Motorola and Mitsubishi have been mostly involved with developing this technique and have claimed that this production is imminent to be commercialized. Table 3.6 explains some physical properties of a Celgard 2500 separator.

Table 3.6. Physical properties of a Celgard 2500 separator [127].

Thickness	25 $\mu\text{m}$
Width	85 mm
Length	60 m
Net weight	0.4 lb
Porosity	39%
Pore size	$0.21 \times 0.05 \mu\text{m}$

### 3.1.7. LiClO<sub>4</sub>

Lithium perchlorate (provided by Sigma-Aldrich Co., 95+% A.C.S reagent) is a white crystalline lithium salt with very high solubility in a variety of polar solvents. It has the largest oxygen to weight ratio between the perchlorate family. One of the main attractions of LiClO<sub>4</sub> is that it does not experience the oxidation on the negative electrode or anode, making it extensively applicable for lithium battery electrolyte. In addition to its higher anodic stability, higher solubility and ionic conductivity than other lithium salts are significant. LiClO<sub>4</sub> is also less hygroscopic than other lithium salts which makes it more stable to moisture. The easy handling of LiClO<sub>4</sub> and low cost are other reasons for its popularity. Reported by Rajendran et al., LiClO<sub>4</sub> owns a small ionic radius but larger anions compared to other Li salts which will result in lower dissociation energy [93].

Figure 3.7 and Table 3.7 illustrate the chemical structure and some physical properties of LiClO<sub>4</sub> respectively.

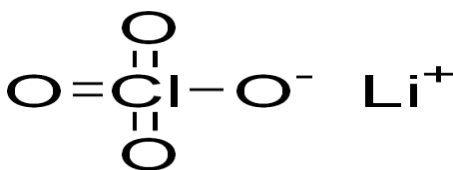


Figure 3.7. Chemical structure of LiClO<sub>4</sub> [8].

Table 3.7. Physical properties of LiClO<sub>4</sub> [8].

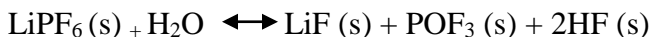
Melting point	236 °C
Appearance	White solid
Molecular weight	106.39 g.mol <sup>-1</sup>
Density	2.42 g.cm <sup>-3</sup>
Solubility in water	60 g/100 mL
Boiling point	430 °C

### 3.1.8. LiPF<sub>6</sub> in EC:DMC:DEC (4:2:4 in volume)

LiPF<sub>6</sub>, provided by MTI Corp. was used a lithium salt solution in combination with a PC-LiClO<sub>4</sub> system. As discussed in section 2.1.2 & 2.3.2 of chapter 2, LiPF<sub>6</sub> allocates the most balanced features of an ideal electrolyte for lithium ion batteries. EC:DMC:DEC is by far the best commercialized solution for solvating LiPF<sub>6</sub> in order to minimize the production of toxic components during the decomposition of LiPF<sub>6</sub>. As discussed earlier, the decomposition of LiPF<sub>6</sub> occurs through following equation:



The PF<sub>5</sub> (g) is a very reactive Lewis acid gas and can react with the solvent and increase the pressure within the cell. LiPF<sub>6</sub> is highly reactive to H<sub>2</sub>O and needs a moisture free environment for maintenance. The following equation expresses the reactivity of LiPF<sub>6</sub> to H<sub>2</sub>O molecules:



All the experimental procedures in order to fabricate a lithium ion battery using LiPF<sub>6</sub> as salt will need an inert environment to minimize the side reactions caused by moisture. In this work, all the maintenance and experimental procedures using LiPF<sub>6</sub> solution were done inside an argon glovebox. Table 3.8 contains some physical properties of the LiPF<sub>6</sub> in the EC:DMC:DEC solution. Also, Figure 3.8 shows the chemical structure of LiPF<sub>6</sub> including its solution components EC:DMC:DEC. As can be seen in Figure 3.8, the differences in solvent chemical structures give rise to their complementary properties. As discussed earlier in section 2.1.2, EC can make very good solid electrolyte interface (SEI) that can protect the graphite from additional reactions with electrolyte components. The



presence of DEC and EMC with long polymeric chain can at the same time enhances the viscosity and solubility of lithium salts [128].

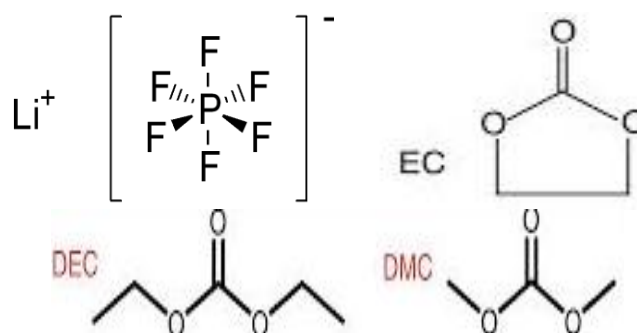


Figure 3.8. Chemical structures of LiPF<sub>6</sub>, EC, DEC and DMC [129].

Table 3.8. Physical properties of LiPF<sub>6</sub> in EC:DMC:DEC [130].

Electrolyte Salt	1 mol/L LiPF <sub>6</sub> in EC+DMC+DEC; 4:2:4 in volume
Net weight	4 lbs
Max. Voltage	4.5V
Moisture	≤ 20 ppm
Free acid (HF)	≤ 50 ppm
Density	1.22 ± 0.03 g/ml @ 25°C
Electrical conductivity	10 ± 0.5 mS/cm

### 3.1.9. NH<sub>3</sub>OH

Ammonium hydroxide or simply ammonia can be regarded as NH<sub>3</sub> (aq). However the alkali nature of hydroxide implies the [NH<sub>4</sub><sup>+</sup>][OH<sup>-</sup>] composition. The interaction between ammonia and water will dissociate the cations and anions followed by the equilibrium bellow:



In this equation, every 1M of ammonia solution results in almost 1.42% of ammonium with the pH of 11.63, providing a very basic environment. Figure 3.8 and Table 3.9 contain the chemical structure and some physical properties of  $\text{NH}_3\text{OH}$  respectively.

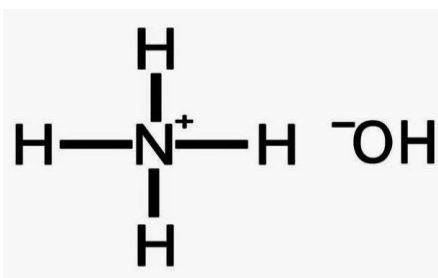


Figure 3.9. Chemical structure of  $\text{NH}_3\text{OH}$  [131].

Table 3.9. Physical properties of  $\text{NH}_3\text{OH}$  [13].

Melting point	-57.5 °C
Appearance	Colorless liquid with fishy smell
Molar mass	35.04 g.mol <sup>-1</sup>
Density	0.91 g.cm <sup>-3</sup>
Solubility in water	miscible
Boiling point	27 °C

### 3.1.10. TEOS

TEOS has a chemical formula of  $\text{Si}(\text{OC}_2\text{H}_5)_4$  and tetrahedral molecular structure shown in figure 3.10, which is mostly used as a precursor for preparing  $\text{SiO}_2$ . The process of converting TEOS to nano particles of  $\text{SiO}_2$  is called hydrolyzation of TEOS in which ethanol will be a side production shown in Eqn. 3-1 of section 3.1.4. Depending on the

nature of the catalyst used for this hydrolyzation process, TEOS could have basic or acidic properties in which  $\text{NH}_3\text{OH}$  was used as the catalyst. When the hydrolyzed TEOS is dried, the solvents will evaporate but there will still be unreacted cross-linking of -OR and -OH groups in the final basic  $\text{SiO}_2$  compound [32]. Table 3.10 shows some physical properties of TEOS.

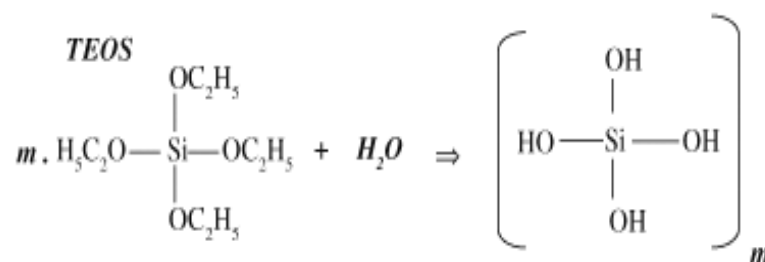


Figure 3.10. Molecular structure of  $\text{Si}(\text{OC}_2\text{H}_5)_4$  used as a precursor for preparing  $\text{SiO}_2$  [132].

Table 3.10. Physical properties of TEOS.

Melting point	-77°C
Appearance	Colorless liquid with alcohol-like smell
Molar mass	208.33 g.mol <sup>-1</sup>
Density	0.933 g.cm <sup>-3</sup>
Solubility in water	Non-soluble
Boiling point	168 °C

### 3.1.11. $\text{HNO}_3$

Nitric acid is a highly corrosive acid with a colorless appearance; however the solution tends to yellow color if the water and oxides of nitrogen decomposes. Nitric acid is commonly used for adding nitro-groups to organic molecules. Since it owns a very high oxidizing factor, treating the nano filler  $\text{TiO}_2$  in our work with the subsequent acid

will produce positively charged nano fillers with acidic properties. This will cause the TiO<sub>2</sub> nano particles to lose electron and act as cations [17, 133]. Figure 3.11 and Table 3.11 illustrate the chemical structure and physical properties of HNO<sub>3</sub>.

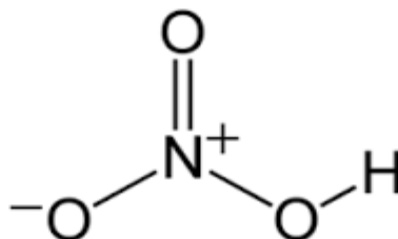


Figure 3.11. Molecular structure of HNO<sub>3</sub> [17].

Table 3.11. Physical properties of HNO<sub>3</sub>.

Melting point	-42° C
Appearance	Colorless , yellow (decomposed) or red (highly concentrated fuming acid)
Molar mass	63.01 g.mol <sup>-1</sup>
Density	1.5129 g.cm <sup>-3</sup>
Solubility in water	miscible
Boiling point	83° C

## 3.2. Preparation of the CGPE coated PP separators

### 3.2.1. O<sub>2</sub> plasma treatment of trilayer PP separator membrane

Trilayer PP separator was cut into proper size and cleaned with lab-related tissue papers provided by Kimberley-Clarck which had been already vapored with acetone as shown in Figure 3.12. The separators were then placed inside the Harrick PDC-32G

plasma system followed by high vacuum level evacuation and intensity of 18W. The plasma was generated for several time frames in which the optimized length was selected to be 20 minutes, where there was no visible burning effect at each side of the PE separator.

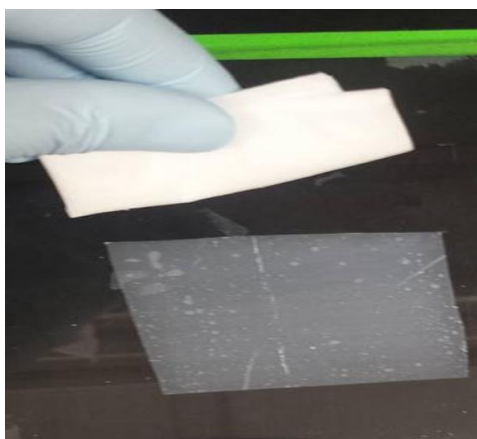


Figure 3.12. Cleaning the separator using acetone vapored lab tissues.

### 3.2.2. Preparation of modified inorganic fillers

Followed by Eqns. 3-1 & 3-2,  $\text{TiO}_2$  acid treatment and hydrolyzation of TEOS were done individually through three steps. Initially, the mixture solution of  $\text{NH}_4\text{OH}$ : TEOS: deionized-water(DIW); (1:2:2) and  $\text{TiO}_2$ : DIW:  $\text{HNO}_3$ ; (0.1:1:1) were ultrasonicated for 20 mins separately at room temperature. In hydrolyzed TEOS mixture, the phase separated gel was then coated on a glass substrate to dry at  $100\text{ }^\circ\text{C}$  for one hour on hotplate. Finally, the  $\text{SiO}_2$  nano fillers were extracted from the hydrolyzed solution. Subsequently, acid treated  $\text{TiO}_2$  was coated and dried under the same circumstances followed by extraction of  $\text{TiO}_2$  [134, 135]. Figure 3.13 shows the phase separated gel TEOS after hydrolyzation and before drying.

NH <sub>4</sub> OH catalyst
-----------------------------

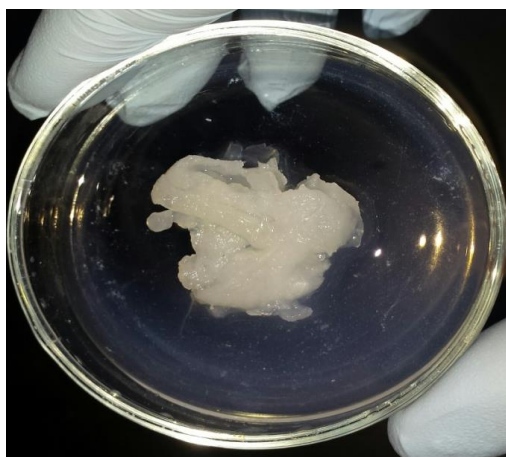
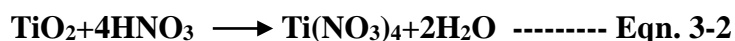


Figure 3.13. Phase separated gel TEOS after hydrolyzation and before drying.

### 3.2.3. Composite gel polymer coating on trilayer PP separator

Using solution casting techniques as reported in other literatures [66], O<sub>2</sub>-plasma treated separators were coated with their respective solutions with mixture ratio of PVDF-HFP: basic/ acidic modified fillers: DMF: Acetone; 0.1:0.01:0.6:0.4. Two different samples were kept inside the Argon glove box for 24 h to remove all the residue solvents before soaking them in lithium salt solution [136, 137]. Figure 3.14a & 3.14b show the basic CGPE coated on trilayer PP separator before dipping in lithium salt solution and schematic diagram of a trilayer PP separator coated by composite gel electrolyte respectively.

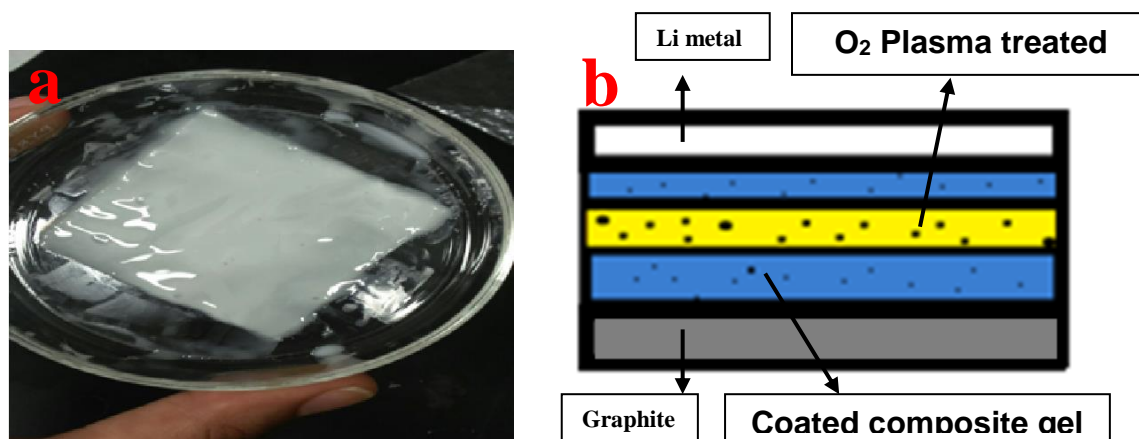


Figure 3.14. (a) Basic CGPE coated on trilayer PP separator before dipping in lithium salt solution. (b) Schematic diagram of a trilayer PP separator coated by composite gel electrolyte.

### 3.2.4. Incorporation of liquid electrolyte into composite gel polymer coated trilayer PP separator membrane

To avoid the direct exposure of the coated separators in Figure 3.15, the Petri dishes were then covered with aluminum foil which had a few holes on them. The dried coated separators were then bathed in 1M PC-LiClO<sub>4</sub>+LiPF<sub>6</sub> in EC: DMC:DEC (4:2:4 in volume) solution as 300% wt. of PVDF-HFP to form the final CGPE before sealing the half cell battery as can be seen in Figure 3.15 [137].



Figure 3.15. CGPE coated PP separators in Petri dishes covered by aluminum foil with holes.

### 3.2.5. Characterization of the trilayer PP before and after coating the CGPE

The water contact angle measurement of the PE separator was performed by the Data Physics OCA 20 system before and after the O<sub>2</sub> plasma treatment. Scanning electron microscope (SEM) and Energy Dispersive X-ray Spectroscopy (EDS) were also employed to observe the pore size of the porous electrolyte membrane and concentration ratio of the lithium ion respectively in the CGPE using a Hitachi S-4300N system. Later, Hydrion Spectral pH Strips were used to determine the pH of the acid treated TiO<sub>2</sub> and hydrolyzed TEOS ceramic filler contents separately. Figures 3.16 & 3.17 show the Contact Angle Measurement and SEM-EDS systems respectively.



Figure 3.16. Contact Angle Measurement system.



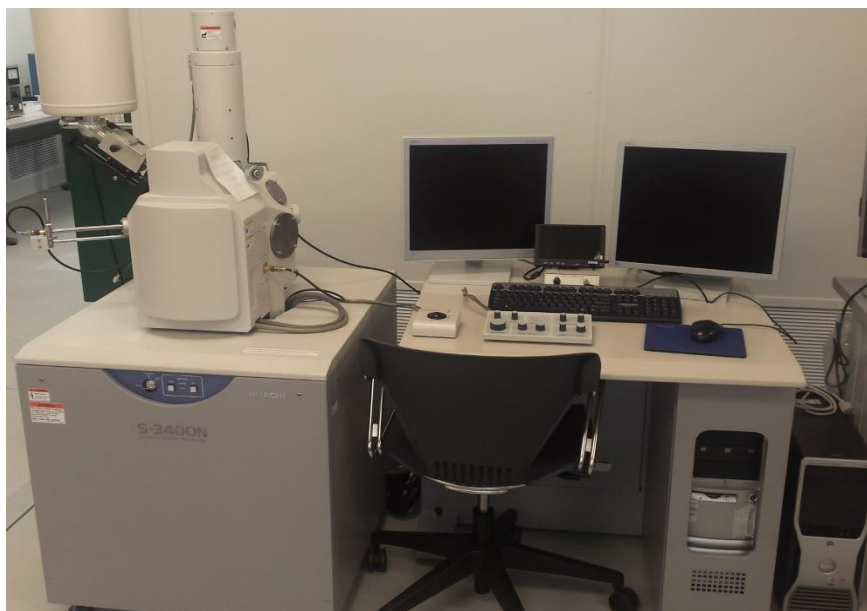


Figure 3.17. SEM-EDS Measurement system.

### 3.2.6. Electrochemical measurements

For electrochemical impedance spectroscopy (EIS) measurement, the prepared CGPEs coated on trilayer PP separators were symmetrically sandwiched between two stainless steels and then sealed using the CR2032 coin cells. Frequency range of 0.01 Hz to 100000 Hz and an ac excitation voltage of 10 mV were applied to the model cells [138]. After measuring the bulk resistance of sandwiched cells via EIS, ionic conductivity was calculated from Eqn. 3-3:

$$\sigma = T \cdot (R_b \cdot A)^{-1} \text{ ----- Eqn. 3-3}$$

In which  $T$  and  $R_b$  stand for thickness and bulk resistance of the CGPE coated trilayer PP separator and  $A$  represents the area of electrode. CV measurement was carried out with potential window of 0.01V 3 V for 5 cycles with scan rate of  $0.2 \text{ mV} \cdot \text{s}^{-1}$ . Finally, the galvanostatic charge and discharge cycles of the half cell batteries were conducted at room temperature using the LAND CT2001A battery tester in potential window of 0.01-

3V versus  $\text{Li}^+/\text{Li}$  at different constant current rate of C/20, C/8, C/4, C/2 and C. Specific charge and discharge capacity of the half cells were then determined using the active mass of the working electrode.

Figure 3.18 & 3.19 show the system setup used for EIS (Electrochemical Impedance Spectroscopy)/ CV (Cyclic Voltammetry) and LAND CT2001A battery tester respectively. Generally, there are 2 sets of cables in EIS/CV system. After recognizing which cable is for working electrode/anode (red cable) and which one is for reference electrode /Li metal (green cable), the half cell was connected into the circuit and the experiment was run.



Figure 3.18. System setup used for Electrochemical Impedance Spectroscopy (EIS) and Cyclic Voltammetry (CV).

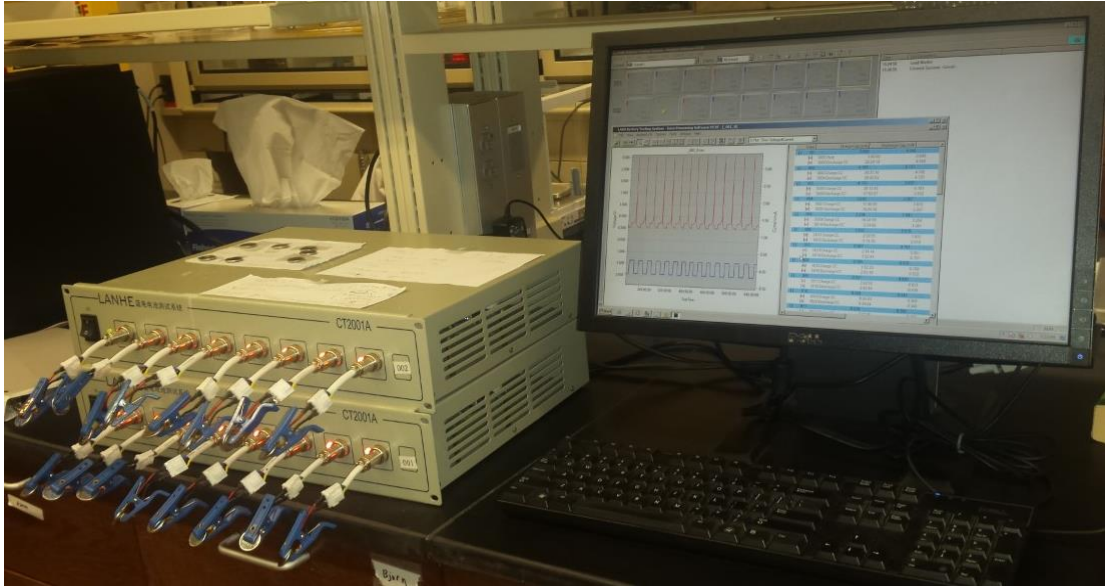


Figure 3.19. LAND CT2001A battery tester system setup.

## CHAPTER 4. RESULTS AND DISCUSSIONS

### 4.1. Characterization of trilayer PP separator before and after O<sub>2</sub> plasma treatment

Figures 4.1a, 4.1b, 4.1c & 4.1 d show the water contact angle of trilayer PP separator before O<sub>2</sub> plasma treatment, after 10 minutes, 15 minutes and 20 minutes of O<sub>2</sub> plasma treatment at each side respectively. As can be seen, the contact angle had a decreasing trend of 112°, 51°, 49° and 30°.

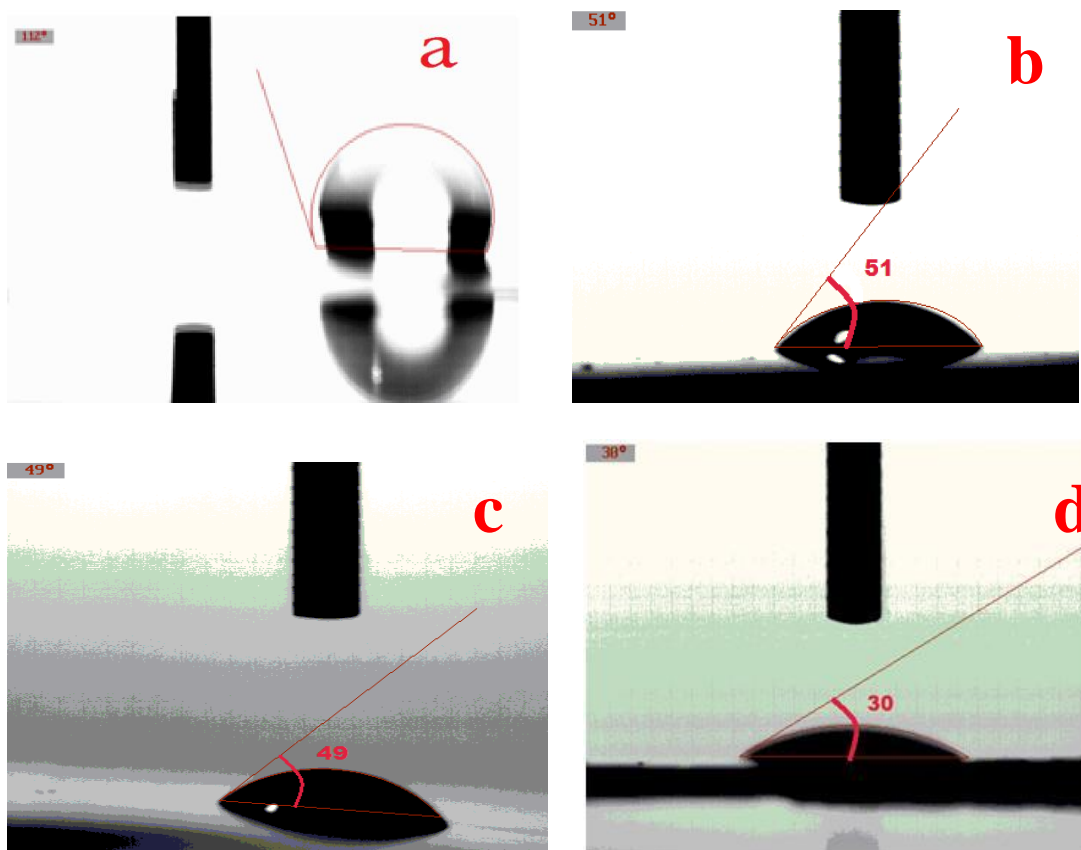


Figure 4.1. Trilayer PP separator (a) before O<sub>2</sub> plasma treatment (b) after 10 minutes, (c) after 15 minutes and (d) after 20 minutes of O<sub>2</sub> plasma treatment at each side respectively.

When the trilayer PP separator was treated for more than 20 minutes, the surface started changing color from white to dark yellow, witnessing the burning of the membrane.

Figure 4.2a & 4.2b show the color change in trilayer PP membrane at 20 and 25 minutes of treatment at each side respectively.

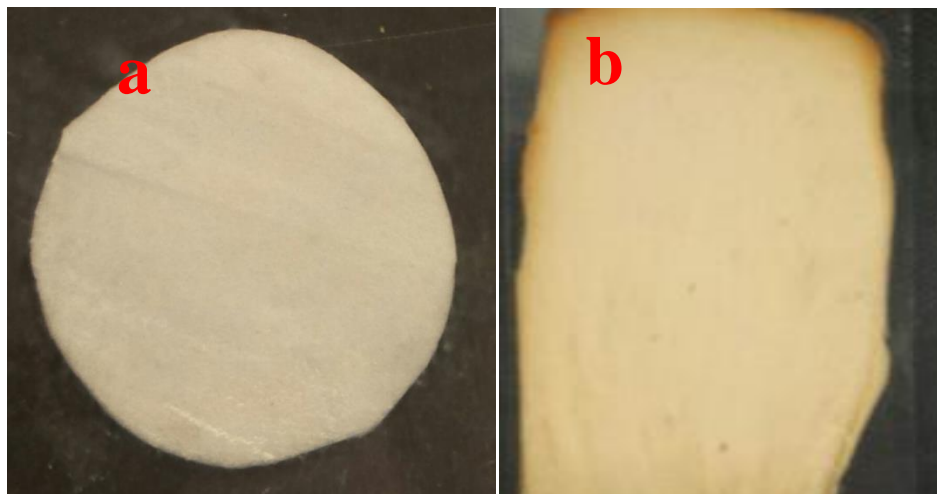


Figure 4.2. Trilayer PP membrane (a) after 20 minutes (b) after 25 minutes of plasma treatment at each side respectively.

The reduction of  $82^\circ$  in contact angle from  $112^\circ$  to  $30^\circ$  after a 20 minute plasma treatment at each side demonstrated the effectiveness of the  $O_2$  plasma treatment in increasing the wettability of the trilayer PP membranes. Polyolefin-based separators such as PE (polyethylene) and PP (polypropylene) separators suffer from poor hydrophilicity which will limit their wettability by liquid electrolyte [136, 139, 140]. Enhancement in the electrolyte uptake is due to the formation of polar hydroxyl functional groups (O-H) on the surface of the trilayer PP separator which will lead to higher surface energy and therefore enhanced interaction with polar functional groups within the electrolyte. Similar observations were done by Kim *et al.* using different types of polyolefin-based separators used for lithium ion batteries [141].

Plasma treatment can modify the surfacial properties of the polymers without sacrificing their bulk properties. Exposing  $O_2$  gas to the electromagnetic power as

mentioned in section 3.2.1, dissociates the gas molecule by forming a chemically reactive gas which modifies the featured trilayer PP separator surface. Considering the atomic level, different species with their relative energy level are produced during plasma such as ions, free radicals and electrons. The free radicals are those which are uncharged but lacking a pair in their valence band. These types of species are mostly responsible for the improved covalent bondings between the separator and the electrolyte component. The reason of choosing oxygen as the initiating gas for plasma was because plasma oxygen gas can break the C-C bonds of trilayer PP separator, so that the top layer of trilayer PP separator will be ablated. Technically, oxygen does oxidative reaction by forming polar groups such as hydroxyl and carboxyl on the separator surface, leading to increases in surface energy. This enhanced surface energy is the key to enhanced wettability and hydrophilicity of separator. Figure 4.3 shows the formation of polar groups on trilayer PP membrane [142].

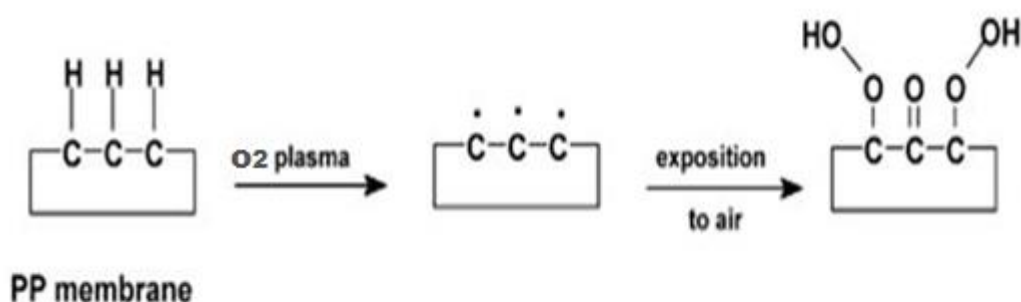


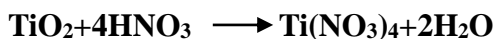
Figure 4.3. Formation of polar groups on trilayer PP membrane [142].

Based on the figure above, plasma treatment enhances the surface energy and consequently reactivity of the membrane by formation of active sites to initiate the uniformity of coated polymer throughout the membrane. In addition, surface modification of the polyolefin separators through plasma treatment is the most inexpensive method

among the numerous methods mentioned in section 2.3.4. The interfacial bonding between electrodes and the separator is very effective in long-term use of a lithium ion battery. Since even a very small faulty interface can create an extremely uneven distribution of the current due to the high interfacial resistance in the faulty areas. This can eventually lead to the formation of SEI layer on the anode which increases the impedance of the battery.

#### 4.2. Characterization of modified inorganic nano fillers

Hydrion Spectral pH Strips' color change demonstrated acidic property of acid treated TiO<sub>2</sub> and basic property of the hydrolyzed TEOS as shown in Figure 4.4 Acid treated TiO<sub>2</sub> had color order close to pH range of 1 to 2 while basic compound of hydrolyzed TEOS had color order close to PH range of 8 to 9. When the TiO<sub>2</sub> nano particles were dipped into the 1M nitric acid, the hydrogen atoms were adsorbed onto the TiO<sub>2</sub> surface through proton exchange at the oxide/water interface as seen in equation below [143, 144]. This was followed by the dissociation of titanium nitride into protonated titanium and nitrate anions in higher temperatures. As can be seen in figure 4.4, the pH range of around 1 to 2 was achieved for the nitric acid treated TiO<sub>2</sub>, corresponding to the pH of 2 for Nitric acid [31].



In the hydrolyzed TEOS, as discussed in sections 3.1.9 and 3.1.10, the interaction between ammonia and water dissociates the cations and anions followed by the equilibrium bellow:



In this equation, every 1M of ammonia solution results in almost 1.42% of ammonium with the pH of 11.63, providing a very basic environment. Since the pH properties of the extracted SiO<sub>2</sub> nano particles depended on the catalyst used for hydrolyzation of TEOS, the SiO<sub>2</sub> nano particles had basic properties. Therefore, when the hydrolyzed TEOS was dried, the solvents was evaporated but there were still the unreacted cross-linking of -OR and -OH groups in the final basic SiO<sub>2</sub> compound [32]. It was reported by Brinker *et al.* that pH of around 9.95 is expected for a hydrolyzed TEOS using a 0.05M ammonia catalyst [145]. Using the same molar ratio of catalyst, pH of around 9 was achieved in this work.

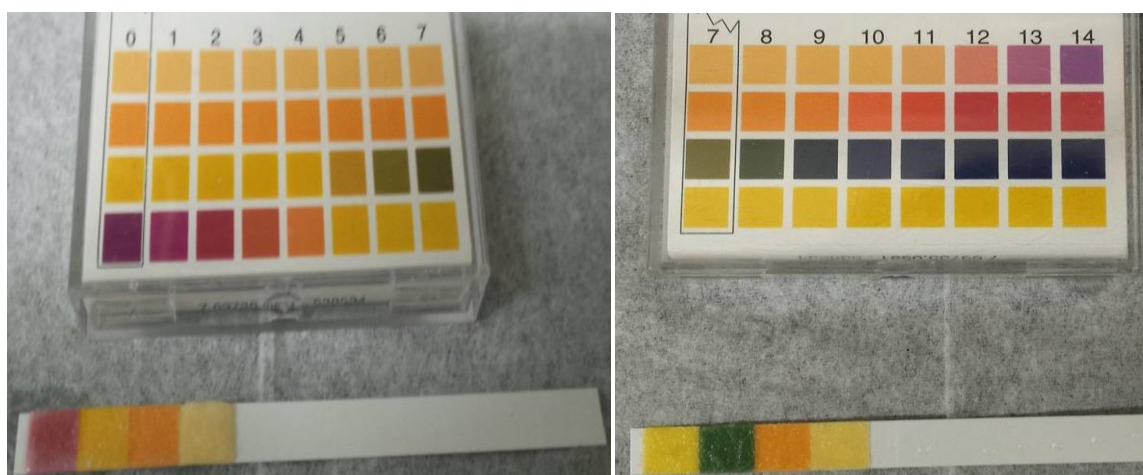


Figure 4.4. acid treated TiO<sub>2</sub> coated on pH strip on the left and hydrolyzed TEOS coated on the pH strip on the right; colors comparison with the pH numbers.

### 4.3. SEM images of the composite gel polymer electrolyte before and after coating on trilayer PP separator

Figures 4.5a & 4.5b show the SEM images of CGPE with several pore-like structures with diameters in the range of 12.6 to 30 $\mu$ m. As seen in Figures 4.5c & 4.5d,



the SEM images of CGPE coated on trilayer PP separator before  $\text{LiClO}_4+\text{LiPF}_6$  solution bath show that the pore diameter decreased to the range of 390 to 520 nm due to the submicron pore size structure of trilayer PP separator [141]. Figures 4.5e & 4.5f show SEM images of porous CGPE coated on trilayer PP separator after  $\text{LiClO}_4+\text{LiPF}_6$  bath. Compared to Figure 4.5c & 4.5d, the pore morphology transformed from circular to spherical shape which is a result of the liquid electrolyte uptake by the available pores. Commonly, the pore size is controlled by the choice of solvents or other evaporating additives [104]. Table 4.1 shows the pore diameter range of CGPE under different conditions. The diameter measurements were done under 10  $\mu\text{m}$  magnifications.

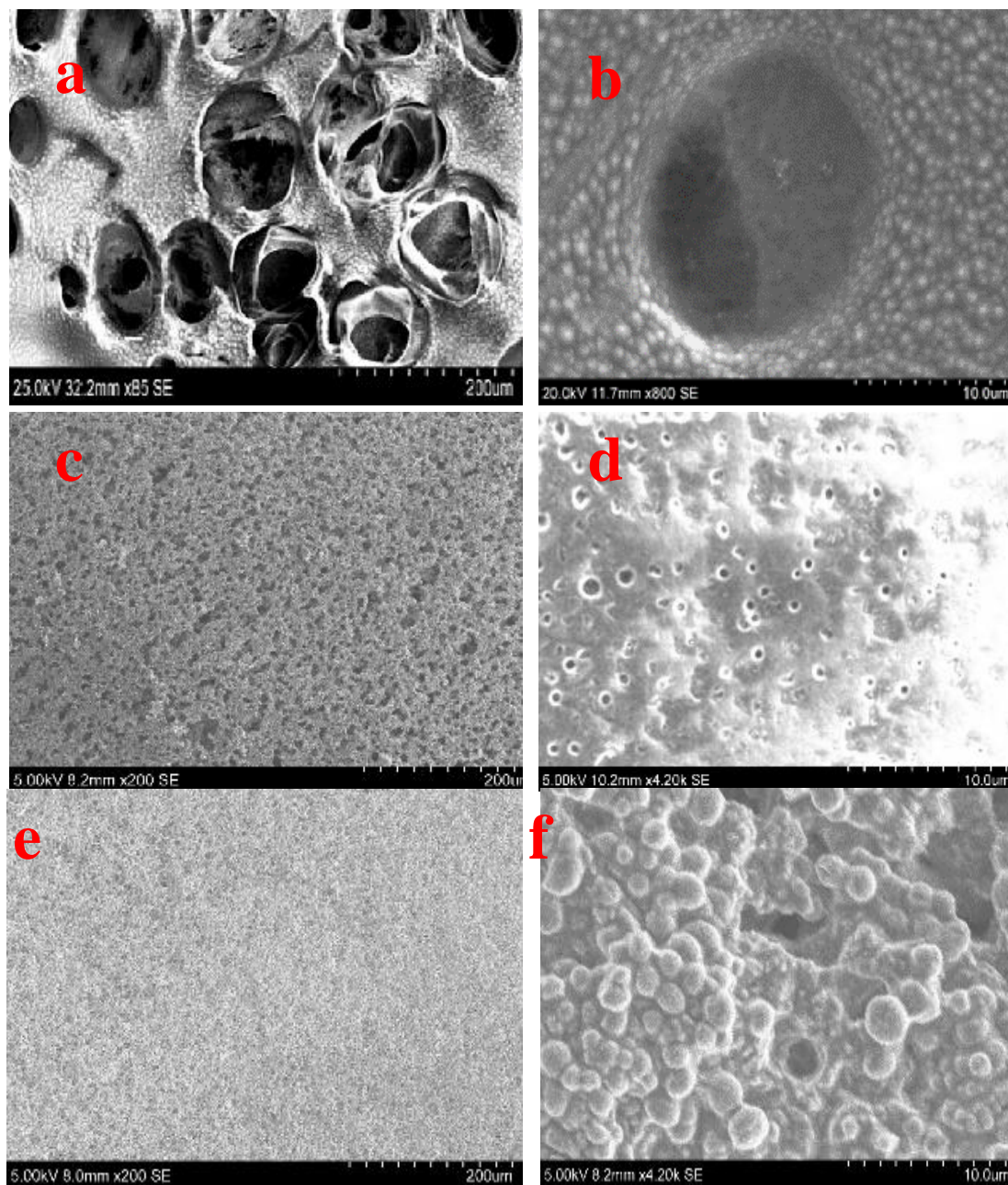


Figure 4.5. SEM image of (a&b): CGPE before coating on trilayer PP separator, (c&d): Coated CGPE before  $\text{LiClO}_4 + \text{LiPF}_6$  solution bath and (e&f): Coated CGPE after  $\text{LiClO}_4 + \text{LiPF}_6$  solution bath with 200 & 10  $\mu\text{m}$  magnification respectively.

Table 4.1. Pore diameter range of CGPE under different conditions.

<b>Film type</b>	<b>Pore diameter range (um)</b>
CGPE before coating on trilayer PP separator	12.6 to 30μm
Coated CGPE before LiClO <sub>4</sub> +LiPF <sub>6</sub> solution bath	390 to 520 nm
Coated CGPE after LiClO <sub>4</sub> +LiPF <sub>6</sub> solution bath	420-610 nm

#### 4.4. EDS measurement of CGPE membrane after LiClO<sub>4</sub>+LiPF<sub>6</sub> solution bath

Table 4.2 shows the weight contribution of carbon, oxygen, hydrogen (3 dominant elements of PVDF-HFP) and lithium in CGPE. As can be seen, carbon and oxygen with the larger molar masses of 15.99 and 12.01 respectively accounted for the higher concentration ratio of 44.13 and 30.87% within the CGPE membrane. Although lithium and hydrogen showed lower concentration ratios of 11.24 and 13.75%, smaller atomic size and (molar mass) of these elements and oxidization of Li to Li<sub>2</sub>O could also attributed to their more limited detection by EDS tools. The 11.24% concentration ratio of lithium salt in EDS measurement followed by the results of SEM imaging in Figure 4.5e & 4.5f proved the successful incorporation of lithium ions into the composite gel polymer matrix after the incorporation of lithium salt solution.

Table 4.2. Weight contribution of carbon, oxygen, hydrogen (3 dominant elements of PVDF-HFP) and lithium in CGPE.

<b>Elt.</b>	<b>Intensity (c/s)</b>	<b>Conc. (wt.%)</b>	<b>Molar mass (g/M)</b>
H	3.00	<b>13.756</b>	<b>1.008</b>
Li	4.62	<b>11.244</b>	<b>6.941</b>
C	13.24	<b>44.130</b>	<b>12.0107</b>
O	8.22	<b>30.87</b>	<b>15.9994</b>

## 4.5. Electrochemical measurements

### 4.5.1. Electrochemical Impedance Spectroscopy (EIS)

As can be seen in figures 4.6a, 4.6b & 4.6c, bulk resistance of 1.2 k  $\Omega$ , 11.9  $\Omega$  and 7.7  $\Omega$  were achieved for GPE without the nano-fillers, basic CGPE and acidic CGPE corresponding to the ionic conductivity of  $0.99 \times 10^{-2}$ , 1 and 1.56  $\text{mS}\cdot\text{cm}^{-1}$  respectively as gathered in Table. 4.3. The thickness of the GPE and area of the electrode are  $T = 1.5 \text{ mm}$  and  $A = 4\pi \text{ cm}^2$  using Eqn. 3-3.

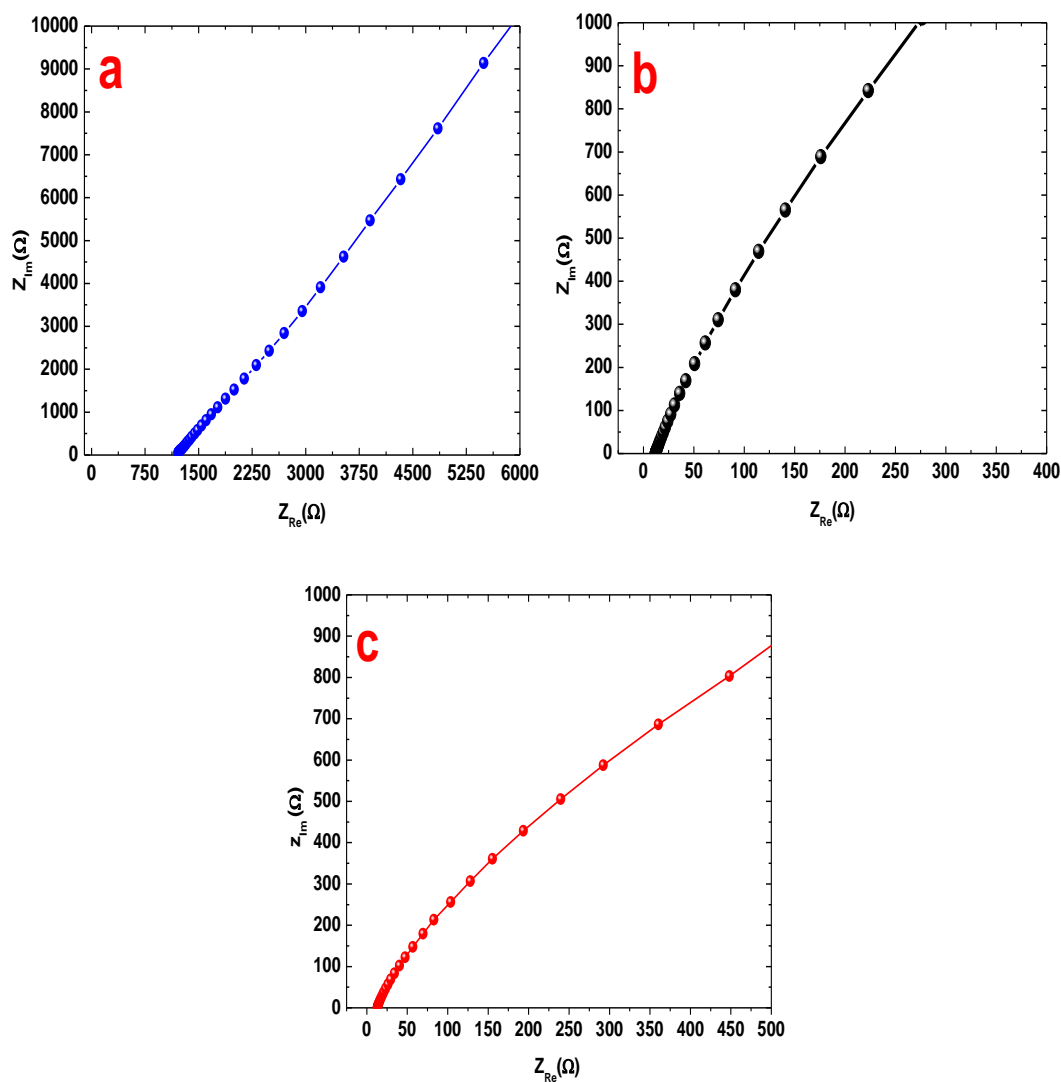


Figure 4.6. EIS of (a) GPE without nano fillers (b) acidic CGPE and (c) basic CGPE.

Table 4.3. Bulk resistance and ionic conductivity of different types of GPE.

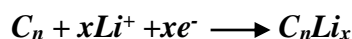
Type of electrolyte	Bulk resistance ( $Z_{re}$ ) ( $\Omega$ )	Ionic conductivity $\text{mS}\cdot\text{cm}^{-1}$
GPE without the nano-fillers	1.2 k	$0.99 * 10^{-2}$
basic CGPE	11.9	1
acidic CGPE	7.7	1.56

Followed by Kumar, Chung and Samiea *et al.*, nano fillers within the polymer electrolyte matrix increased the lithium ion transference number as well as the ionic conductivity due to their dipole interaction with the polymer matrix. Also, the lower glass transition temperature caused by addition of nano fillers resulted in easier segmental motion of the polymeric chains. This means that the voids provided by these sorts of motions gave rise to smoother flow of ions along the polymer backbone and chain [123-125]. Another critical reason for significant enhancement of ionic conductivity after addition of nano fillers is the better interfacial properties of the electrolyte in contact with the electrodes due to mechanical stability of ceramic particles [66]. As discussed in section 2.3.3, Lewis acid-base interactions are technically responsible for the contribution of the composite gel polymer membrane in transferring the lithium ions. The polar groups in modified nano fillers dissolved the lithium salt, leading to a columbic interaction between salt cations and surface hydroxyl (OH) anions of  $\text{TiO}_2$  and  $\text{SiO}_2$ . In this work, the modification of nano fillers by forming the polar groups on their surface caused a difference between bulk resistances of the basic CGPE compared to that of acidic one. This tendency could be related to the concentration of free ions after salt dissociation.

Acidic TiO<sub>2</sub> has had more hydroxyl groups which interact with salt cations, leading to acidic CGPE to have the higher concentration of free-ion.

#### 4.5.2. Cyclic Voltammetry (CV) measurement of the half cell lithium ion battery

Figures 4.7a & 4.7b show two major reactions happening in cyclic voltammetry (CV) measurement of Li-ion half cell, corresponding to reduction and oxidation of graphite. Reduction of graphite in half cell discharging process happens as Li<sup>+</sup> is being inserted into the graphite layers shown in equation below:



Oxidation of graphite in half cell charging process happens as Li<sup>+</sup> is being extracted from charged graphite shown in equation below:



According to figures 4.7a & 4.7b, oxidation peaks happening at (0.56 V, 0.1 mA) and (0.46 V, 0.012 mA) for acid and basic CGPE respectively. The sharper the peak of a reaction, the easier the reaction is done. As can be seen in CV plots, oxidation of graphite anode has sharper peak in acidic CGPE with current level of 0.1 mA compared to 0.012 mA for the basic CGPE. Likely, the reduction peaks happening at (0.31 V, -0.268 mA) for acidic CGPE and (0.291 V, -0.26 mA) for basic CGPE demonstrate a significant difference in the uniformity of the peaks in acidic CGPE compared to the basic CGPE. More stability of the acidic CGPE peaks prove the more immune environment with less affected by side reactions. These results could be attributed to the number of free cations and anions after salt's dissociation. After the modification of the nano fillers, dissociation of the lithium salt can occur through the interaction of anions in salt and surface OH groups of TiO<sub>2</sub> and SiO<sub>2</sub>. Acidic compound can accommodate the most number of OH

groups that can interact with lithium salt; therefore the reactions happening in CGPE with acidic properties can have the best overall performance.

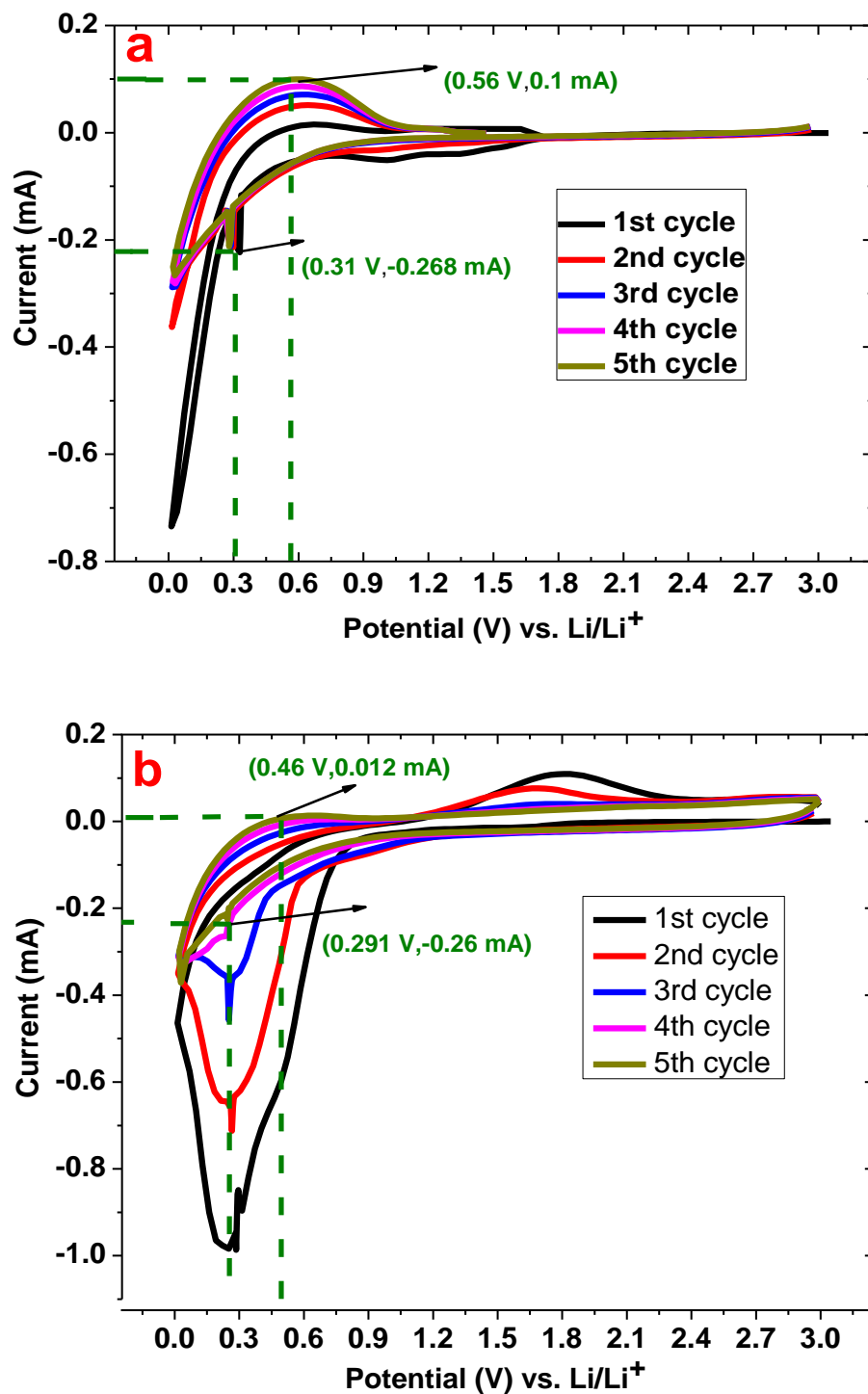
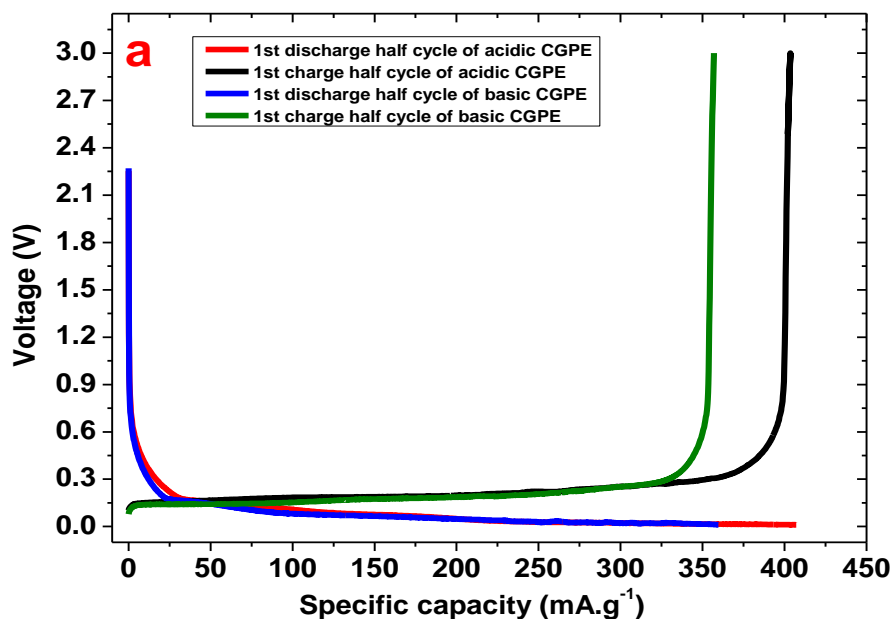


Figure 4.7. Cyclic voltammograms of (a) acidic CGPE and (b) basic CGPE.

### 4.5.3. Charge and discharge cycle of the half cell lithium ion battery

Figures 4.8a & 4.8b show galvanostatic discharge and charge curves of CGPE for the 1<sup>st</sup> and 40<sup>th</sup> cycles respectively. As can be seen in figure 4.8a, reversible capacities of 408.5 and 347.18 mA.h.g<sup>-1</sup> were observed for 1<sup>st</sup> cycle of acidic and basic CGPE respectively. Figure 4.8b also demonstrates the reversible capacities of 317 and 247 mA.h.g<sup>-1</sup> for 40<sup>th</sup> cycle of acidic and basic CGPE respectively. Higher capacity in acidic compound can be attributed to the larger dissociation rate observed in EIS and CV measurements. In basic compound, when the hydrolyzed TEOS was dried, the solvents was evaporate but there was still unreacted cross-linking of -OR and -OH groups [32]. Likely, acid treated TiO<sub>2</sub> had excess protons in HNO<sub>3</sub> which was adsorbed on the surface of oxygen in a neutral anatase TiO<sub>2</sub>. In acidic compound, the higher concentrations of the hydroxyl functional groups resulted in higher dissociation rate of lithium salt in a CGPE compared to that of basic compound [33].





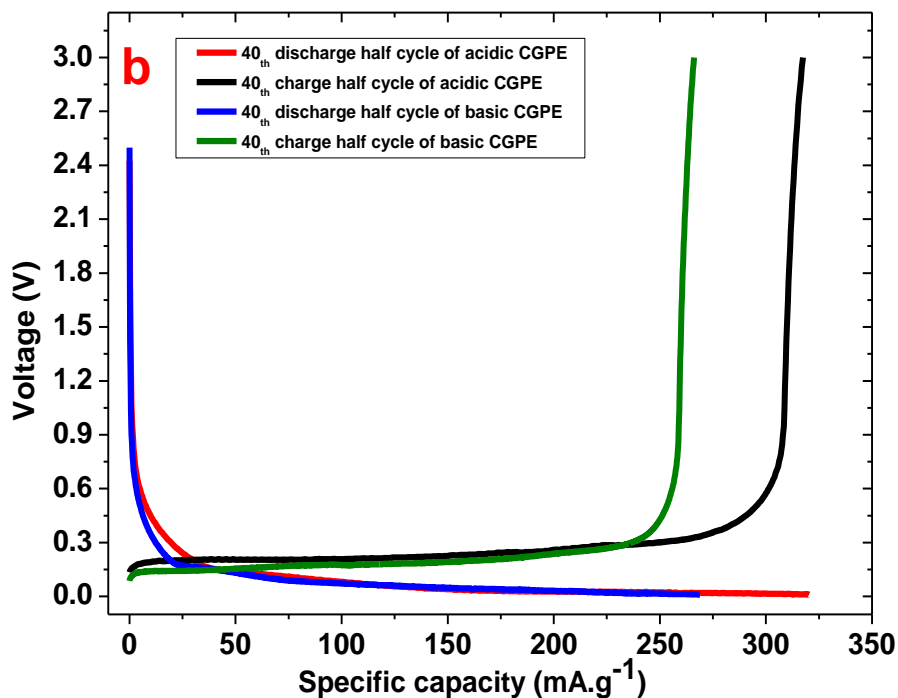


Figure 4.8. Galvanostatic charge-discharge voltage profiles of acidic and basic CGPE for (a) 1st cycle and (b) 40<sup>th</sup> cycle @ C/20.

#### 4.5.4. Rate capability measurement of the half cell lithium ion batteries

Rate capabilities of both CGPE half cells are shown in figure 4.9 at different constant current rates of C/20, C/8, C/4, C/2, C and again back to C/20. Table 4.4 & 4.5 summarize the specific capacities of acidic and basic CGPE at different constant current rates respectively. The rate capabilities of both CGPE half cells show better compatibility of cells' performance under C/20 compared to higher constant current rates. The fade of specific capacity in higher constant current rate of C/8 to C is happening slightly more in acidic CGPE than that of basic. This can be attributed to the accumulation of higher density of dissociated ions in acidic CGPE that could not successfully travel towards the electrodes through the electrolyte membrane under the electric field. In higher constant current rate, the level of current being applied to the half cell increases while the time for

a full cycle accordingly decreases. In this work, since the concentration of the ionic species such as -OH functional groups was enhanced, the transfer of the ions throughout the electrolyte membrane could face a higher traffic. The slightly lower capacity rate in acidic CGPE in higher constant current rates was followed by the higher number of free ions that were unsuccessful to travel through the electrolyte membrane in a designated time. Meaning that in C/20 rate, a constant current rate of 0.2 mA took almost 20 h to fully charge and discharge the half cell. While in C rate, it took almost one hour for the half cell to go through a full charge and discharge cycle under 1 mA of applied constant current. This can tell us that under an optimized charge/discharge current rate, the performance of the acidic CGPE is overly better.

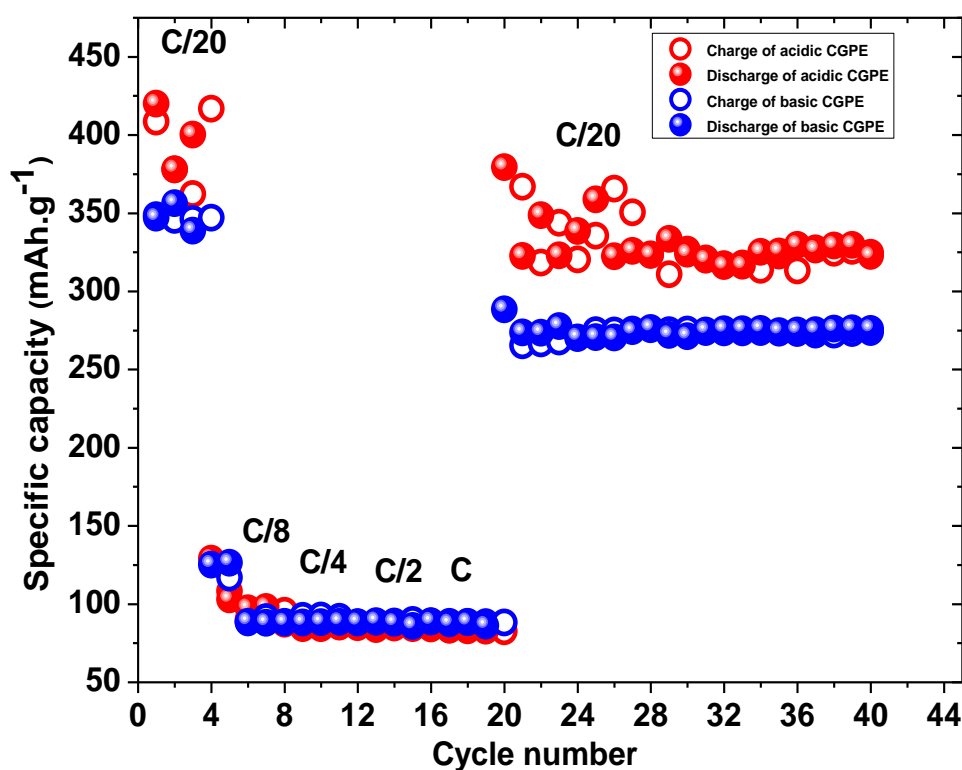


Figure 4.9. Rate capability of acidic and composite gel polymer electrolyte half cells @ different constant current rates.

Table 4.4. Specific capacity of acidic CGPE at different cycle numbers and constant current rates.

Cycle number	Specific charge capacity range (mAh.g <sup>-1</sup> )	Specific discharge capacity range (mAh.g <sup>-1</sup> )	Constant current rate
1-4	362-416	128-420	C/20
5-8	89-108	87-103	C/8
9-12	85-86	84-86	C/4
13-16	85-87	84-85	C/2
17-20	82-83	82-379	C
21-40	310-375	282-399	C/20

Table 4.5. Specific capacity of basic CGPE at different cycle numbers and constant current rates.

Cycle number	Specific charge capacity range (mAh.g <sup>-1</sup> )	Specific discharge capacity range (mAh.g <sup>-1</sup> )	Constant current rate
1-4	345-348	125-356	C/20
5-8	88-116	84-116	C/8
9-12	82-92	88	C/4
13-16	88-89	86-88	C/2
17-20	88	86-288	C
21-40	265-275	270-277	C/20

## CHAPTER 5. CONCLUSIONS

### 5.1. Summary

The American Physical Society presaged that the household demand of energy is claimed to increase by 30% in the next 10 years. The urge for an affordable and clean source of energy as an alternative for the fossil fuel paved the way for renewable energy power plants. Unfortunately, the fluctuation nature of these sources makes them insufficient and/or unstable for all time use. Introducing the storage system can stabilize the renewable energy sources [5].

Secondary batteries can be addressed by their rechargeable nature compared to primary batteries. Primary batteries are more cost effective and have higher energy density, initial voltage and capacity while are not mostly recyclable or sufficient for portable use since they cannot be recharged. Among all the battery prototypes, alkaline and zinc-carbon batteries from primary batteries and lithium ion, lead acid, and nickel cadmium from secondary batteries are the most commonly used devices in which lithium ion batteries have dominated the market in last decades due to their higher specific energy, specific capacity, cycle durability, columbic efficiency, easier maintenance, very low self discharge rate and more simple charge/discharge cycling properties [49].

The development of battery industry has been through a long journey since the 17<sup>th</sup> century. In 1985 Japanese scientist Akira Yoshino managed to build the first lithium ion battery device where the battery was rechargeable with dominant advantages over its lithium battery prototypes in case of electrode stability over charge and discharge cycling, paving its way to commercialization of lithium ion batteries in 1991 by Sony. In 1997, lithium polymer batteries with solid polymer/composite electrolyte were introduced

where the safety drawbacks of the initial prototypes were eliminated but the ionic conductivity of the batteries have been critical issue due to the lower ion transfer rate in a solid state compared to that of a liquid [28].

Gel polymer electrolyte containing PVdF-HFP as the polymer host was first proposed by Capiglia *et al.* where changing the concentration of the lithium salt altered the ionic conductivity in a wide range of  $10^{-8}$  to  $10^{-2}$  S.cm<sup>-1</sup>. The popularity of lithium ion vs. lithium metal batteries yet is technically due to the more immune nature of lithium ion based batteries when it comes to unfavorable reactions such as decomposition of the electrodes and SEI layer formation [51, 53]. However, there is a strong need for a highly conductive gel polymer electrolyte for lithium polymer batteries to replace the current organic liquid electrolyte with leakage and ignition issues. In this work, the objective was to develop a highly conductive gel polymer electrolyte for lithium polymer batteries through solution casting the mixture of PVDF-HFP and charge modified nano fillers on an O<sub>2</sub> plasma treated trilayer PP separator.

Solid electrolyte itself has two main categories: (I) inorganic solid electrolyte such as ceramics, and (II) solid/gel organic polymer electrolyte which can be doped with inorganic fillers and shape the composite polymer electrolyte. Polymer gels own closer conduction mechanism to liquid electrolyte than that of solid. While gel polymer electrolyte normally possesses a lower ionic conductivity of around  $10^{-3}$  Scm<sup>-1</sup> at room temperature compared to  $10^{-2}$  Scm<sup>-1</sup> order of magnitude for liquid electrolytes, gel polymers have improved safety and flexibility. In a PVdF-HFP), HFP provides an amorphous phase in which the liquid electrolyte is trapped and ion movements happens through the more porous structure. Also, the PVdF phase due to its crystalline properties

contributes in mechanical stability [65-71]. Plasticizing the polymer matrix will decrease the regional viscosity and facilitate the transfer of the mobile lithium ions through smoother paths. Also, the mechanical stability of the polymer matrix can be enhanced by adding nano fillers such as  $\text{Al}_2\text{O}_3$ ,  $\text{TiO}_2$ ,  $\text{SiO}_2$  and etc. The active fillers can contribute in total ionic conduction of the electrolyte due to the presence of the Li ions in their structure e.g.  $\text{LiAl}_2\text{O}_3$  while passive fillers such as  $\text{TiO}_2$  and  $\text{SiO}_2$  are not involved in Li ion conduction process. Among the variety of the salts,  $\text{LiClO}_4$  has attracted a lot of attention because of its high stability in ambient atmosphere. However, the chemical and thermal consistency of  $\text{LiPF}_6$  makes it the most balanced salt [66]. In our work, the gel type polymer electrolyte was coated on to the commercial trilayer PP separator membrane where the absorption properties of the highly hydrophobic separator membranes were enhanced through irradiation of plasma which increases the surface energy of the separator due to emergence of oxide dangling bonds. [106, 111].

## 5.2. Conclusion

In this work, the method offered by Li *et al.* was improved by modifying the surface charge properties of  $\text{SiO}_2$  and  $\text{TiO}_2$  nano fillers through acid and base treatments in the CGPE membranes and their effects on the half-cell Li ion battery performance was examined [98]. pH treatment of neutral  $\text{TiO}_2$  to acidic active filler and neutral  $\text{SiO}_2$  to basic active filler caused modified surface charge properties on the passive nano fillers which were the novelty of this work. The better adhesion of gel polymer electrolyte itself on the trilayer PP separator was due to the  $\text{O}_2$  plasma treatment of the separator prior to gel coating. Also, the submicron pore size of the gel polymer electrolyte after coating on trilayer PP separator was suitable to assure the possibility of internal short circuit by

electrode material or formation of diffused SEI layer are minimized. Also, after the incorporation of  $\text{LiClO}_4+\text{LiPF}_6$  solution into the CGPE coated trilayer PP separator, the pore morphology transformed from circular to spherical shape which was a result of the liquid electrolyte uptake by the available pores. Capacities of 408.5/317.0 mAh/g for acidic CGPE and 347.1/247.0 for basic CGPE were achieved for 1<sup>st</sup> and 40<sup>th</sup> cycles respectively, in which the sharper oxidation/reduction peaks in acidic CGPE represent faster Li ion transfer kinetics compared to the basic one. Also, impedance studies showed us that the addition of ceramic filler reduced the bulk resistance at the interfaces, in which the ionic conductivity increased from the range of  $10^{-5}$  to  $10^{-3}$  after addition of charge modified nano fillers due to the reduction in bulk resistance of CGPE at the interfaces.

### 5.3. Future work

Gel and solid polymer have the ionic conductivities of between  $10^{-8}$  to  $10^{-2}$   $\text{Scm}^{-1}$  depending on the structure of the electrolyte membrane while for liquid electrolyte it always lays at around  $10^{-2}$   $\text{Scm}^{-1}$ . In such a case, enhancing the ion transport rate in a solid membrane is the most challenging approach for a safer lithium ion battery. First and foremost, for a solid or gel polymer membrane to have acceptable ionic conductivity, a highly porous structure of polymer electrolyte membrane is required. Two common ways to achieve a good ionic conductor polymer membrane are as followed: (I) introducing alternative polymer blends such as PVDF-HFP co-polymer that has complimentary properties of both polymer hosts. (II) cross linking the polymer hosts by incorporating side chains that work as channels for lithium ions' transport. The selection of non-flammable and more volatile organic plasticizers and addition of an active nano-filler

with large size anions to attract more number of lithium cations are among the most popular methods of ionic conductivity enhancement as well [146]. The CGPE prepared in this work can be implemented in a full cell lithium ion battery for further applications such as combining it with a thin film solar cell where the leakage of the liquid electrolyte is a primary issue in order to seal the full cell lithium polymer battery-solar cell in one combined device.



## REFERENCES

- [1] T. Cotterman, "Transforming America's intelligent electrical infrastructure," IEEE-USA2013.
- [2] B. McGuire. (2015, 7/26/2016). *The Changing Earth* Available: [http://rockyrexscience.blogspot.com/2015\\_04\\_01\\_archive.html](http://rockyrexscience.blogspot.com/2015_04_01_archive.html)
- [3] P. Eiamlamai, "Polymer electrolytes based on ionic liquids for lithium batteries," Université Grenoble Alpes, 2015.
- [4] M. E. V. Team, "A Guide to Understanding Battery Specifications," December 2008.
- [5] E. E. P. Denholm, B. Kirby, M. Milligan, "The role of energy storage with renewable electricity generation," January 2010.
- [6] T. Randall. (Feb. 25, 2016). *Here's How Electric Cars Will Cause the Next Oil Crisis*. Available: <http://www.bloomberg.com/features/2016-ev-oil-crisis/>
- [7] I. r. e. agency, "Battery storage for renewable: market status and technology," January 2015.
- [8] K. Hamilton, "Energy Storage: State of the Industry," Energy Storage Association2015.
- [9] M. H. J. F. Rohan, S. Patil, D. P. Casey, T. Clancy, "Energy Storage: Battery Materials and Architectures at the Nanoscale," Tyndall National InstituteMarch 2013.
- [10] B. Kramer-Miller. (5/12/2016). *What Investors Need To Know About Lithium Ion Batteries*. Available: <http://seekingalpha.com/article/3811586-investors-need-know-lithium-ion-batteries>
- [11] R. S. Treptow, "The lead-acid battery: its voltage in theory and practice," *Journal of chemical education*, vol. 79 p. 334, 2002.
- [12] U. Irfan. (December 18, 2014). *How Lithium Ion Batteries Grounded the Dreamliner*. Available: <http://www.scientificamerican.com/article/how-lithium-ion-batteries-grounded-the-dreamliner/>
- [13] (December 11, 2006). *Lithium Polymer Batteries: A Review*. Available: <http://www.treehugger.com/gadgets/lithium-polymer-batteries-a-review.html>
- [14] A. F.-B. NEWS. (Thursday, 27 February). *Riddle of 'Baghdad's batteries'*. Available: <http://news.bbc.co.uk/2/hi/science/nature/2804257.stm>
- [15] B. University. (5/27/2016). *when was the battery invented*. Available: [http://batteryuniversity.com/learn/article/when\\_was\\_the\\_battery\\_invented](http://batteryuniversity.com/learn/article/when_was_the_battery_invented)
- [16] E. P. Krider, "Benjamin Franklin and the first lighting conductors," 2004.
- [17] O. Levi, "Alessandro Volta and the voltaic pile," 2011.
- [18] W. B. Jensen, "The Daniell cell," October 2013.
- [19] C. W. B. M. BRAIN, C. PUMPHREY (2016, 6/12/2016). *How Batteries Work*. Available: <http://electronics.howstuffworks.com/everyday-tech/battery1.htm>
- [20] "History of the battery," in *Wikipedia*, ed.
- [21] (7/5/2016). *THE ALEXANDER CELL*. Available: <http://www.pipeline-corrosion-control.co.uk/Nigeria/ProcHTML/proc13.htm>
- [22] "Lead-acid battery," in *Wikipedia*, ed.
- [23] "Camille Alphonse Faure," in *Wikipedia*, ed.

- [24] (2016, 6/18/2016). *Carl Gassner – inventor of dry cell battery*. Available: <http://www.worldofchemicals.com/32/chemistry-articles/carl-gassner-inventor-of-dry-cell-battery.html>
- [25] (6/20/2016). *The Lead-Acid Car Battery*. Available: <http://schoolworkhelper.net/the-lead-acid-car-battery/>
- [26] (2016, 7/4/2016). *The Laclanche Cell*. Available: <http://astarmathsandphysics.com/o-level-physics-notes/256-the-leclanche-cell.html>
- [27] (6/28/2016). *The Oldest Battery* Available: <http://thegreatbattery.yolasite.com/the-oldest-battery.php>
- [28] P. J. DeMar, "Nickel-Iron," IEEE-USA, IEEE 33rd international Telecommunications Energy Conference 2011.
- [29] "History of the battery " in *Wikipedia*, ed.
- [30] "John B. Goodenough," in *Wikipedia*, ed.
- [31] "Rachid Yazami," in *Wikipedia*, ed.
- [32] B. University. (5/6/2016). *Lithium Ion Safety Concerns*. Available: [http://batteryuniversity.com/learn/article/lithium\\_ion\\_safety\\_concerns](http://batteryuniversity.com/learn/article/lithium_ion_safety_concerns)
- [33] "Micheal Armand Hammer " in *Wikipedia* ed.
- [34] A. M. Stephan, "Review on gel polymer electrolytes for lithium batteries," *European Polymer Journal*, vol. 42, pp. 21-42, 2006.
- [35] O. V. Y. Y. V. Baskakova, O. N. Efimov, "Polymer gel electrolytes for lithium batteries," *Russian chemical reviews*, vol. 81, pp. 367-380, 2012.
- [36] M. Kucharski, T. Łukaszewicz, and P. Mrozek, "New electrolyte for electrochromic devices," *Opto-Electronics Review*, vol. 12, pp. 175-180, 2004.
- [37] J.-H. K. K. J. Kim, M.-S. Park, H. K. Kwon, H. Kim, Y.-J. Kim, "Enhancement of electrochemical and thermal properties of polyethylene separators coated with polyvinylidene fluoride-hexafluoropropylene co-polymer for Li-ion batteries," *Journal of Power Sources*, vol. 198, pp. 298-302, 2012.
- [38] K. S. N. A. M. Stephan, "Review on composite polymer electrolytes for lithium batteries," *Journal of Polymer*, vol. 47, pp. 5952-5964, 2006.
- [39] A. K. D. Saikia, "Fast ion transport in P(VDF-HFP)-PMMA-PC-LiClO<sub>4</sub>-TiO<sub>2</sub> composite gel polymer electrolytes," *Indian Journal of Pure & Applied Physics*, vol. 41, pp. 961-966, 2003.
- [40] R. Zhang, "Advanced gel polymer electrolyte for lithium-ion polymer batteries," Master thesis and dissertation, Iowa State University, 2013.
- [41] P. V. V. Aravindan, S. Madhavi, A. Sivashanmugam , R. Thirunakaran , S. Gopukumar, "Improved performance of polyvinylidene fluoride-hexafluoropropylene based nanocomposite polymer membranes containing lithium bis(oxalato)borate by phase inversion for lithium batteries," *Journal of Solid State Sciences*, vol. 13, pp. 1047-1051, 2013.
- [42] D. Y. T. W. W. Cui, "Electrospun poly(lithium 2-acrylamido-2-methylpropanesulfonic acid) fiber-based polymer electrolytes for lithium-ion batteries," *Journal of applied polymer science*, vol. 126, pp. 510-518, 2012.
- [43] "List of battery types," in *Wikipedia*, ed.

- [44] B. unievrstiy. (6/15/2016). *Global Battery market Information-Nickel based batteries*. Available: [http://batteryuniversity.com/learn/article/nickel\\_based\\_batteries](http://batteryuniversity.com/learn/article/nickel_based_batteries)
- [45] B. University. (6/14/2016). *Global Battery Markets Information*. Available: [http://batteryuniversity.com/learn/article/global\\_battery\\_markets](http://batteryuniversity.com/learn/article/global_battery_markets)
- [46] B. University. (6/14/2016). *Global Battery market Information-Lead based batteries*. Available: [http://batteryuniversity.com/learn/article/lead\\_based\\_batteries](http://batteryuniversity.com/learn/article/lead_based_batteries)
- [47] S. V. A.K. Shukla, B. Hariprakash, "Nickel-based rechargeable batteries," *Journal of power sources*, vol. 100, pp. 125–148, 2001.
- [48] A. Kasaei, "Course of development of lithium-ion battery, and future outlook," March 2013.
- [49] "Lithium ion battery " in *Wikipedia*, ed.
- [50] B. University. (6/17/2016). *Global Battery market Information-lithium based batteries*. Available: [http://batteryuniversity.com/learn/article/lithium\\_based\\_batteries](http://batteryuniversity.com/learn/article/lithium_based_batteries)
- [51] M. Yuan, "Poly (Ethylene Oxide)/Graphene Oxide Polymer Nanocomposite Electrolyte for Lithium Ion Batteries," Thesis for master of Engineering Science, University of Houston, 2013.
- [52] (5/3/2016). *BATTERY CELL COMPARISON*. Available: <http://www.epectec.com/batteries/cell-comparison.html>
- [53] T. B. R. D. Linden. (2001). *Handbook of batteries (3rd ed.)*.
- [54] C. Woodford. (6/4/2016). *Lithium-ion batteries*. Available: <http://www.explainthatstuff.com/how-lithium-ion-batteries-work.html>
- [55] H. Y. W. Li, K. Yan, G. Zheng, Z. Liang, Y. M. Chiang, Y. Cui, "The synergetic effect of lithium polysulfide and lithium nitrate to prevent lithium dendrite growth," *Journal of nature communications*, vol. 10.1038/ncomms8436, June 2015.
- [56] J. B. Goodenough, "Report on Rechargeable Batteries, Old and New," University of Texas at Austin 2015.
- [57] (December 7, 2015). *Basic technology of high thermally-durable all-solid-state lithium ion battery developed*. Available: <https://www.sciencedaily.com/releases/2015/12/151207100007.htm>
- [58] S. M. P. V. V. Aravindan, A. Sivashanmugam , R. Thirunakaran , S. Gopukumar, "Improved performance of polyvinylidene fluoride-hexafluoropropylene based nanocomposite polymer membranes containing lithium bis(oxalato)borate by phase inversion for lithium batteries," *Journal of Solid State Sciences*, vol. 13, pp. 1047-1051, 2013.
- [59] M. J. G. B. J. Landi , C. D. Cress† , R. A. DiLeo, R. P. Raffaele "Carbon nanotubes for lithium ion batteries," *Energy & Environmental Science*, vol. 2, pp. 638-654, 2009.
- [60] J. W. Fergus, "Recent developments in cathode materials for lithium ion batteries," *Journal of Power Sources*, vol. 195, pp. 939–954, 2010.
- [61] F. W. N. Nitta, J. T. Lee, G. Yushin, "Li-ion battery materials: present and future," *Journal of materials today*, vol. 18, pp. 252-264, 2015.

- [62] A. K. T. Kawamura, M. Egashira, S. Okada, and J.-I. Yamaki, "Thermal stability of alkyl carbonate mixed-solvent electrolytes for lithium ion cells," *Journal of Power Sources*, vol. 104, pp. 260-264, 2002.
- [63] D. S. B. D. McCloskey, R. M. Shelby, G. Girishkumar, and A. C. Luntz, "Solvents' Critical Role in Nonaqueous Lithium–Oxygen Battery Electrochemistry," *Journal of Physical Chemistry Letters*, vol. 2, pp. 1161-1166, 2011.
- [64] Y. Y. W. J. Y. Song, and C. C. Wan, "Review of gel-type polymer electrolytes for lithium-ion batteries," *Journal of Power Sources*, vol. 77, pp. 183-197, 1999.
- [65] J. Y. Song, Y. Y. Wang, and C. C. Wan, "Review of gel-type polymer electrolytes for lithium-ion batteries," *Journal of Power Sources*, vol. 77, pp. 183-197, 2// 1999.
- [66] A. Manuel Stephan and K. S. Nahm, "Review on composite polymer electrolytes for lithium batteries," *Polymer*, vol. 47, pp. 5952-5964, 7/26/ 2006.
- [67] R. Miao, B. Liu, Z. Zhu, Y. Liu, J. Li, X. Wang, *et al.*, "PVDF-HFP-based porous polymer electrolyte membranes for lithium-ion batteries," *Journal of Power Sources*, vol. 184, pp. 420-426, 2008.
- [68] Y. Li, Y. Yin, K. Guo, X. Xue, Z. Zou, X. Li, *et al.*, "Tuning pore structure of the poly(vinylidene difluoride hexafluoropropylene) membrane for improvement in rate performance of Li–oxygen battery," *Journal of Power Sources*, vol. 241, pp. 288-294, 11/1/ 2013.
- [69] V. Aravindan, P. Vickraman, S. Madhavi, A. Sivashanmugam, R. Thirunakaran, and S. Gopukumar, "Improved performance of polyvinylidene fluoride–hexafluoropropylene based nanocomposite polymer membranes containing lithium bis(oxalato)borate by phase inversion for lithium batteries," *Solid State Sciences*, vol. 13, pp. 1047-1051, 5// 2011.
- [70] J. Wilson, G. Ravi, and M. A. Kulandainathan, "Electrochemical studies on inert filler incorporated poly (vinylidene fluoride - hexafluoropropylene) (PVDF - HFP) composite electrolytes," *Polímeros*, vol. 16, pp. 88-93, 2006.
- [71] D. Saikia and A. Kumar, "Ionic conduction in P (VDF-HFP)/PVDF–(PC+ DEC)–LiClO<sub>4</sub> polymer gel electrolytes," *Electrochimica Acta*, vol. 49, pp. 2581-2589, 2004.
- [72] C.-Y. Chiang, Y. J. Shen, M. J. Reddy, and P. P. Chu, "Complexation of poly(vinylidene fluoride):LiPF<sub>6</sub> solid polymer electrolyte with enhanced ion conduction in 'wet' form," *Journal of Power Sources*, vol. 123, pp. 222-229, 9/20/ 2003.
- [73] N. Shukla and A. K. Thakur, "Role of salt concentration on conductivity optimization and structural phase separation in a solid polymer electrolyte based on PMMA-LiClO<sub>4</sub>," *Ionics*, vol. 15, pp. 357-367, 2009.
- [74] S. P. D. Bresser, B. Scrosati, "Recent progress and remaining challenges in sulfur-based lithium secondary batteries – a review," *Journal of chemical communications*, vol. 49, pp. 10545-10562.
- [75] A. A. M. V. I. Volkov, "NMR methods for studying ion and molecular transport in polymer electrolytes," *Russian academy of science and turpion*, vol. 82, pp. 248-272, 2013.

- [76] T. K. Wui, "Studies on the properties of PMMA-based polymer electrolyte for lithium rechargeable battery," master of Engineering Science, Tunku Abdul Rhaman.
- [77] K. S. N. A. M. Stephan, "Review on composite polymer electrolytes for lithium batteries," *Polymer*, vol. 47, pp. 5952-5964, 2006.
- [78] J. C. P. Hu, Y. Duan, Z. Liu, G. Cui, L. Chen, "Progress in nitrile-based polymer electrolytes for high performance lithium batteries," *Journal of Materials Chemistry A*, 2016.
- [79] Y. J. S. C.-Y. Chiang, M. J. Reddy, P. P. Chu, "Complexation of poly(vinylidene fluoride):LiPF<sub>6</sub> solid polymer electrolyte with enhanced ion conduction in 'wet' form," *Journal of Power Sources*, vol. 123, pp. 222-229, 2003.
- [80] A. K. T. I. N. Shukla, "Role of salt concentration on conductivity optimization and structural phase separation in a solid polymer electrolyte based on PMMA-LiClO<sub>4</sub>," vol. 15, pp. 357-367, 2009.
- [81] F. Croce, L. Persi, B. Scrosati, F. Serraino-Fiory, E. Plichta, and M. A. Hendrickson, "Role of the ceramic fillers in enhancing the transport properties of composite polymer electrolytes," *Electrochimica Acta*, vol. 46, pp. 2457-2461, 5/1/ 2001.
- [82] L. P. F. Croce, B. Scrosati, F. Serraino-Fiory, E. Plichta, M. A. Hendrickson, "Role of the ceramic fillers in enhancing the transport properties of composite polymer electrolytes," *Electrochimica Acta*, vol. 46, pp. 2457-2461, 2001.
- [83] A. S. M. A. Lewandowski, "Ionic liquids as electrolytes for Li-ion batteries—An overview of electrochemical studies," *Journal of power sources*, vol. 194, pp. 601-609, 2009.
- [84] T. A. A. N. Madria, N. G. Nair, A. Vadapalli, Y. W. Huang, S. C. Jones, V. P. Reddy, "Ionic liquid electrolytes for lithium batteries: Synthesis, electrochemical, and cytotoxicity studies," *Journal of power sources*, vol. 234, pp. 277-284, 2013.
- [85] K. Binnemans, "Ionic Liquid Crystals," *Chemical Reviews*, vol. 105, pp. 4148-4204, 2005.
- [86] H. Crichton. (2013, March 22, 2013). *Polymer electrolytes integrated with ionic liquids*. Available: <http://www.materialsvIEWS.com/polymer-electrolytes-integrated-with-ionic-liquids/>
- [87] S. H. C. J. M. G. Cowie, "Electrolytes Dissolved in Polymers," *Annual Review of Physical Chemistry*, vol. 40, pp. 85-113, 1989.
- [88] J.-S. C. H.-M. Xiong, D.-M. Li, "Controlled growth of Sb<sub>2</sub>O<sub>5</sub> nanoparticles and their use as polymer electrolyte fillers," *Journal of Materials Chemistry*, vol. 13, pp. 1994-1998, 2003.
- [89] Y. T. R. Kanno, T. Ichikawa, K. Nakanishi, O. Yamamoto, "Carbon as negative electrodes in lithium secondary cells," *Journal of Power Sources*, vol. 26, pp. 535-543, 1989.
- [90] H. C. E. T. C. Nardelli, B. Robaire, "Toxicogenomic Screening of Replacements for Di(2-Ethylhexyl) Phthalate (DEHP) Using the Immortalized TM4 Sertoli Cell Line," *PLoS ONE*, vol. 10, p. p. e0138421, 200.
- [91] W. H. Meyer, "Polymer Electrolytes for Lithium-Ion Batteries," *Advanced materials*, vol. 10, pp. 439-448, 1998.

- [92] P. N. K. P. C. Sekhar, A. K. Sharma, "Effect of plasticizer on conductivity and cell parameters of (PMMA+NaClO<sub>4</sub>) polymer electrolyte system," *Journal of applied physics*, vol. 2, pp. 1-6, 2012.
- [93] M. S. S. Rajendran, R. Subadevi, "Investigations on the effect of various plasticizers in PVA–PMMA solid polymer blend electrolytes," *Materials Letters*, vol. 58, pp. 641-649, 2004.
- [94] (2006). *Making polyemrs*. Available: <http://slideplayer.com/slide/6974541/>
- [95] A. K. A. M. M. E. Jacob, "FTIR studies of DMF plasticized polyvinylidene fluoride based polymer electrolytes," *Electrochimica Acta*, vol. 45, pp. 1701-1706, 2000.
- [96] S. S. R. Baskaran, N. Kuwata, J. Kawamura, T. Hattori, "Conductivity and thermal studies of blend polymer electrolytes based on PVAc–PMMA," *Journal of solid state ionics*, vol. 177, pp. 2679-2682, 2006.
- [97] K. Xu, "Nonaqueous Liquid Electrolytes for Lithium-Based Rechargeable Batteries," *Journal of chemical reviews*, vol. 104, pp. 4303-4417.
- [98] X. Li, J. He, D. Wu, M. Zhang, J. Meng, and P. Ni, "Development of plasma-treated polypropylene nonwoven-based composites for high-performance lithium-ion battery separators," *Electrochimica Acta*, vol. 167, pp. 396-403, 6/10/ 2015.
- [99] Q.-B. Lin, L.-W. Wang, and S.-H. Huang, "Effects of different treatment of TiO<sub>2</sub> electrodes on photovoltaic characteristics of dye-sensitized solar cells," *Surface Engineering and Applied Electrochemistry*, vol. 51, pp. 394-400, 2015.
- [100] G. Parashar, D. Srivastava, and P. Kumar, "Ethyl silicate binders for high performance coatings," *Progress in Organic Coatings*, vol. 42, pp. 1-14, 6// 2001.
- [101] D. Fu, B. Luan, S. Argue, M. N. Bureau, and I. J. Davidson, "Nano SiO<sub>2</sub> particle formation and deposition on polypropylene separators for lithium-ion batteries," *Journal of Power Sources*, vol. 206, pp. 325-333, 5/15/ 2012.
- [102] E. Zelazowska, M. Borczuch-Laczka, and E. Rysiakiewicz-Pasek, "Sol–gel derived organic–inorganic hybrid electrolytes for thin film electrochromic devices," *Journal of Non-Crystalline Solids*, vol. 353, pp. 2104-2108, 6/15/ 2007.
- [103] C.-Y. Chiang, M. Jaipal Reddy, and P. P. Chu, "Nano-tube TiO<sub>2</sub> composite PVdF/LiPF<sub>6</sub> solid membranes," *Solid State Ionics*, vol. 175, pp. 631-635, 11/30/ 2004.
- [104] B. Kurc and T. Jesionowski, "Modified TiO<sub>2</sub>-SiO<sub>2</sub> ceramic filler for a composite gel polymer electrolytes working with LiMn<sub>2</sub>O<sub>4</sub>," *Journal of Solid State Electrochemistry*, vol. 19, pp. 1427-1435, 2015// 2015.
- [105] F. Croce, G. B. Appetecchi, L. Persi, and B. Scrosati, "Nanocomposite polymer electrolytes for lithium batteries," *Nature*, vol. 394, pp. 456-458, 07/30/print 1998.
- [106] J. Fang, A. Kellarakis, Y.-W. Lin, C.-Y. Kang, M.-H. Yang, C.-L. Cheng, *et al.*, "Nanoparticle-coated separators for lithium-ion batteries with advanced electrochemical performance," *Physical Chemistry Chemical Physics*, vol. 13, pp. 14457-14461, 2011.
- [107] Y.-H. A. Y.-J. Lim, N.-J. Jo, "Polystyrene-Al<sub>2</sub>O<sub>3</sub> composite solid polymer electrolyte for lithium secondary battery," *Nanoscale Research Letters*, vol. 7, pp. 1-6, 2012.

- [108] M.-K. Song, J.-Y. Cho, B. W. Cho, and H.-W. Rhee, "Characterization of UV-cured gel polymer electrolytes for rechargeable lithium batteries," *Journal of Power Sources*, vol. 110, pp. 209-215, 7/20/ 2002.
- [109] K. J. Kim, J.-H. Kim, M.-S. Park, H. K. Kwon, H. Kim, and Y.-J. Kim, "Enhancement of electrochemical and thermal properties of polyethylene separators coated with polyvinylidene fluoride-hexafluoropropylene co-polymer for Li-ion batteries," *Journal of Power Sources*, vol. 198, pp. 298-302, 1/15/ 2012.
- [110] J. Y. Lee, Y. M. Lee, B. Bhattacharya, Y.-C. Nho, and J.-K. Park, "Separator grafted with siloxane by electron beam irradiation for lithium secondary batteries," *Electrochimica Acta*, vol. 54, pp. 4312-4315, 7/15/ 2009.
- [111] J. W. Fergus, "Ceramic and polymeric solid electrolytes for lithium-ion batteries," *Journal of Power Sources*, vol. 195, pp. 4554-4569, 8/1/ 2010.
- [112] "Polyvinylidene fluoride," in *wikipedia*, ed.
- [113] J. M. D. Tamer S. Ahmed, George W. Roberts, "Continuous Copolymerization of Vinylidene Fluoride with Hexafluoropropylene in Supercritical Carbon Dioxide: High-Hexafluoropropylene-Content Amorphous Copolymers," *Macromolecules*, vol. 41, pp. 3086-3097, 2008.
- [114] (2016). *Poly(vinylidene fluoride-co-hexafluoropropylene)*. Available: <http://www.sigmaaldrich.com/catalog/product/aldrich/427187?lang=en&region=US>
- [115] "Dimethylformamide," in *wikipedia*, ed.
- [116] M. Z. A. Munshi, Ed., *Handbook of Solid State Batteries and Capacitors*. 1995, p.^pp. Pages.
- [117] Y. T. Doron Aurbacha, Boris Markovskya, Elena Markevicha, Ella Zinigrada, Liraz Asrafa, Joseph S. Gnanaraja, Hyeong-Jin Kimb, "Design of electrolyte solutions for Li and Li-ion batteries: a review," *Elsevier-Electrochimica Acta*, vol. 50, pp. 247-254 November 2004.
- [118] W.-B. L. Chung-Wen Kuo, Pin-Rong Chen, Jian-Wei Liao, Ching-Guey Tseng, Tzi-Yi Wu, "Effect of Plasticizer and Lithium Salt Concentration in PMMA-based Composite Polymer Electrolytes," *ELECTROCHEMICAL SCIENCE*, vol. 8, pp. 5007 - 5021, 1 April 2013 2013.
- [119] "Propylene carbonate," in *wikipedia*, ed.
- [120] A. A. F. Z. Ismail A.M. Ibrahim, Mohamed A. Sharaf, "Preparation of spherical silica nanoparticles: Stober silica," *Journal of American Science*, vol. 6, pp. 985-989, 2010.
- [121] Saed. (2012-13). *CHEM 104 Study Guide*. Available: <https://www.studyblue.com/notes/n/chem-104-study-guide-2012-13-saed-/deck/9715125>
- [122] Z. A. M. H. Samira Bagheria, Amin Termeh Yousefib, Sharifah Bee Abdul Hamid, "Progress on mesoporous titanium dioxide: Synthesis, modification and applications," *Microporous and Mesoporous Materials*, vol. 218, pp. 206-222, 2015.
- [123] L. G. S. B. Kumar, R.J. Spry, "on the origin of conductivity enhancement in polymer-ceramic composite electrolytes," *J. Power Sources* vol. 96, pp. 337-342, 2001.

- [124] Y. W. S.H. Chung, L. Persi, F. Croce, S.G. Greenbaum, B. Scrosati, "Enhancement of ion transport in polymer electrolytes by addition of nanoscale inorganic oxides," *J. Power Sources*, vol. 97-98, pp. 644-648, 2001.
- [125] A. B. B.M. Abdel-Samiea, R. Khalil1, Eslam Mohamed Sheha, H. Tsuda and T. Matsui, "The Role of TiO<sub>2</sub> Anatase Nano-Filler to Enhance the Physical and Electrochemical Properties of PVA-Based Polymer Electrolyte for Magnesium Battery Applications " *Journal of Materials Science and Engineering*, vol. 3, pp. 678-689 2013.
- [126] R. S. Baldwin, "A Review of State-of-the-Art Separator Materials for Advanced Lithium-Based Batteries for Future Aerospace Missions," Glenn Research Center, Cleveland, Ohio, National Aeronautics and Space Administration 2009.
- [127] (2013). *Li-ion Battery Separator Film (25um thick x 85mm W x 60m L, Celgard ) - EQ-bsf-0025-60C*. Available: <http://www.mtixtl.com/separatorfilm-EQ-bsf-0025-60C.aspx>
- [128] A. Moretti. *What are the advantages and disadvantages of ethylene carbonate and propylene carbonate?* Available: [https://www.researchgate.net/post/What\\_are\\_the\\_advantages\\_and\\_disadvantages\\_of\\_ethylene\\_carbonate\\_and\\_propylene\\_carbonate](https://www.researchgate.net/post/What_are_the_advantages_and_disadvantages_of_ethylene_carbonate_and_propylene_carbonate)
- [129] D. Ortiz, V. Steinmetz, D. Durand, S. Legand, V. Dauvois, P. Maitre, *et al.*, "Radiolysis as a solution for accelerated ageing studies of electrolytes in Lithium-ion batteries," *Nat Commun*, vol. 6, 04/24/online 2015.
- [130] (2013). *Electrolyte LiPF<sub>6</sub> for LiCoO<sub>2</sub> Lithium-ion Battery R&D, 1Kg in Stainless Steel Container - EQ-LBC3051C*. Available: <http://www.mtixtl.com/ElectrolyteLiPF6forLiCoO2Lithium-ionbatteryRandD1KginaSafeStainle.aspx>
- [131] N. J. S. M.R.Gilberg. (29 April 2016). *Ammonium Hydroxide* Available: [http://cameo.mfa.org/wiki/Ammonium\\_hydroxide](http://cameo.mfa.org/wiki/Ammonium_hydroxide)
- [132] F. S. c. Elizabeth Fonseca dos Reisa, Andrey Pereira Lagea, Romulo Cerqueira Leitea, Luiz Guilherme Heneineb, Wander Luiz Vasconcelosc, Zelia Ines Portela Lobatoa, Herman Sander Mansur, "Synthesis and Characterization of Poly (Vinyl Alcohol) Hydrogels and Hybrids for rMPB70 Protein Adsorption " *Materials Research*, vol. 9, pp. 185-191, December 29, 2005 2006.
- [133] L.-W. W. Q.-B. Lin, and S.-H. Huang, "Effects of different treatment of TiO<sub>2</sub> electrodes on photovoltaic characteristics of dye-sensitized solar cells,," *Surface Engineering and Applied Electrochemistry*, vol. 51, pp. 394-400, 2015.
- [134] K.-H. Park, E. M. Jin, H. B. Gu, S. E. Shim, and C. K. Hong, "Effects of HNO<sub>3</sub> treatment of TiO<sub>2</sub> nanoparticles on the photovoltaic properties of dye-sensitized solar cells," *Materials Letters*, vol. 63, pp. 2208-2211, 10/31/ 2009.
- [135] A. M. Buckley and M. Greenblatt, "The Sol-Gel Preparation of Silica Gels," *Journal of Chemical Education*, vol. 71, p. 599, 1994/07/01 1994.
- [136] P. K. Chu, J. Y. Chen, L. P. Wang, and N. Huang, "Plasma-surface modification of biomaterials," *Materials Science and Engineering: R: Reports*, vol. 36, pp. 143-206, 3/29/ 2002.
- [137] D. Aurbach, Y. Talyosef, B. Markovsky, E. Markevich, E. Zinigrad, L. Asraf, *et al.*, "Design of electrolyte solutions for Li and Li-ion batteries: a review," *Electrochimica Acta*, vol. 50, pp. 247-254, 11/30/ 2004.



- [138] H. P. Zhang, P. Zhang, G. C. Li, Y. P. Wu, and D. L. Sun, "A porous poly(vinylidene fluoride) gel electrolyte for lithium ion batteries prepared by using salicylic acid as a foaming agent," *Journal of Power Sources*, vol. 189, pp. 594-598, 4/1/ 2009.
- [139] S. Guruvenket, G. M. Rao, M. Komath, and A. M. Raichur, "Plasma surface modification of polystyrene and polyethylene," *Applied Surface Science*, vol. 236, pp. 278-284, 9/15/ 2004.
- [140] M. T. van Os and E. University of Twente. Department of Chemical, *Surface Modification by Plasma Polymerization: Film Deposition, Tailoring of Surface Properties and Biocompatibility*: Print Partners Ipskamp, 2000.
- [141] Jun Young Kim 1, \* and Dae Young Lim 3,\* , "Surface-Modified Membrane as A Separator for Lithium-Ion Polymer Battery " *energies*, vol. 3, pp. 866-885, 2010.
- [142] J. Y. Kim and D. Y. Lim, "Surface-modified membrane as a separator for lithium-ion polymer battery," *Energies*, vol. 3, pp. 866-885, 2010.
- [143] Z.-S. Wang, M. Yanagida, K. Sayama, and H. Sugihara, "Electronic-insulating coating of CaCO<sub>3</sub> on TiO<sub>2</sub> electrode in dye-sensitized solar cells: improvement of electron lifetime and efficiency," *Chemistry of Materials*, vol. 18, pp. 2912-2916, 2006.
- [144] K.-H. Park, E. M. Jin, H. B. Gu, S. E. Shim, and C. K. Hong, "Effects of HNO<sub>3</sub> treatment of TiO<sub>2</sub> nanoparticles on the photovoltaic properties of dye-sensitized solar cells," *Materials Letters*, vol. 63, pp. 2208-2211, 2009.
- [145] C. J. Brinker, "Hydrolysis and condensation of silicates: effects on structure," *Journal of Non-Crystalline Solids*, vol. 100, pp. 31-50, 1988.
- [146] H. J. Walls, M. W. Riley, R. R. Singhal, R. J. Spontak, P. S. Fedkiw, and S. A. Khan, "Nanocomposite Electrolytes with Fumed Silica and Hectorite Clay Networks: Passive versus Active Fillers," *Advanced Functional Materials*, vol. 13, pp. 710-717, 2003.